AD-A114 655 FEDERAL AVIATION ADMINISTRATION TECHNICAL CENTER ATL--ETC F/G 1/2
REDUCTION AND ANALYSIS OF MODE C ALTITUDE DATA COLLECTED AT HI@--ETC(U)
MAR 82 R RIGOLIZZO

UNCLASSIFIED DOT/FAA/CT-81/53 DOT/FAA/EM-82/9 NL

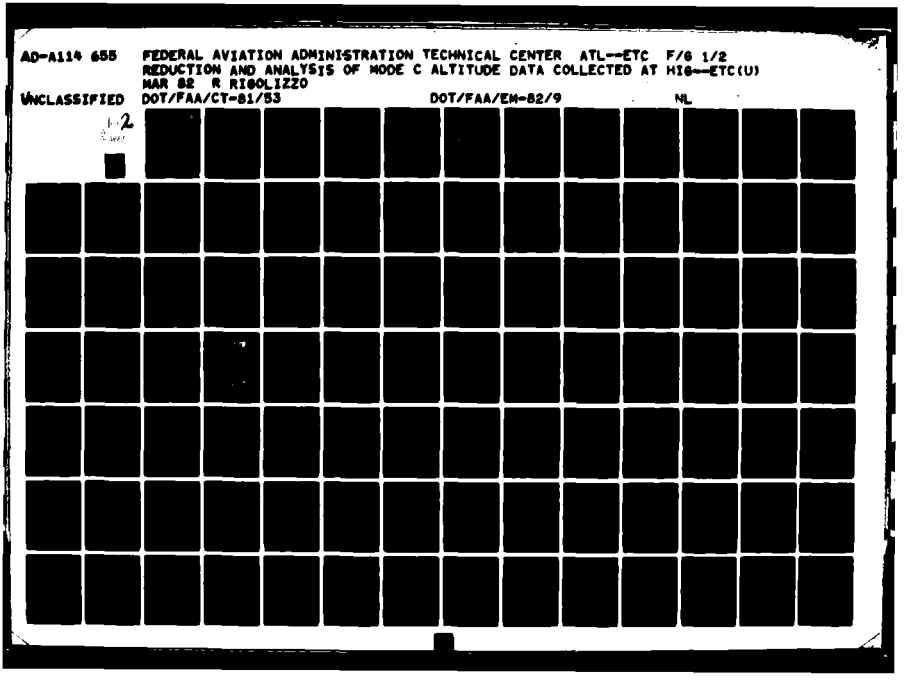

13

DOT/FAA/EM-82/9
DOT/FAA/CT-81/53

Reduction and Analysis of Mode C Altitude Data Collected at High Altitudes Over the Continental United States

Robert Rigolizzo

Prepared By
FAA Technical Center
Atlantic City Airport, N.J. 08405

March 1982

Final Report

U.S. Department of Transportation
Federal Aviation Administration
Office of Systems Engineering Management
Washington, D.C. 20590

NOTICE

This document is disseminated under the sponsorship of the Department of Transportation in the interest of information exchange. The United States Government assumes no liability for the contents or use the.eof.

The United States Government does not endorse products or manufacturers. Trade or manufacturer's names appear herein solely because they are considered essential to the object of this report.

Technical Report Documentation Page

1. Report No.	2. Government Accession No.	3. Recipient's Catalog No.
DOT/FAA/EM-82/9	AD-A114655	

4. Title and Subtitle

REDUCTION AND ANALYSIS OF MODE C ALTITUDE DATA COLLECTED AT HIGH ALTITUDES OVER THE CONTINENTAL UNITED STATES

5. Report Date	March 1982
6. Performing Organization Code	
8. Performing Organization Report No.	DOT/FAA/CT-81/53

7. Author(s)

Robert Rigolizzo

9. Performing Organization Name and Address

Federal Aviation Administration
Technical Center
Atlantic City Airport, New Jersey 08405

10. Work Unit No. (TRAIS)	
11. Contract or Grant No.	012-102-230
13. Type of Report and Period Covered	Final September 1977 - April 1978
14. Sponsoring Agency Code	

12. Sponsoring Agency Name and Address

U.S. Department of Transportation
Federal Aviation Administration
Office of Systems Engineering Management
Washington, D.C. 20590

15. Supplementary Notes

16. Abstract

This report describes the reduction and analysis of mode C altitude data collected over the en route centers of Cleveland, Ohio; Memphis, Tennessee; and Albuquerque, New Mexico. The data were gathered under the aegis of the separation standards program primarily for the study of lateral navigation performance over the continental United States at high altitudes.

This study provides a procedure for estimating the vertical flight technical error as evidenced from mode C altitude data recorded at the en route centers. It does not account for basic altimeter system error or flight technical error biases and/or fluctations that are not observable in the ground-derived mode C reported altitude. The data are fitted to six different analytical distributional forms. The effect that data quantization has on the estimation of the parameters of the distributions is examined. Then statistical tests are performed to evaluate the appropiateness of each distributional model in representing the histogram of the mode C deviations.

A preliminary analysis is conducted to investigate the association betwee[illegible] C altitude and aircraft environmental performance characteristics commonly [illegible] in evaluating separation criteria, as well as identifying aircraft attributes [illegible] are of major interest when evaluating vertical flight technical error.

17. Key Words	18. Distribution Statement
Flight Technical Error Transponded Mode C Altitude Vertical Separation Standards Aircraft Height-Keeping Systems	Document is available to the U.S. public through the National Technical Information Service, Springfield, Virginia 22161

19. Security Classif. (of this report)	20. Security Classif. (of this page)	21. No. of Pages	22. Price
Unclassified	Unclassified	99	

METRIC CONVERSION FACTORS

Approximate Conversions to Metric Measures

Symbol	When You Know	Multiply by	To Find	Symbol
		LENGTH		
in	inches	*2.5	centimeters	cm
ft	feet	30	centimeters	cm
yd	yards	0.9	meters	m
mi	miles	1.6	kilometers	km
		AREA		
in^2	square inches	6.5	square centimeters	cm^2
ft^2	square feet	0.09	square meters	m^2
yd^2	square yards	0.8	square meters	m^2
mi^2	square miles	2.6	square kilometers	km^2
	acres	0.4	hectares	ha
		MASS (weight)		
oz	ounces	28	grams	g
lb	pounds	0.45	kilograms	kg
	short tons (2000 lb)	0.9	tonnes	t
		VOLUME		
tsp	teaspoons	5	milliliters	ml
Tbsp	tablespoons	15	milliliters	ml
fl oz	fluid ounces	30	milliliters	ml
c	cups	0.24	liters	l
pt	pints	0.47	liters	l
qt	quarts	0.95	liters	l
gal	gallons	3.8	liters	l
ft^3	cubic feet	0.03	cubic meters	m^3
yd^3	cubic yards	0.76	cubic meters	m^3
		TEMPERATURE (exact)		
°F	Fahrenheit temperature	5/9 (after subtracting 32)	Celsius temperature	°C

*1 in = 2.54 (exactly). For other exact conversions and more detailed tables, see NBS Misc. Publ. 286, Units of Weights and Measures, Price $2.25, SD Catalog No. C13.10:286.

Approximate Conversions from Metric Measures

Symbol	When You Know	Multiply by	To Find	Symbol
		LENGTH		
mm	millimeters	0.04	inches	in
cm	centimeters	0.4	inches	in
m	meters	3.3	feet	ft
m	meters	1.1	yards	yd
km	kilometers	0.6	miles	mi
		AREA		
cm^2	square centimeters	0.16	square inches	in^2
m^2	square meters	1.2	square yards	yd^2
km^2	square kilometers	0.4	square miles	mi^2
ha	hectares (10,000 m^2)	2.5	acres	
		MASS (weight)		
g	grams	0.035	ounces	oz
kg	kilograms	2.2	pounds	lb
t	tonnes (1000 kg)	1.1	short tons	
		VOLUME		
ml	milliliters	0.03	fluid ounces	fl oz
l	liters	2.1	pints	pt
l	liters	1.06	quarts	qt
l	liters	0.26	gallons	gal
m^3	cubic meters	35	cubic feet	ft^3
m^3	cubic meters	1.3	cubic yards	yd^3
		TEMPERATURE (exact)		
°C	Celsius temperature	9/5 (then add 32)	Fahrenheit temperature	°F

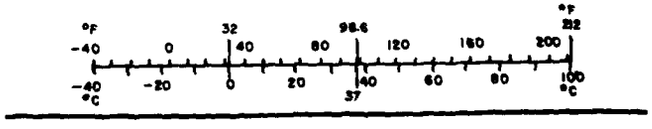

PREFACE

This work could not have been initiated without the help of several key personnel within the Analysis Branch of the Systems Simulation and Analysis Division. Dale Livingston provided all the Cleveland mode C data used during the lateral separation study in a reduced form suitable for computer analysis. He also contributed to clarifying many facets of the data anomalies and collection procedures and provided consultation on the efficient use of the Honeywell computer time-sharing system. Dorothy Hanlon, Iva Callio, and Doris Westervelt meticulously selected the level-flight portions of the data, keyed it into the computer, and performed editing via the time-sharing system. It is largely due to their diligence that a high degree of credibility can be given to the reduced data. Paul Bradbury performed consultation regarding operating procedures of air traffic controllers in the National Airspace System (NAS) environment. Allen Busch and Brian Colamosca provided assistance in statistical analysis, as well as constructive guidance and support in assembling this report. Thomas Funke (Drexel University Student) wrote several highly efficient time-sharing programs and provided consultation on many vaguely described time-sharing commands.

Professor Neil Polhemus of Princeton University provided the lateral separation Fortran distribution fitting program and valuable analytic support throughout this study.

The work discussed in this report was conducted under NAFEC Program Document 01-203, FAA Subprogram 012-102, Project 012-102-230. The FAA Technical Center Program Manager was Brian F. Colamosca.

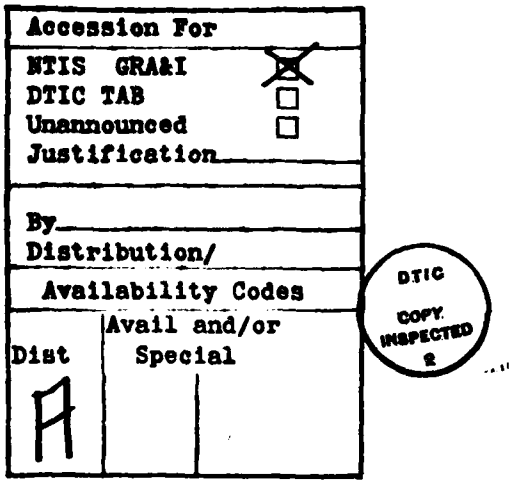

BLANK PAGE

TABLE OF CONTENTS

LIST OF ILLUSTRATIONS

LIST OF ILLUSTRATIONS (Continued)

LIST OF ILLUSTRATIONS (Continued)

LIST OF TABLES

BLANK PAGE

INTRODUCTION

PURPOSE.

The purpose of this study was to construct the distribution of level flight mode C altitude deviations from assigned altitude as collected over the en route centers of Cleveland, Memphis, and Albuquerque; investigate the utility of mode C reported altitude in representing vertical flight technical error (FTE); examine the association between mode C altitude and aircraft performance characteristics; and identify aircraft attributes that are of major interest when evaluating vertical FTE. This report describes the procedure employed to reduce and analyze the collected mode C altitude data and defines the limitations encountered due to its structure.

BACKGROUND.

Due to the increase in air traffic and improved avionics systems, several organizations have proposed evaluating the feasibility of reducing aircraft vertical separation above flight level 290 over the continental United States (CONUS). Currently, the vertical separation minima for instrument flight rule (IFR) aircraft are 2,000 feet at and above flight level 290 and 1,000 feet below flight level 290. This evaluation would necessarily entail obtaining an estimate of vertical displacement from assigned flight level pressure height for a large number of aircraft. Vertical deviation represents the inability of aircraft avionic systems to, first, measure and, second, maintain altitude at a given atmospheric pressure level. The first (the inability of the aircraft system to measure a given pressure level) is called altimeter system error (ASE). It is usually divided into the two components of static pressure error and altimeter instrument error. Static pressure error represents the deviation which occurs due to measuring aircraft ambient pressure and transmitting that pressure to the altimeter. Altimeter instrument error represents the deviation which occurs in transforming from pressure input to altitude in feet and displaying this value to the aircraft crew. The second (the inability of the aircraft system to maintain a given flight level) is called vertical FTE.

In the early 1960's, several studies were initiated by the International Air Transport Association (IATA) to investigate the feasibility of reducing vertical separation to 1,000 feet over the North Atlantic. These studies precipitated several data collection efforts. One such effort employed radar altimeter equipped jet aircraft that were capable of accurately measuring height above the ocean (reference 1). During this effort, flight crews manually recorded barometric altimeter altitude, radar altimeter altitude, assigned altitude, time, and position data at predetermined locations. Subsequently, when two aircraft recorded data within predetermined geographical and time constraints, their relative vertical separation was computed. This system provided the first simultaneous in-flight data on altimeter system, flight technical, and total vertical errors between aircraft pairs. Unfortunately, the quantity of independent data was insufficient to confidently demonstrate that reduced vertical separation standards were safe.

At about the same time, a National Aeronautics and Space Administration (NASA) data collection was conducted to evaluate the vertical FTE of 19 commercial transports for almost 10,000 hours of stabilized cruise flight (reference 2). This data was

employed in several subsequent Royal Aircraft Establishment (RAE) reports, where the aggregate distribution is clearly more heavily tailed than normal (references 3 and 4). This observation, supported by results from other studies, demonstrated that the classical Gaussian methods of analysis were not applicable in the vertical domain, and the requirement for a large quantity of data became a necessity.

Since the early 1960's, several studies were conducted on a limited number of aircraft to establish static pressure errors. The most significant of these studies is the Department of Defense (DOD) (AIMS) pitot-static systems calibration (reference 5). (Note: AIMS is an acronym derived from other acronyms — Air Traffic Control Radar Beacon System (ATCRBS), Identification Friend or Foe (IFF), Mark XII Identification System, and System.) The purpose of this test was to ensure that all DOD aircraft altimeter systems perform within a tolerance of 250 feet. This analysis was based on the unproven assumption that once an aircraft's altimeter system is within 250 feet, it will remain within that tolerance for an indefinite period. This assumption was questioned at the 1976 Air Data Systems Conference, and the conclusion was made that a study was needed to establish improved maintenance procedures for aircraft pitot-static systems (reference 6).

Other countries have recently investigated the possibility of reducing vertical separation over national airspace. The French have proposed an interim solution of reducing separation to 1,500 feet above flight level 290 and increasing separation to 1,500 feet for one or more flight levels below. Japan has already collected significant amounts of level flight FTE data on all Nippon Airways L1011 and Japanese Air Lines (JAL) B747 aircraft at high altitudes. In addition, at the 1978 Review of General Concepts of Separation Panel (RGCSP) in Paris, France, they presented preliminary data collection results obtained by measuring the relative vertical distance between aircraft pairs using a ground-based pulse radar with a fan beam antenna. Available literature suggests that this is the only ongoing effort to measure vertical separation.

While automatic altitude reporting enhances air traffic controller capability to maintain aircraft separation and reduce communications, it also provides a source of information regarding the frequency and magnitude of vertical FTE. This report will present the results of reducing and analyzing mode C beacon reported altitude data. This information will at times be used as a surrogate for vertical FTE, and as such, it can be somewhat distorted. Sources contributing to the distortion include 100-foot quantization, transponder crossover, linkage system bias, and the difference between pilot and copilot altimeter readings.

DATA COLLECTION AND REDUCTION

LATERAL DATA COLLECTION.

The data utilized in this study were collected from September 1977 to April 1978. Its purpose was to provide quantitative support for the lateral very high frequency omnidirectional radio range (VOR) navigation performance study of aircraft at high altitudes over CONUS. The procedure — supervising, gathering and reducing data — was conducted by the Federal Aviation Administration (FAA) Technical Center, under the aegis of the Separation Standards Program.

The three en route centers chosen as data collection sites were Cleveland, Memphis, and Albuquerque. At each en route center, an FAA Technical Center representative was present to direct and coordinate each phase of the collection, and a special data processor and recorder was installed between the data receiver group and the system maintenance monitor console (SMMC) to record digital transponded data. The processor and recorder were packaged into one unit and received messages at the input to the SMMC. Hence, it did not interface with normal Air Route Traffic Control Center (ARTCC) operations. For all aircraft within the operational range of three National Airspace System (NAS) surveillance radars that were associated with each ARTCC, the unit's recorder had the capability to automatically transfer onto magnetic tape time, azimuth, range, mode C encoded altitude, beacon code, and an identification corresponding to each surveillance radar. The processing component had the capability to restrict information to within a cylindrical coordinate segment; with angular sector limits defined by azimuth, cylinder radius limits defined by range, and height limits defined by altitude. Each limiting value was predetermined before the data collection so that transponded data were recorded only for those aircraft on routes of interest. The routes chosen for each center are displayed in figures 1 to 3. The lower limit on mode C altitude was set to 19,000 feet, and supplementary information was collected to associate transponded radar data with parameters such as aircraft identity, type, and speed. This collation was accomplished through flight strips and observer logs. After each data collection day, all flight strips associated with the en route sectors containing prechosen routes were assembled, sorted, and set aside at the ARTCC. After the 14-day holding period the en route center mailed these flight strips to the FAA Technical Center. During the data collection, observers were stationed at an unused air traffic controller radar scope to record duplicate strip information and provide written remarks and comments on any aircraft that exhibited poor lateral navigation performance. Finally, voice tape communication recordings for each day were obtained in parallel with normal operations to aid in identifying supplementary information. This collection was scheduled for 4 to 5 months and designed to collect information on 15,000 aircraft passes. At completion, the entire package of transponded radar magnetic tape data, flight strips, observer logs, and voice communication recordings were sent to the FAA Technical Center (figure 4).

DATA REDUCTION.

Once the data were received at the FAA Technical Center, the transponded radar magnetic tapes were processed. Aircraft data were restructured so that all the information pertaining to each aircraft, on each route segment, was blocked into data sets. Route segments were defined for each Center as the distance between VOR's. Further, the transponded range and azimuth values were transformed and rotated into a rectangular coordinate system. One axis represented distance from a VOR on route, and one axis represented a lateral deviation from route. Mode C altitude was not converted. Aircraft beacon codes were matched to aircraft identity, and each data set was labeled with supplementary information. Those aircraft data sets within the en route center coverage, and not on prechosen routes, were eliminated. The remaining data sets were filtered, smoothed, and transferred to magnetic discs for ease in computer processing. Simultaneously, the flight strip and observer log data were reduced, restructured, and stored on magnetic discs. All of the above was accomplished as part of the lateral VOR study.

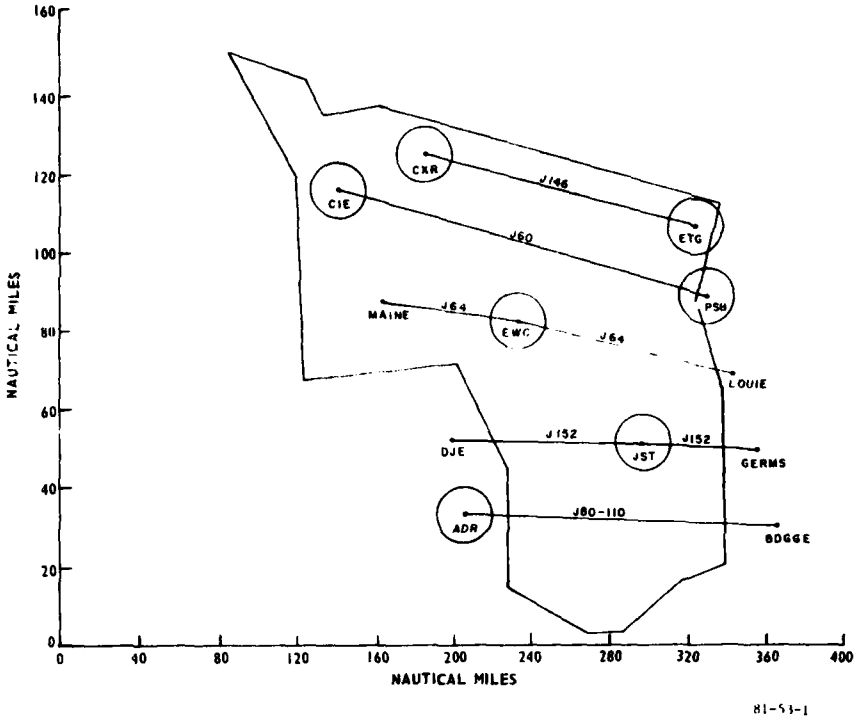

FIGURE 1. CLEVELAND HIGH ALTITUDE OUTER SECTOR BOUNDARIES AND DATA COLLECTION ROUTE SEGMENTS

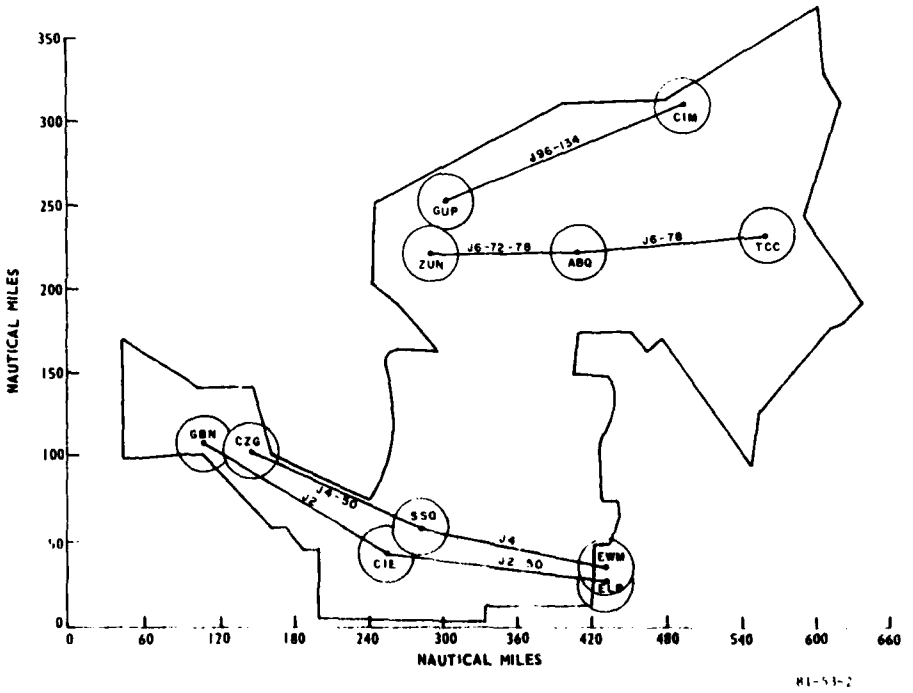

FIGURE 2. ALBUQUERQUE HIGH ALTITUDE OUTER SECTOR BOUNDARIES AND DATA COLLECTION ROUTE SEGMENTS

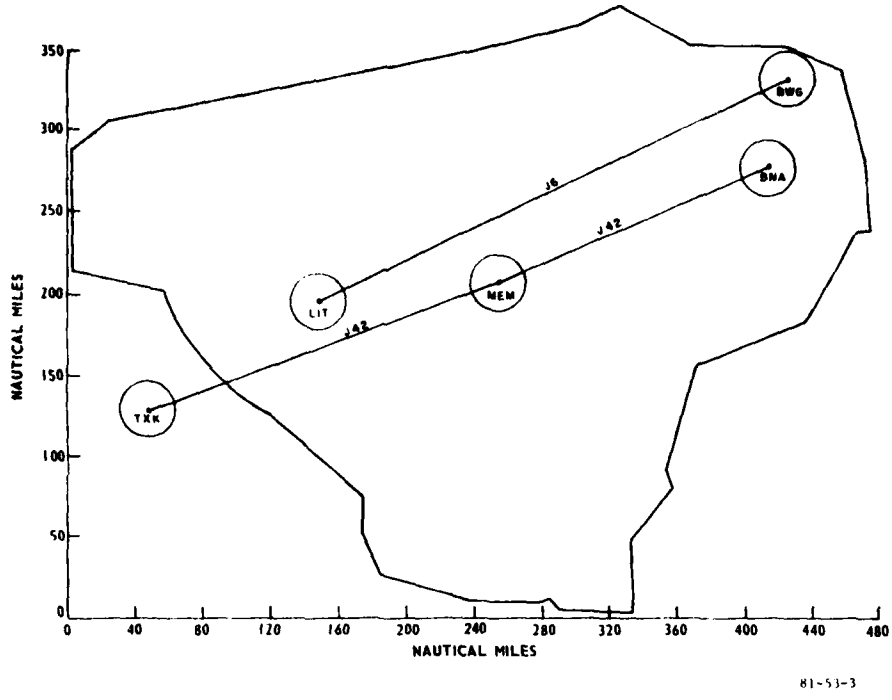

FIGURE 3. MEMPHIS HIGH ALTITUDE OUTER SECTOR BOUNDARIES AND DATA COLLECTION ROUTE SEGMENTS

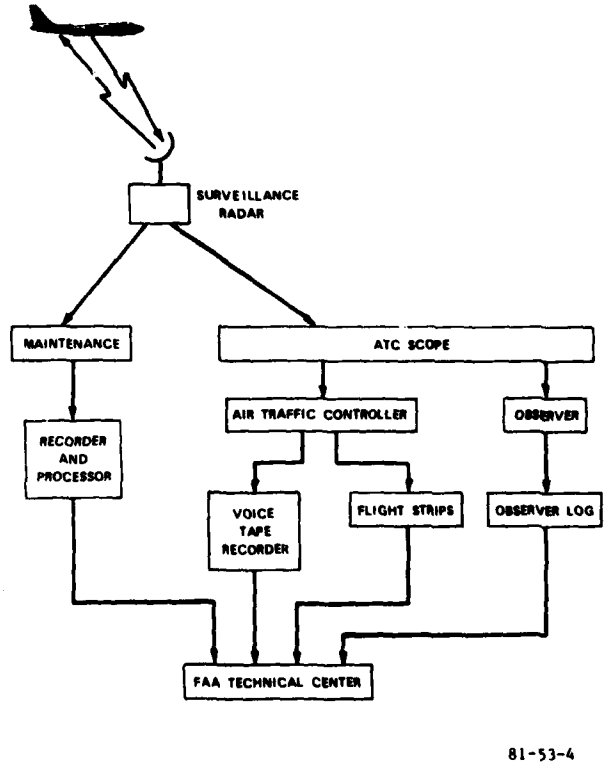

FIGURE 4. SUMMARIZED DATA COLLECTION PROCEDURES

For the vertical study, the data were reprocessed in a similar manner, except that no filtering or smoothing of digital mode C altitude was performed and the data were stored on magnetic tapes. Utilizing these tapes, the data were further reduced to time versus mode C altitude, and hard copy computer listings were generated.

Since the primary objective of the data collection was to obtain information related to lateral aircraft performance, vertical flight profiles consisted of ascending, descending, and level-flight aircraft. To partition level-flight data, each computer listing was visually examined by statistical clerks familiar with aircraft operational procedures. Employing the criteria defined in appendix A, the times associated with the beginning and end of level-flight segments were marked and tabulated. Subsequent to tabulating this information for each data collection day, it was collated with aircraft identity, beacon code, data set count, and the statistical clerks' estimate of level-flight time interval as represented by the digital computer listing. Finally, it was entered onto a computer generated disc file by means of a time-sharing terminal (table 1).

TABLE 1. SAMPLE LEVEL FLIGHT START AND END TIMES TABULATION

Data Set Count	Center/Day	Aircraft Identity	Start Time (Seconds)	End Time (Seconds)	Digital Altitude (Feet)
1	M339	BN212	53,724.9	53,896.7	290
1	M339	BN212	54,147.9	54,916.0	330
2	M339	BN212	54,925.7	55,542.3	330
3	M339	N1125	54,727.8	54,914.5	410
3	M339	N1125	55,225.6	55,437.9	370
3	M339	N1125	56,623.3	55,478.1	350
4	M339	N1125	57,309.7	57,309.7	800
5	M339	BN18	55,314.2	57,305.8	370
6	M339	EA51	54,710.7	56,624.0	310
7	M339	N966L	55,676.2	57,750.7	-390
8	M339	N552N	57,042.4	57,042.4	900
9	M339	N552N	57,072.4	58,768.7	350
10	M339	BN27	62,023.9	60,203.3	350

Several conditions existed during the construction of the level-flight beginning and end timetable that required special attention. They are as follows: (1) An aircraft data set observed at several level-flight segments was divided into as many parts. For example, on data set 1, in table 1, an aircraft identified as BN212 was observed in level flight at both altitudes 290 and 330. (2) An aircraft profile observed in nonlevel flight during the entire data set between VOR stations had a code of 800 set for altitude, and both start and end times were set equal (e.g. data set 4 in table 1). (3) An aircraft's flight profile that contained unreasonable data had a code of 900 set for altitude, and start and end times were set equal (e.g. data set 8 in table 1). (4) An aircraft observed in level flight above 29,000 feet, and not at an odd numbered flight level, had its digital assigned altitude temporarily set to the nearest negative odd numbered altitude. For example, if an aircraft was observed in level flight at altitude 380, a digital assigned altitude of -370 or -390 was tabulated and input on to the computer disc file (e.g. data set 7 in table 1). This identified that aircraft for further analysis. (5) An aircraft's vertical flight profile that exhibited unusually abnormal behavior was also tagged by setting the altitude negative.

For each day of data collected, a printout of the level-flight beginning and end timetable was created and verified against the original data by a different statistical clerk. All modifications and corrections were made directly onto the computer disc file via the time-sharing terminal. Upon completion, a time histogram of aircraft level-flight data segments was generated by matching the reduced time versus mode C altitude data with the level-flight file and using the following definition:

> The amount of time spent at a given mode C altitude for a specific aircraft data set is the difference between the time associated with given mode C the altitude and the time associated with the next chronological mode C altitude for that aircraft's data set.

Hence, an aircraft tracked by one surveillance radar, might exhibit a time interval between each mode C observation of approximately 10 to 12 seconds (depending on the scan rate of the radar). An aircraft tracked by two surveillance radars, might exhibit two mode C observations in 10 to 12 seconds. The time between successive mode C observations was dependent on the geometrical relationship between the two radars and the tracked aircraft. The data recorded for this study had from one to three surveillance radars tracking aircraft, and it was possible to have three asynchronous observations every 10 to 12 seconds. For example, consider the data in table 2. Two surveillance radars are tracking an aircraft, and each has a scan rate of approximately 10 seconds. The time interval between observations oscillates from about 3.5 to 6.7 seconds due to the relative location of the radars and the aircraft. Altitude changes are at times 58332.4 and 58342.5. Hence, the amount of time estimated at altitude 350, 349, and again at 350 was 13.6, 10.1, and 20.3 seconds, respectively. This information can be summarized in a time histogram as shown in table 3. Column 2 is the total time tracked, and the remaining columns are the amount of time tracked at or deviating from assigned altitude. The sample exemplified in table 2 is shown as case 11. In this case, the aircraft was tracked for a total of 44 seconds. The amount of time at 350 (zero-deviation from assigned altitude) was 33.9 seconds. The amount of time spent at 349 (100 feet below assigned altitude) was 10.1 seconds. The time spent at all other levels was zero.

TABLE 2. SAMPLE DIGITAL MODE C ALTITUDE AND TIME OBSERVATIONS

Observation Count	Time Of Observation	Time Difference	Digital Altitude
1	58,318.8		350
		3.5	
2	58,322.3		350
		6.7	
3	58,329.0		350
		3.4	
4	58,332.4		349
		6.7	
5	58,339.1		349
		3.4	
6	58,342.5		350
		6.6	
7	58,349.1		350
		3.6	
8	58,352.7		350
		6.6	
9	58,359.3		350
		3.5	
10	58,362.8		350

Associated with each time histogram is supplementary information obtained from the lateral data collection computer disc files, and augmented by information contained on the flight strip and observer log data. A sample of supplementary information is shown in table 4. The records of observed altitude are presented in columns 5, 6, and 7. They are obtained from flight data strips, observer logs, and digital data, respectively. The first two altitude records were used to aid in verifying the digital data assigned altitude. This procedure will be discussed in the next section. All the remaining columns except 9, are self-explanatory. In that column, the codes 1, 2, 3, and 4 are used to identify an aircraft as commercial, military, general aviation, and unknown, respectively. A time histogram file and supplementary data file were constructed for each aircraft level-flight segment observed over the en route centers of Cleveland, Memphis, and Albuquerque. These reduced data files will be the basis for most of the analysis discussed in this report.

TABLE 3. SAMPLE TIME HISTOGRAM DATA

Data Set	Total Time In Level Flight (seconds)	Time (seconds) spent deviating from altitude (feet)										
		etc.	-400	-300	-200	-100	0	100	200	300	400	etc.
1	830.0						830.0					
2	891.0					891.0						
3	730.0						730.0					
4	2052.0					10.0	1981.0	61.0				
5	863.0						863.0					
6	1267.0				109.0	1105.0	30.0	13.0	10.0			
7	2154.0				10.0	1194.0	920.0	30.0				
8	1535.0					1535.0						
9	402.0					402.0						
10	2416.0					2416.0						
11	44.0					10.1	33.9					

TABLE 4. SAMPLE SUPPLEMENTARY INFORMATION

Data Set	Center/ Day	Aircraft Identity	Beacon Code	Flight Strip Altitude	Observer Log Altitude	Digital Altitude	Total Time Observed (seconds)	User Code	Type	Weight	Direction	Speed (knots)	Route	Route Segment
1	A326	BN501	2222	310	310	310	1256.3	1	DC8	H	W	419	J4	SSO-EWM
2	A326	AA605	2277	350	310	350	302.0	1	B727		W	431	J4	CZG-SSO
2	A326	AA605	2277	310	310	310	547.2	1	B727		W	431	J4	CZG-SSO
3	A326	AA605	2277	310	310	310	1244.5	1	B727		W	431	J4	SSO-EWM
4	A326	AA229	3413	310	350	350	116.6	1	B727		W	411	J4	CZG-SSO
5	A326	AA229	3413	310	350	350	1326.0	1	B72		W	411	J4	SSO-EWM
6	A326	WILY26Z	4201	290	330	330	706.0	2	T38		E	532	J4	CZG-SSO
7	A326	WILY26Z	4201	290	330	330	230.7	2	T38		E	532	J4	SSO-EWM
7	A326	WILY28Z	4204	290	330	370	115.7	2	T38		E	527	J4	SSO-EWM
8	A326	WILY28Z	4204	290	290	290	230.9	2	T38		E	527	J4	SSO-EWM

DECONTAMINATION OF MODE C ALTITUDE DATA

Automatically transponded data has as its primary function the relaying of aircraft positional information to the ATC system. In this manner, reducing voice communications, increasing efficiency, and providing a real-time system to aid controllers in performing their duties. The transponded signal may be identified as either mode A, B, C, or D, depending on the time interval between pulses. The signal corresponding to the aircraft's transmitted pressure altitude is mode C and is characterized by a series of pulses spaced 1.45 microseconds apart. It is capable of defining altitude from -1,000 to 126,750 feet in 100-foot intervals. The signal is referenced to 29.92 inches of mercury (Hg) independent of the altimeter setting within the aircraft.

The accuracy requirment of mode C altitude is that it must correspond to within 125 feet of pressure altitude (referenced to 29.92-inch Hg) on a 95 percent basis. This tolerance was originally derived under the following considerations. Mode C is quantized to 100-foot intervals and this results in a possible 50-foot error; the encoder switching point uncertainty and the linkage from the input source to the encoder results in a possible 50-foot error (assuming common input source to both the encoder and the pilot's altimeter); and the drive mechanism, the linkage from the encoder to the altimeter, and the altimeter setting results in a possible 25-foot error. The sum of these three errors accounts for in the 125-foot tolerance. Subsequent studies indicate this tolerance to be pessimistic for aircraft with a common input pressure source (reference 7). However, in addition to the above errors, there exists several other sources of error, mostly environmental, that contribute to the difference between transmitted mode C altitude as displayed on the air traffic controller cathode-ray tube (CRT) and pressure altitude, as displayed on the pilot's altimeter. The effect these parameters have on distorting FTE as evidenced by mode C altitude will now be examined.

TEST CRITERIA.

Environmental deviations such as antenna shading, reflection of signals, data processing, multiple aircraft transmitting on the same beacon code, and faulty transmitters, produce inconsistencies that are easily characterized by isolated large fluctuations in mode C altitude. Two procedures were employed to remove these nonrepresentative inconsistencies. The first was a computer-oriented relative median test, and the second was a visual test.

Each set of three contiguous data points was examined during data processing. If the center value was the median, it implied that during this time interval the aircraft vertical flight profile was either constant, increasing, or decreasing, and this altitude was accepted as valid mode C data. If an adjacent value was the median, then this implied that the center value peaked either positive or negative. When the magnitude of this peak was 100 feet, it was considered a changeover, resulting from the switching point of the transponded altitude data, and accepted as valid mode C data. When the magnitude was greater than 100 feet, the rate of climb or descent between the center altitude and its adjacent median was computed, rounded to the nearest 100 feet, and compared to twice the climb rate curve of a typical high-powered military jet. The curve used to specify the climb rates at each altitude was generated by fitting a fourth-degree polynomial to twice the

digital simulation facility (DSF) estimated aircraft climb rates from 5,000 to 45,000 feet (figure 5). If the computed climb rate exceeded the values specified in figure 5, the center altitude was rejected as invalid mode C data. The maximum descent rate was set to 10,000 feet/minute for all altitudes. This test was designed to delete only those deviations that could not possibly be valid FTE's, while allowing for the occurrence of large deviations due to turbulence. For example, consider figures 6 and 7. In figure 6, a large deviation occurred, and is characterized by a continual rise and a gradual descent. In this figure, all points were accepted by the median test, since it is possible that turbulence produced the deviations. In figure 7, a large isolated deviation occurred. The median test automatically removed this point from the data set. This test was not designed to remove two or more contiguous large deviations and accepted values within the performance of a high-powered military jet, yet outside the performance of the aircraft observed. To detect these and other deviations, all aircraft data sets that exhibited deviations of 400 feet or greater were visually examined. Those that had two or more contiguous large deviations, or were outside the performance of the aircraft tracked, were manually modified by editing the time histogram and deleting the amount of time spent at the invalid deviation. Data processing errors or any other inconsistencies detected (such as incorrect definition of flight level segments) were removed in the same manner. All aircraft exhibiting errors of 500 feet or greater were further examined by first creating a package on each one. This package included copies of flight strips, observer logs, vertical deviation time plot, lateral deviation plot, and a voice transcription around the time of the vertical deviation. If, for any reason this data indicated an error caused by sources not related to FTE, that aircraft's data set was either modified or removed from the time histogram file. Simultaneous to examining vertical deviation, a verification of each aircraft's flight level was conducted. A comparison was performed between the digital altitude recorded by the statistical clerks (column 7 of table 4), the flight strip recorded altitudes (column 5 of table 4), and the observer log recorded altitudes (column 6 of table 4). If the digital altitude recorded by the statistical clerks did not match the flight strip or observer log altitudes, that aircraft's identity, beacon code, case number, and en route center of collected data were tabulated. A thorough search of the original flight strips or observer logs usually provided the necessary identification. If not, a voice transcription was requested. For aircraft in level flight below 24,000 feet, there existed incomplete flight strip files and voice transcriptions due to en route center sector altitude boundaries. Hence, all aircraft in level flight below 24,000 feet and those with unverified altitudes were removed from the time histogram file.

PARAMETERS NOT CONSIDERED.

The decontamination process discussed in this section did not account for linkage from pressure input source to the encoder, the encoder to the altimeter, encoder switching point, drive mechanism, altimeter setting uncertainties, and possibly other unknown error sources. These are important factors in evaluating the utility of mode C altitude in representing FTE and cannot be thoroughly analyzed from the collected data. As such, the data in this report could represent a distorted, yet hopefully reasonable estimate of FTE as evidenced by mode C altitude of data collected over the en route centers of Cleveland, Memphis, and Albuquerque. Quantization of data into 100-foot intervals was resolved and will be presented in a later section of this report.

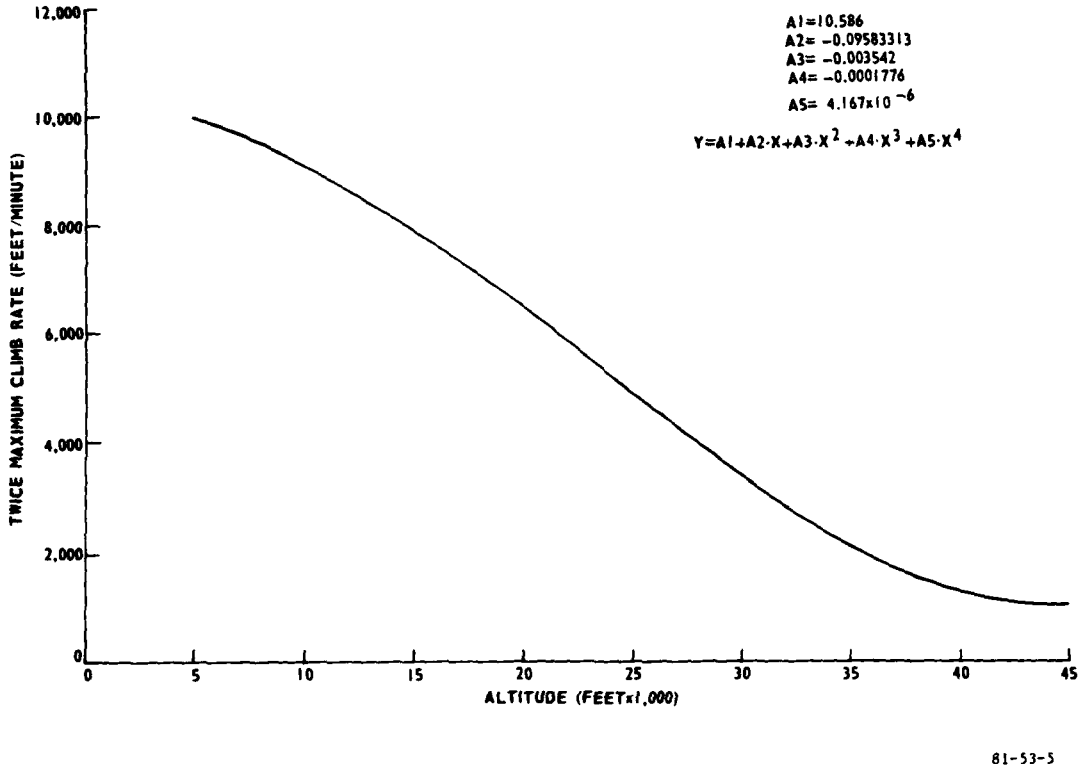

FIGURE 5. TWICE THE CLIMB RATE SPECIFIED FOR A HIGH PERFORMANCE MILITARY JET

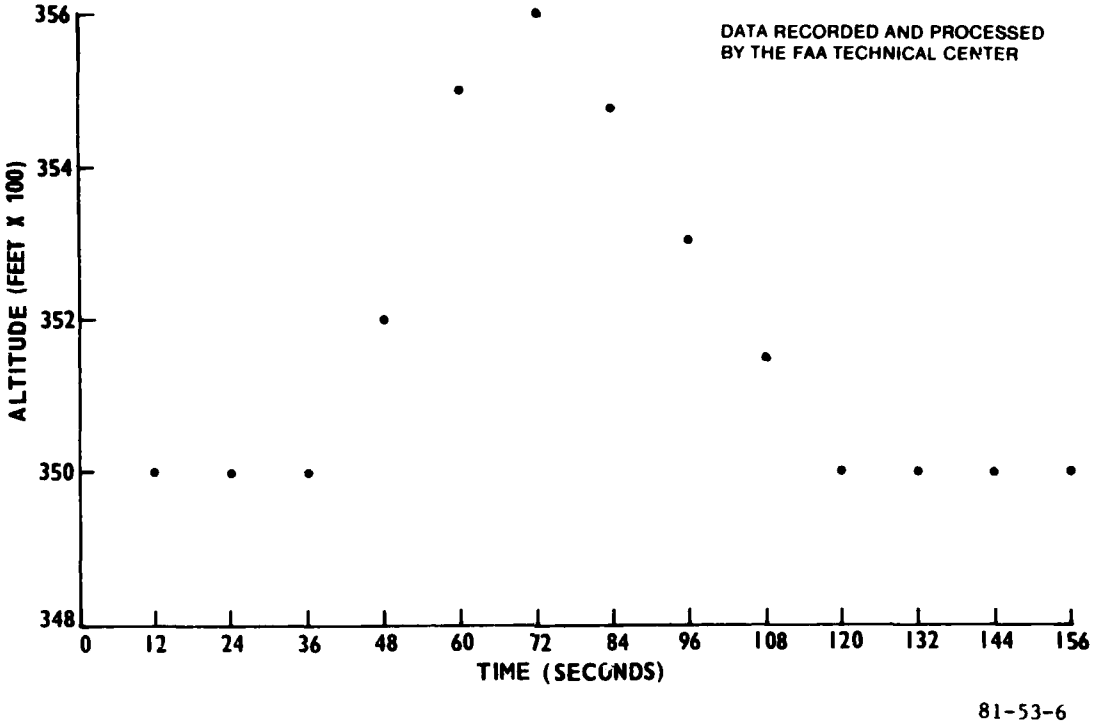

FIGURE 6. SAMPLE MODE C ALTITUDE DEVIATION (CASE 1)

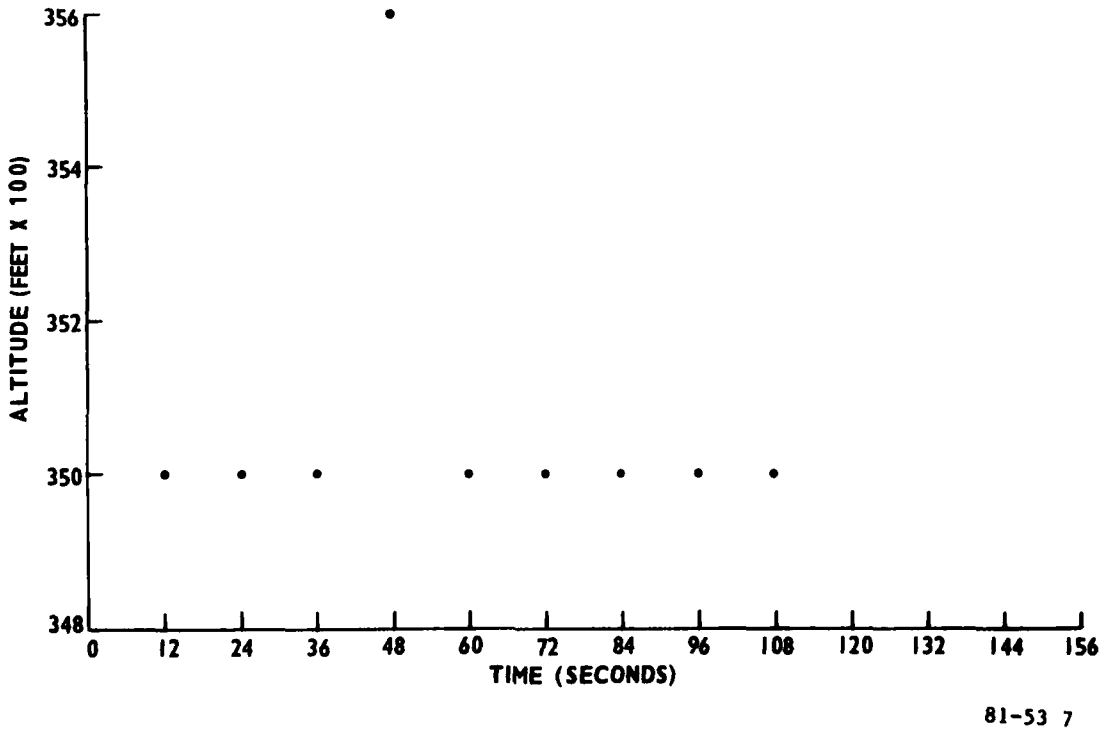

FIGURE 7. SAMPLE MODE C ALTITUDE DEVIATION (CASE 2)

DATA ANALYSIS

HISTOGRAM DATA.

The time histograms for all aircraft level-flight segments were combined into an aggregate histogram representing the length of time observed in each 100-foot interval about assigned flight levels by the data collected over the en route centers of Cleveland, Memphis, and Albuquerque. The relative frequency for each 100-foot interval is plotted on figure 8. This is a culmination of 14,168 aircraft level-flight segments for a total time of 4,904 hours. A mean of 0.4 feet and a skewness about the origin of 0.125 indicate a unimodal and symmetric distribution. The standard deviation about the origin is 61.2 feet and indicates class interval size of 100 feet is approximately 1.6 sigma. The kurtosis (a combined statistical measure of a distributions peakness or flatness near the mean and its abundance or sparsity of values far from the mean) about the origin (zero) is 6.96 and indicates a distribution more peaked and heavily tailed than normal (kurtosis of a normal distribution is 3) and slightly greater than an exponential (kurtosis of a double exponential distribution is 6). Each of the parameters (mean, standard deviation,

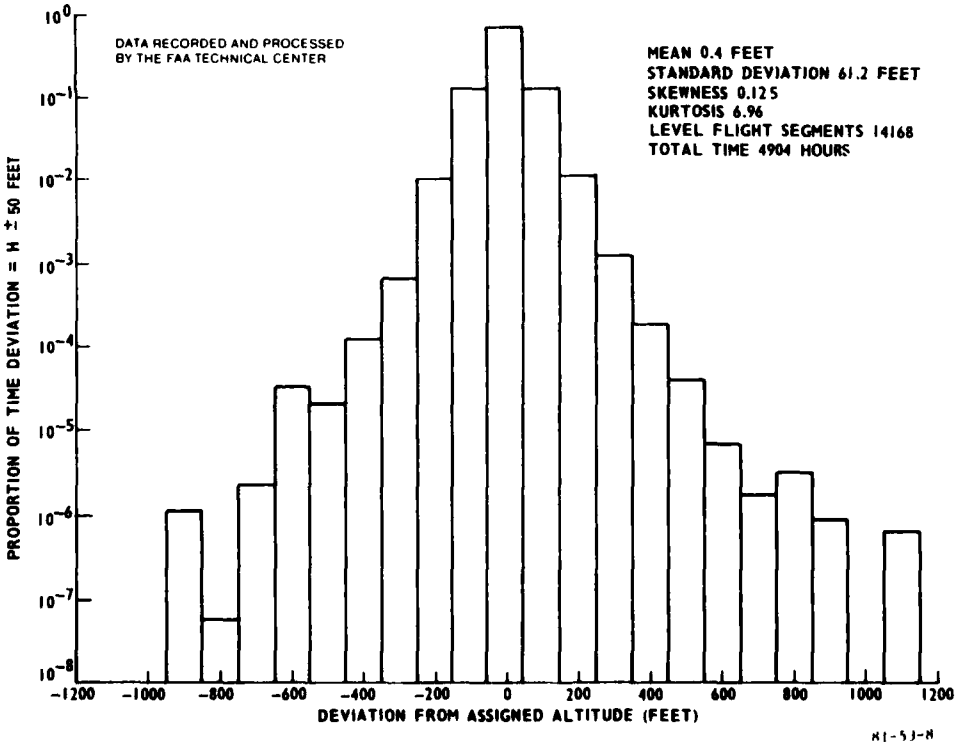

FIGURE 8. AGGREGATE MODE C ALTITUDE TIME HISTOGRAM

skewness, and kurtosis) was obtained by computing moments about the origin from data samples of variable time duration since the amount of time between independent samples of FTE was not determined during this or previous studies. The procedure employed to obtain these parameters avoided estimating the number of independent samples by relating the nth mean power of a time function to the nth moment of a frequency function as described in appendix B. The maximum positive deviation observed from assigned altitude is 1,100 feet, and the maximum negative deviation is 900 feet. The histogram indicates inconsistencies beyond 500 feet that may possibly be due to small sample size. In order to obtain an intuitive perception for the uncertainty associated with the heights of each histogram class interval, estimates of the 95 percent confidence limits were constructed (appendix C). These limits are based on 12,129 individual aircraft observed in level flight during the data collection and are plotted in figure 9. The symbol —●— shows the height of each histogram rectangle and the shaded area about that height shows the computed 95 percent limits. This figure demonstrates a high degree of confidence with respect to the histogram core ($\leq 5\ \sigma$ or 300 feet), and a low degree of confidence with respect to the histogram tail. Constant confidence level height, as displayed beyond 500-foot deviations, is due to the limited sample size. Hence, caution must be exercised in making deductions based on these histogram class interval heights. Finally, this figure clearly demonstrates that the fluctuations of the time histogram for large deviations may very likely be the result of small sample size.

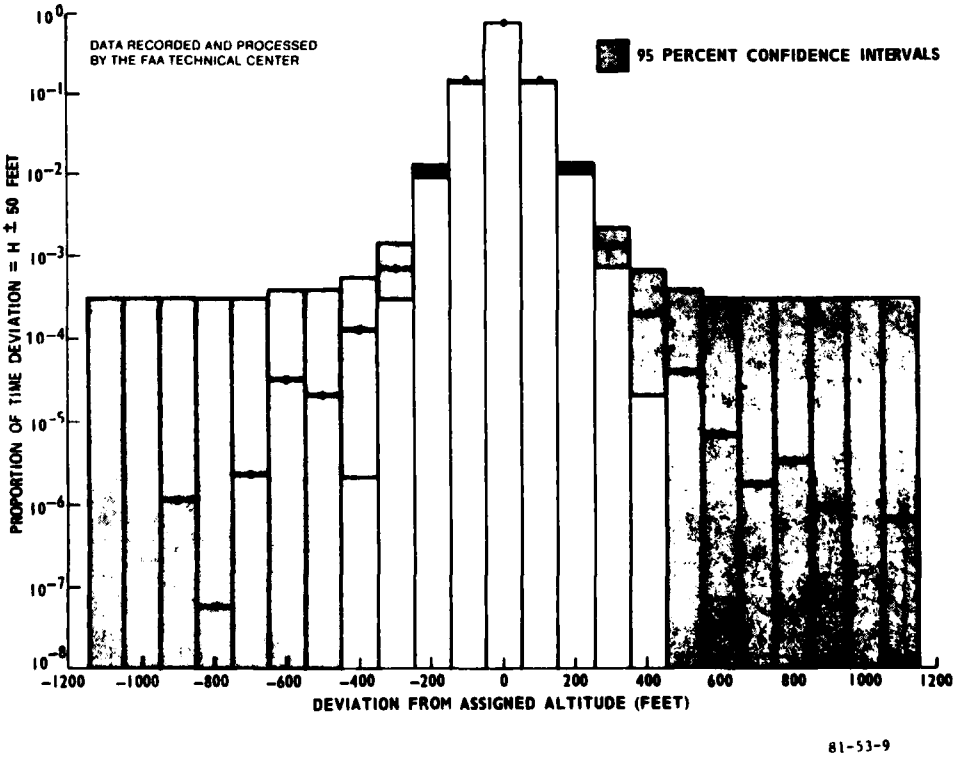

FIGURE 9. AGGREGATE MODE C ALTITUDE TIME HISTOGRAM WITH 95 PERCENT CONFIDENCE INTERVALS

MODEL DISTRIBUTION ESTIMATION TECHNIQUE.

Whenever empirical data are gathered and ordered into a histogram form, the next step is usually an attempt at representation by an analytical model. It provides a parsimonious method of describing the information obtained, is repeatable and establishes a means whereby others can generate similar models and analytically study the problem at hand. Further, unless one is willing to put bounds on maximum errors, their range of possible values usually approaches infinity. This implies that it would require an infinite quantity of data to truly represent the distribution — an impossible task. The preferred method is to collect a sufficient quantity of data so that a reasonable amount of confidence is obtained over the range of major interest. In the case for vertical FTE, this range would be from -2,000 to 2,000 feet. As is demonstrated in figure 9, this data collection did provide reasonable confidence on values ranging from -400 to 400 feet. However, it would have been desirable to collect more data so that more information on the frequency of errors ranging from 500 to 2,000 feet would be obtained. Lacking this information, it would seem reasonable that the true distribution would follow the sparse histogram data in a smooth and consistent manner. Finally, there exists a limit to the range of values in any data set, and it is sometimes necessary to provide frequency estimates of errors beyond those represented in the empirical data. This can only be accomplished through the use of an appropriately fitted model.

A few words of caution. Any model chosen to represent empirical data is a summary. Hence, the estimates generated by utilizing even an appropriate model does not decrease the confidence interval originally estimated for the histogram. Only a larger data collection can accomplish that goal.

The time histogram shown in figure 8 was fit to six distribution models via a modified maximum likelihood procedure. They were normal, double-exponential, double-double exponential, power-exponential, generalized "t" and power-double exponential distributions. The first five distributions and the maximum likelihood algorithm were programed for the lateral separation study under the direction of Professor Neil Polhemus at Princeton University. The power-double exponential distribution was defined and programed during the vertical study. Each distribution is explicity transcribed in appendix D.

Before the method of maximum likelihood could be applied to the time histogram data, it required modification for two reasons. First, it assumed that the number of samples within each class interval were known; and second, it assumed that the data were grouped into small class intervals. The first problem was solved by modifying the algorithm so it required only the relative frequency of samples within each class interval, and the second problem was solved by integrating each distribution model over the 100-foot class intervals of interest. A complete description of the modified maximum likelihood algorithm is given in appendix E. Each model estimate is demonstrated by the relative frequency histograms shown in figures 10 to 15. At the upper right-hand corner of each figure is the estimated standard deviation, kurtosis, and logarithm modified maximum likelihood value. Directly under these variables are each distribution's parameters as defined in appendix D. The mean and skewness for each distribution are not given since the models were structured symmetical about zero (appendix D). The standard deviation estimates range from a low value of 55 feet, for a normal distribution, to a high value 57.23, for a double-double exponential, with most estimates grouping about

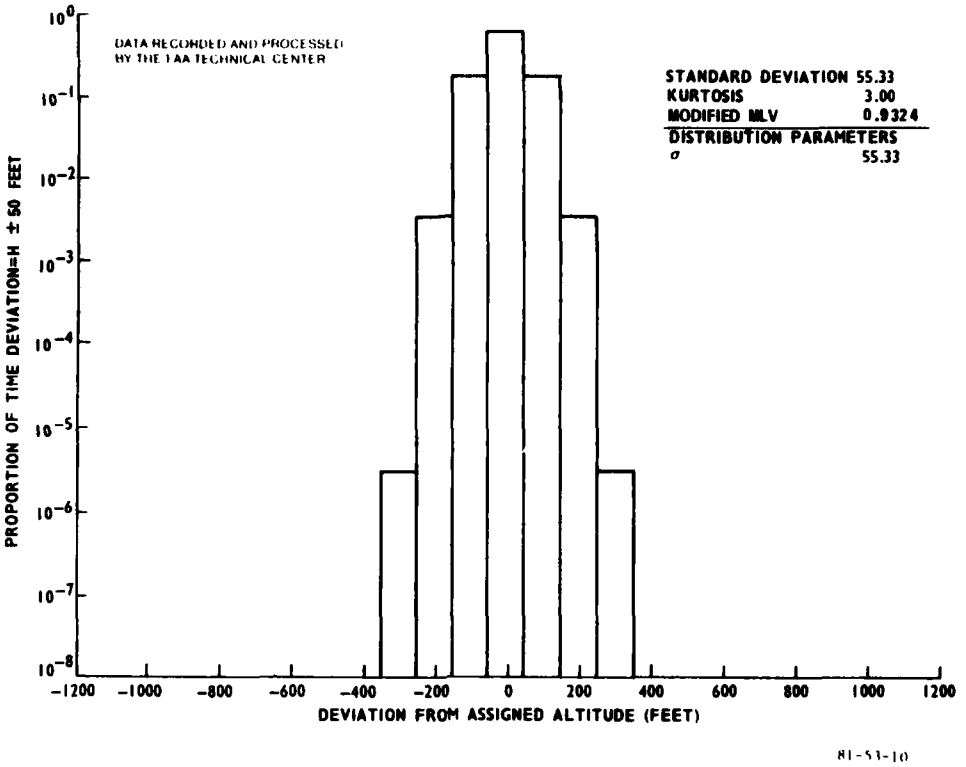

FIGURE 10. NORMAL DISTRIBUTION MODEL ESTIMATE

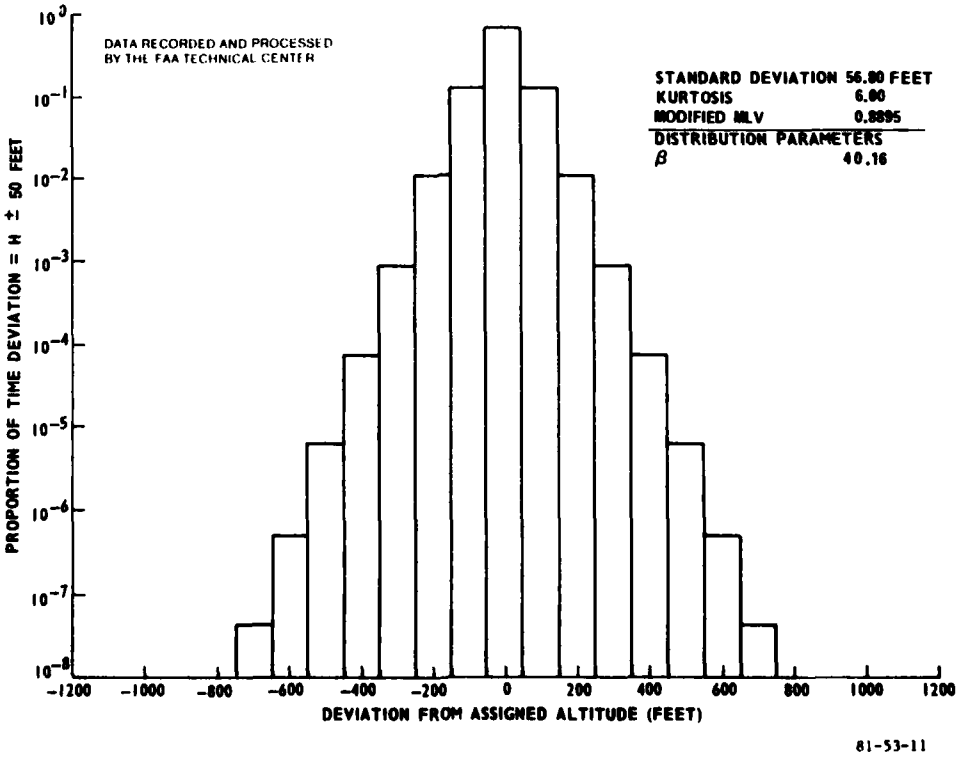

FIGURE 11. DOUBLE-EXPONENTIAL MODEL ESTIMATE

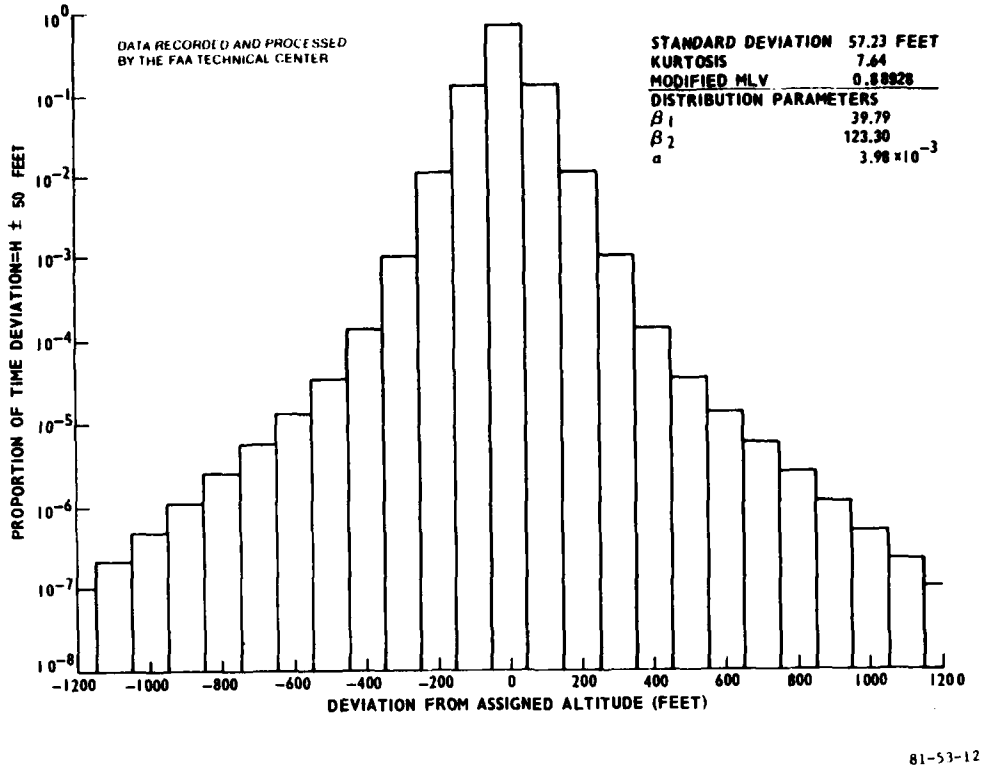

FIGURE 12. DOUBLE-DOUBLE EXPONENTIAL MODEL ESTIMATE

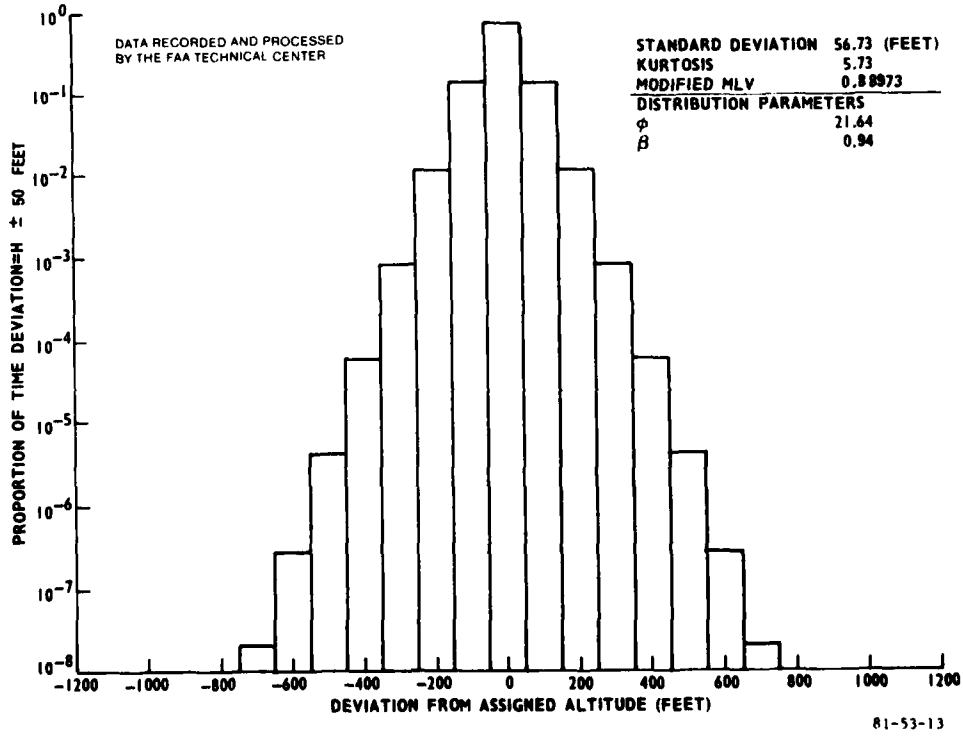

FIGURE 13. POWER-EXPONENTIAL MODEL ESTIMATE

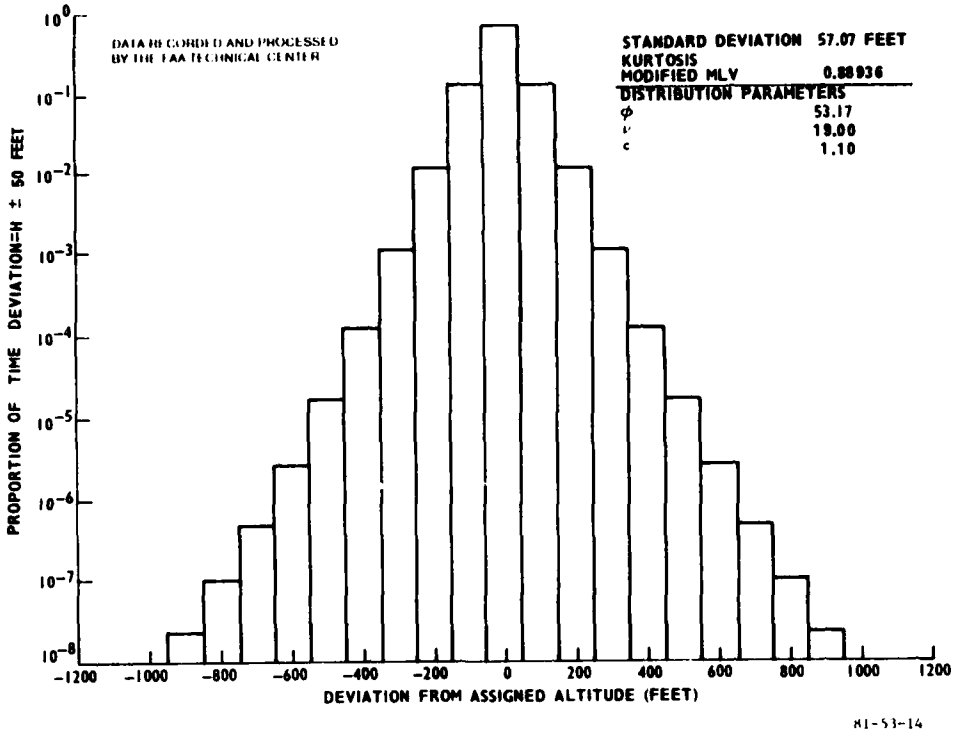

FIGURE 14. GENERALIZED t MODEL ESTIMATE

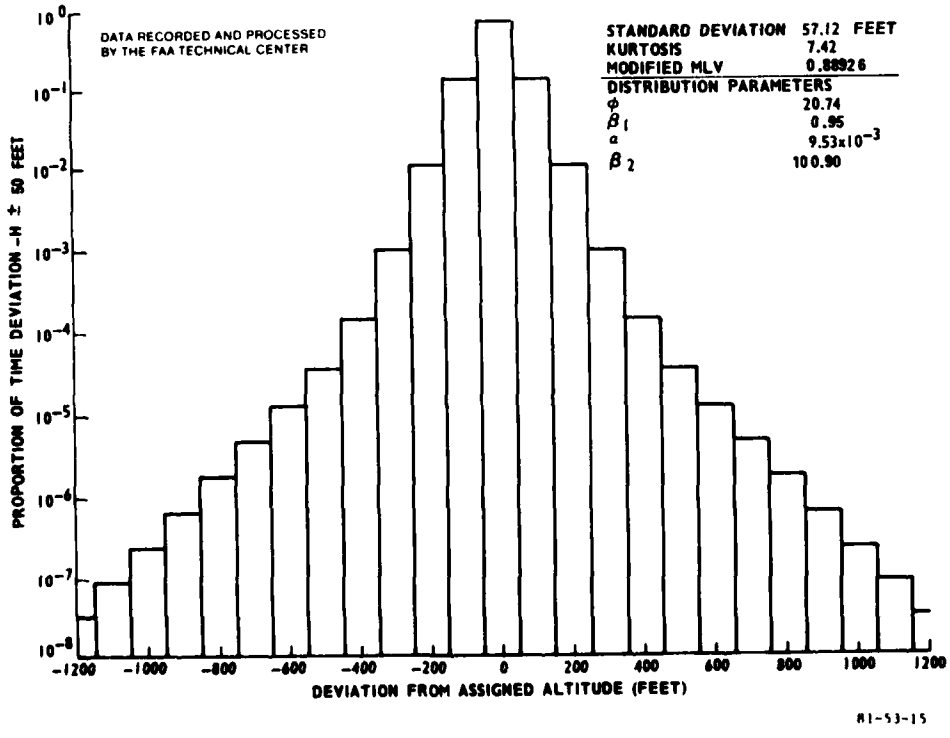

FIGURE 15. POWER-DOUBLE EXPONENTIAL MODEL ESTIMATE

57 feet. Note that the standard deviation of the 100-foot class interval histogram data was 61 feet. This implies that the distortion of quantization on estimating the standard deviation is approximately 4 feet. The modified maximum likelihood natural logarithm value is largest for a normal distribution at 0.9324 and smallest for a power-double exponential distribution at 0.88926 with the double-double exponential distribution only slightly higher at 0.88928. This implies that the power-double exponential distribution provides the closest fit to the empirical data. Recalling the empirical histogram structure (figure 8), it is apparent that a normal distribution grossly underestimates the proportion of errors greater than 100 feet. When compared to figure 9, it is clearly outside most 95 percent confidence limits. The double-exponential and power-exponential distributions are much better models. However, when compared to figure 8, they appear to underestimate the proportion of errors greater than 400 feet. The generalized t distribution is a better model. Still, it appears to underestimate the proportion of errors greater than 600 feet. The double-double exponential and power-double exponential seem to appropriately model the empirical data. However, it now becomes difficult to distinguish each model's goodness of fit, and it would be propitious to have a quantitative goodness-of-fit measure.

Chi-square and Kalmagorov-Smirnov (K-S) tests were implemented by assuming no less than 5 minutes of data within each class interval and using the 12,129 individual aircraft observations as a lower-bound estimate for the number of independent samples. They were applied to each distribution model at the 90 percent confidence level. The normal distribution failed both tests. Since this distribution was also outside most 95 percent histogram limits, it was considered an inappropriate representation of the empirical data and will not be used for further analysis. The power-exponential failed the chi-square test and passed the K-S test. All other distribution passed both tests. Hence, standard statistical procedures provided little insight into model choice for those distributions with similar cores and different tail shapes.

Since the area of major interest in model building for assessing vertical deviations to examine vertical separation standards is in the proportion of large errors, the difference between the log of both the empirical and model histograms were computed and plotted in figures 16 to 20. A positive value represents model underfit. The sample mean and standard deviation of the residuals corresponding 500-foot or greater mode C altitude deviations for each figure are shown in the upper right-hand corner. A model that represents a good fit should have a mean zero, a relatively small variance, and no distinguishable trend. The double-exponential, power-exponential, and generalized t distributions each demonstrate a positive trend as the deviation increases (indicating increased underfit as a function of altitude deviation), have nonzero positive means (indicating that they generally underfit the empirical data), and have relatively large variances. These measures of mean, variance, and trend become generally smaller as the distribution models become more generalized. For example, the power-exponential had a mean and standard deviation of 2.57 and 1.58, respectively, and the generalized t had a mean and standard deviation of 0.95 and 0.81, respectively. All three of the above distributions apparently underfit the empirical tails. On the other hand, double-double and power-double exponential distributions both provide apparently good tail fits. For the latter two distributions, the 500-foot or greater mode C altitude residuals have near-zero mean and no apparent trend (i.e. they exhibit the characteristics of white noise).

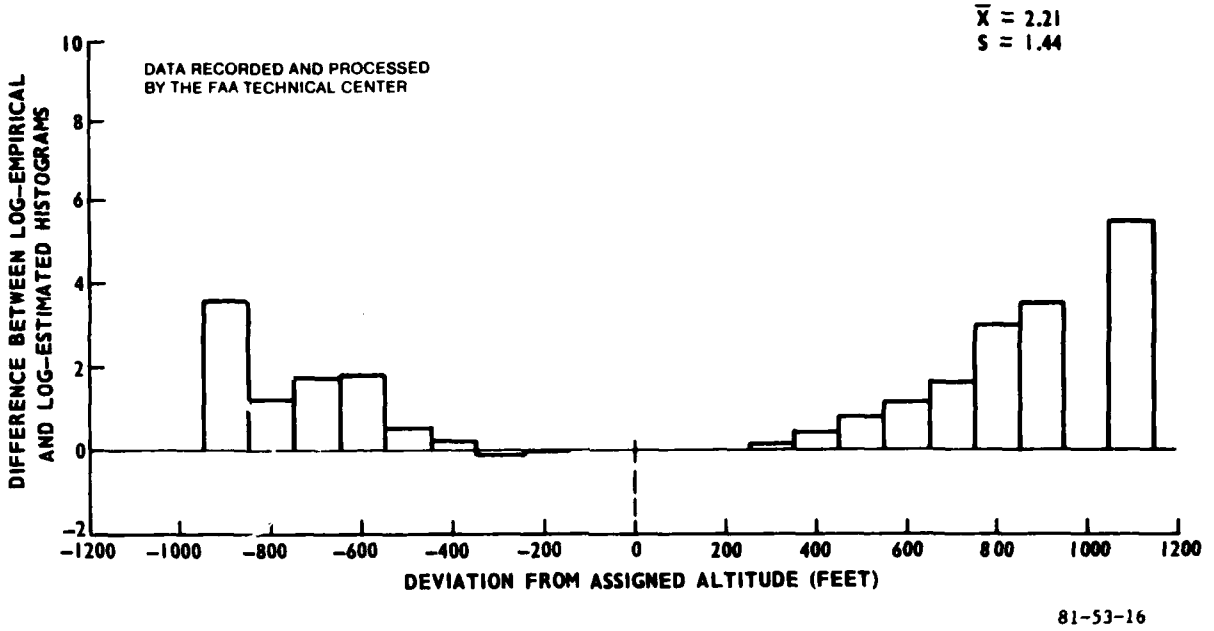

FIGURE 16. DOUBLE-EXPONENTIAL LOGARITHM RESIDUALS

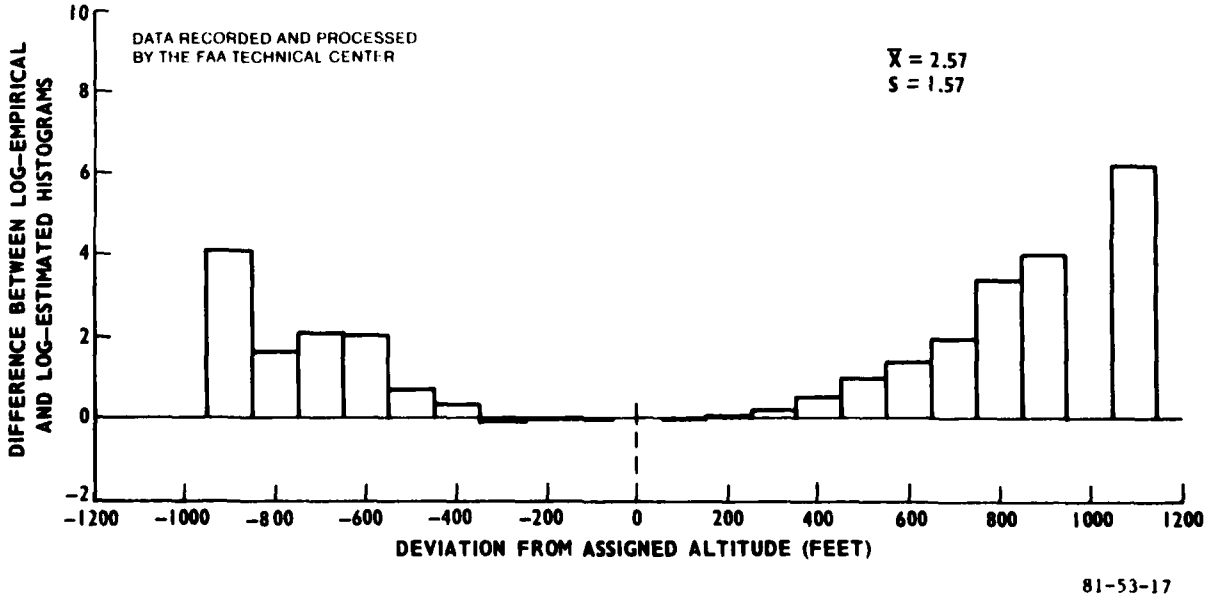

FIGURE 17. POWER-EXPONENTIAL LOGARITHM RESIDUALS

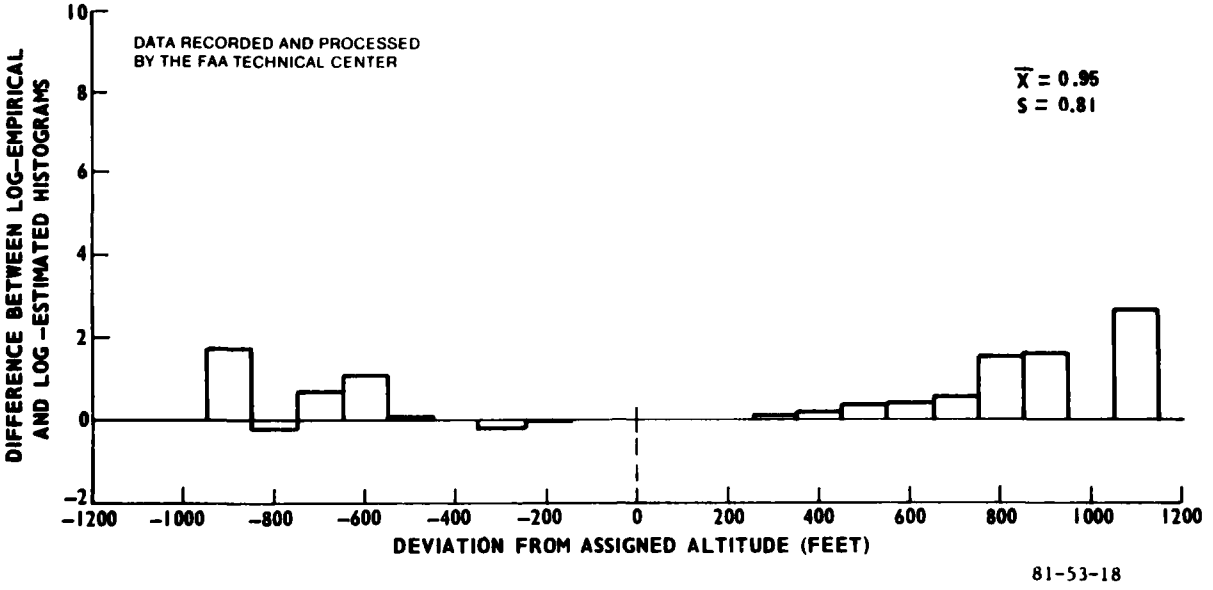

FIGURE 18. GENRALIZED t LOGARITHM RESIDUALS

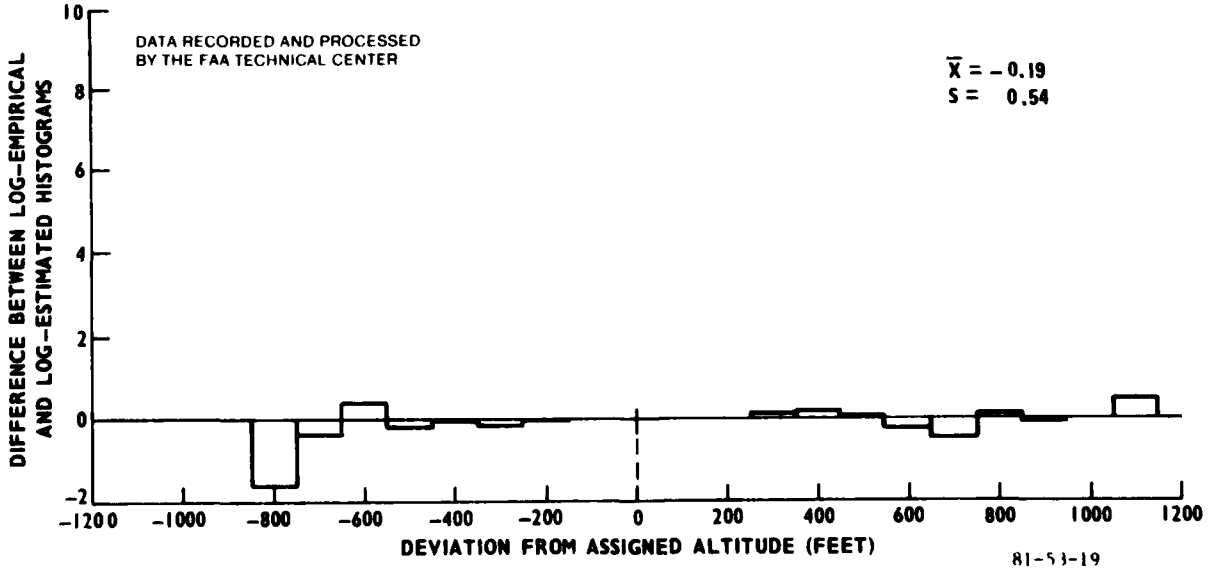

FIGURE 19. DOUBLE-DOUBLE EXPONENTIAL LOGARITHM RESIDUALS

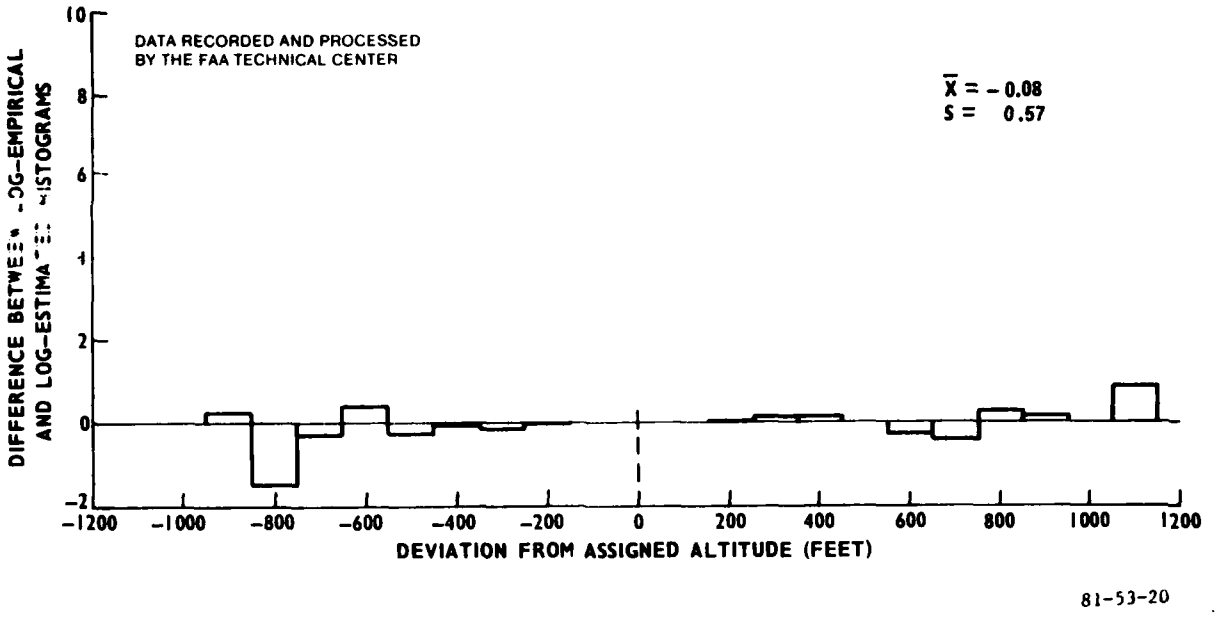

FIGURE 20. POWER-DOUBLE EXPONENTIAL LOGARITHM RESIDUALS

Since the residual mean of a good model is expected to be zero, a two-sided t test was constructed. The hypothesis of this test is that the residuals are normally distributed with mean zero. The t-values are given in table 5 for each model. If the mean is equal to zero, the probability that the t-values fall between -2.093 and 2.093 is 0.95 for 19 degrees of freedom. The double exponential, power-exponential and generalized t distributions fail this test, the hypothesis that the mean is equal to zero is rejected, and these distributions are considered inappropriate in modelling the proportion of mode C deviations greater than or equal to 500 feet. The double-double exponential and power-double exponential distribution pass the t-test, and the hypothesis that the mean is equal to zero is accepted. Due to the structure of the latter two distributions (weighted exponential tail), it was anticipated that each would fit the tail data in a similar manner. However, since the power-exponential distribution is a generalization of the double-exponential distribution, the former should more appropriately model the distribution core. Otherwise, the double-exponential is a more parsimonious model.

TABLE 5. T-TEST FOR ZERO MEAN

Model	t - Value
1. Double-exponential	4.85
2. Power-exponential	5.13
3. Generalized t	3.70
4. Double-double exponential	-1.12
5. Power-double exponential	-0.44

To evaluate the distribution cores more closely, the absolute value of the difference between the empirical and estimated distribution was computed and plotted in figures 21 and 22. The means and standard deviations are again shown in the upper left-hand corner. Figure 21 demonstrates that the double-double exponential is too peaked at zero deviation (overfits the data in this class interval) and falls off too rapidly in the next 100 feet (underfits the data in this class interval). Figure 22 demonstrates the appropriateness of the power-double exponential core with a standard deviation three orders of magnitude less than the double-double exponential. Still, it can be argued that the power-double exponential is an unnecessary overparamaterization, and the double-double exponential is sufficient. The end toward which each effort is directed should be the deciding factor in chosing a model. If the purpose is to study results related to the proportion of errors in the tails, then the double-double exponential may be appropriate. If the purpose is to study results related to the proportion of errors in both the core and tails, then the power-double exponential may be required.

QUANTIZATION. Throughout this analysis, no mention was made concerning the effect quantization has on estimating the distribution parameters and moments, except for the note of an increased standard deviation. To assess quantization, the proportion of errors in each 100-foot class interval was computed by integrating each distribution models density function as estimated by the modified maximum likelihood (MML) technique. This was performed for class intervals ranging from -2,000 to 2,000 feet. These proportions were converted to estimated time observed in each class interval. The first four moments about the origin, the standard deviation, and the kurtosis were computed. Assuming a given model was an appropriate fit, these statistical parameters should match those of the empirical histogram. When, and if, the model is found that produces this match, the effect of quantization on the estimated parameters can be evaluated. From table 6, it can be seen that each distribution modeled provides a reasonable estimate of the second moment. The standard deviation about the origin is equal to the square root of the second moment. The fourth moment is underestimated by all models except the double-double and power-double exponential distribution. It has already been shown that the double-double exponential is too peaked at the origin (figure 21). This results in a high estimate of kurtosis (kurtosis about the origin equals fourth moment about the origin divided by the squared second moment about the origin). The power-double exponential produces the best match of second and fourth moments and necessarily standard deviation and kurtosis. By assuming the power-double exponential to be the model that produces a match between the estimated empirical parameters and the estimated model parameters, the effect quantization has on estimating standard deviation and kurtosis was evaluated by computing the model's quantized and nonquantized parameters (figure 15). For reading continuity the standard deviation, kurtosis, second and fourth moments, and their differences are given in table 7. Notice that quantization increases the model standard deviation and decreases model kurtosis. Since it is well known that quantization increases both the second and fourth moment (reference 8), this result is apparently inconsistent. However, upon examining the differences between modeled and quantized moments, it is observed that quantization increases the second moment squared by 32 percent, and the fourth moment by 23 percent. This causes the ratio to decrease.

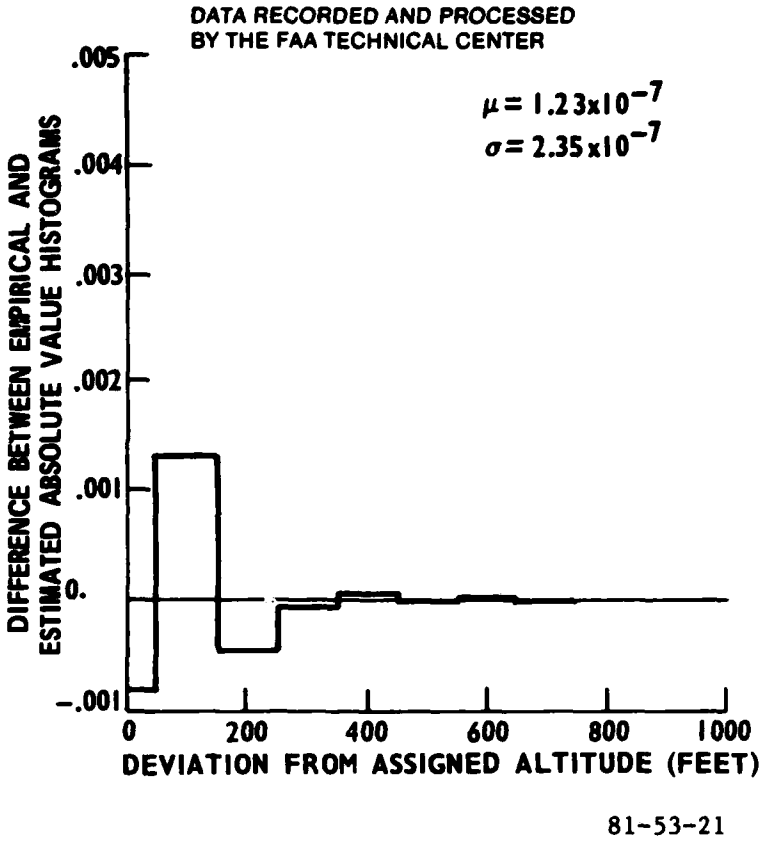

FIGURE 21. DOUBLE-DOUBLE EXPONENTIAL ABSOLUTE RESIDUALS

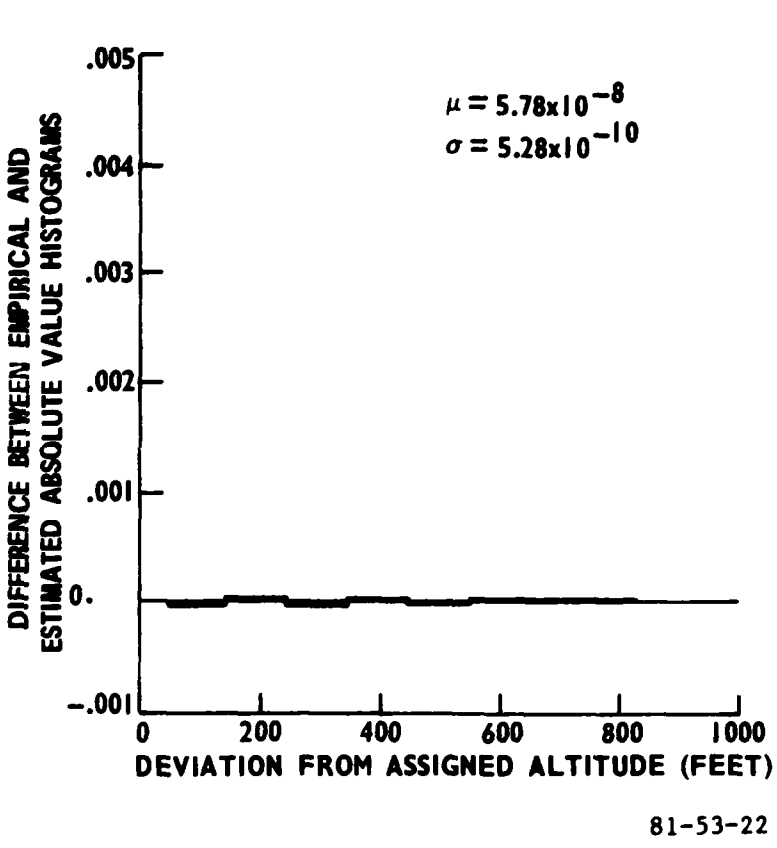

FIGURE 22. POWER-DOUBLE EXPONENTIAL ABSOLUTE RESIDUALS

TABLE 6. PARAMETERS OF QUANTIZED MODEL DISTRIBUTION

Modeled Histograms (Quantized into 100-ft. intervals)	Second Moment	Fourth Moment	Kurtosis
Empirical	3.746×10^3	97.65×10^6	6.96
Normal	3.863×10^3	46.72×10^6	3.13
Double-exponential	3.718×10^3	80.95×10^3	5.88
Power-exponential	3.714×10^3	77.89×10^6	5.648
Generalized t	3.740×10^3	87.71×10^6	6.269
Double-double Exponential	3.754×10^3	100.8×10^6	7.153
Power-double exponential	3.746×10^3	97.72×10^6	6.96

TABLE 7. QUANTIZED VERSUS MAXIMUM LIKELIHOOD PARAMETERS OF THE POWER-DOUBLE EXPONENTIAL

	Second Moment μ_2	Second Moment Squared μ_2^2	Fourth Moment μ_4	Standard Deviation (ft) $\sqrt{\mu_2}$	Kurtosis $\frac{\mu_4}{\mu_2^2}$
Quantized Power-double exponential	3.746×10^3	14.1×10^6	97.72×10^6	61.2	6.96
Maximum Likelihood Power-double exponential	3.263×10^3	10.65×10^6	79.0×10^6	57.1	7.42
Difference	0.483×10^3	3.45×10^6	18.72×10^6	4.1	-0.46

This does not imply that if the data were structured differently (for example, exponential), that quantization would have the same effect. Rather, it implies that the empirical data must be appropriately modeled before quantization can be evaluated.

Throughout the previous discussion, it was also assumed that the MML technique was not affected by 100-foot quantization. That is, given that the true distribution of errors were quantized into 100-foot intervals and the MML technique applied to this histogram, the result would lead back to the true distribution parameters. The preceding procedure was implemented using the power-double exponential as the true distribution. The MML technique converged to the same set of parameters given in table 7 demonstrating that 100-foot quantization did not distort the model estimate. Since the power-double exponential is a qeneralization of the double-double exponential, the normal-double exponential, the power-exponential, the double-exponential, and the normal distribution, the results hold true for this entire class of distributions. This completes the procedure for estimating vertical FTE through the use of mode C altitude data. The reader is cautioned that this procedure is only as reliable as the collected data, and although a methodology has been established to model vertical FTE, the result is subject to the same uncertainties present in the empirical data. This is demonstrated more fully by overlaying the 95 percent confidence limits about the absolute values of the mode C altitude cumulative empirical data on the estimated absolute values of the cumulative power-double exponential model distribution. The results are shown in figure 23. Hence, although the model distribution computed in this analysis is the only relatively current representation of vertical FTE over CONUS, it must be verified by a more extensive data collection. It is felt that the 4,904 hours of data collected during this study are not sufficient to properly characterize the distribution of FTE, and that at least 10,000 hours of mode C altitude data must be gathered in a data collection structured for the vertical domain before a high degree of confidence can be attributed to the distribution model of FTE's.

PROBABILITY OF OVERLAP. The ultimate goal of modeling the time histogram was to obtain an estimate of the probability of vertical FTE overlap at high altitudes over CONUS for 1,000- and 1,500-foot aircraft separation. Due to the high uncertainty associated with the model distribution, as well as not being able to account for errors in the linkage system, it was felt inappropriate to compute the associated probability of vertical FTE overlap. However, a double numerical integration was computer programed during the course of this study. Explicitly, probability of vertical FTE overlap was computed by using the following equation:

$$\int_{-1500}^{1500} f(\bar{\theta}, y) \left[\int_{y-h}^{y+h} f(\bar{\theta}, x - S)\, dx \right] dy$$

Where $f(\bar{\theta}, x)$ is the vertical FTE model distribution, $\bar{\theta}$ is the parameter vector, S is aircraft separation, and h is average aircraft height. This procedure, although established and verified, was not implemented.

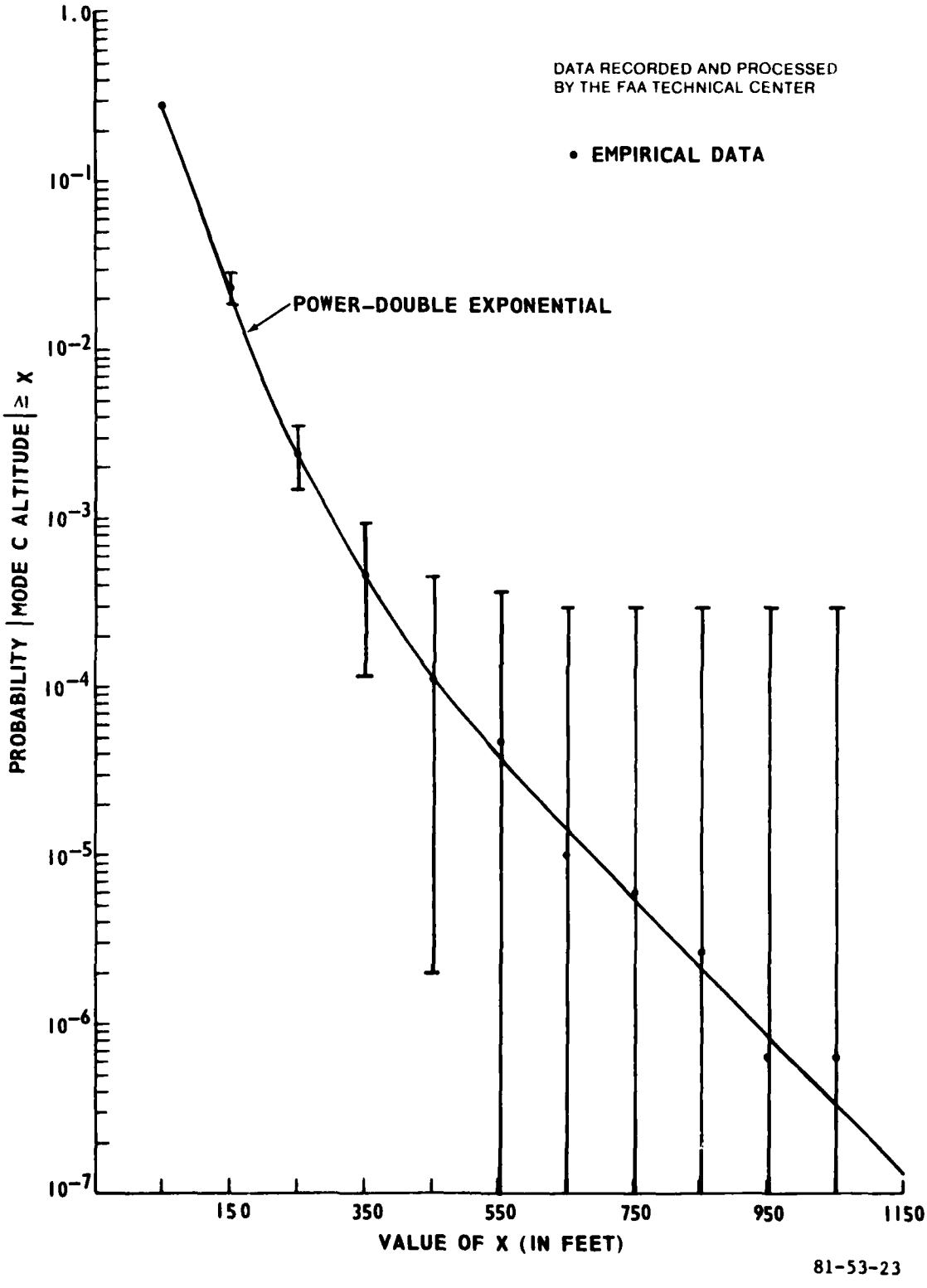

FIGURE 23. POWER-DOUBLE EXPONENTIAL TIME HISTOGRAM WITH 95 PERCENT CONFIDENCE INTERVALS

ATTRIBUTE DATA.

The analysis presented in the previous sections focused on the aggregate distribution of mode C altitude errors. Another aspect of the collected data that requires examination is the number of aircraft that exhibit a particular attribute, for instance, the quantity of B-727 observed. This type of information was readily available through the supplementary data described in table 4. Further, it was decided to relate this information to altitude performance by recording whether a 300-foot or greater deviation occurred during each aircraft's level-flight profile. The attributes examined were en route center, jet-route, aircraft type, aircraft user, direction of travel, level altitude segment, aircraft speed, aircraft weight, and level-flight time (figure 24 to 34). For each figure, the log of the total number of aircraft observed along with the log of the number of aircraft observed with a 300-foot or greater mode C altitude deviation is plotted on bargraphs. The log scaling was chosen in order to more easily compare those events that occurred frequently with those that occurred infrequently. The unshaded bar height is the aircraft frequency log, and the shaded bar height is the 300-foot or greater frequency log. The symbol —●— across each bar represents the expected number of 300-foot or greater mode C deviations (computed by multiplying the number of aircraft contained within a given bar height by the ratio of the aggregate number of 300-foot or greater deviation over the total number of aircraft observed), and the left-most ordinate displays the percentage scale. For example, in figure 24, the aircraft frequency log on route J146 is 3.252, which indicates 1,786 aircraft (14.7 percent of total aircraft count) were observed on this route. The respective 300-foot or greater frequency log is 1.04 indicating 11 aircraft on route J146 were observed with a 300-foot or greater mode C altitude deviation. The expected value is 1.87 indicating that, on the average, 74 of the 1,786 aircraft on route J146 were expected to exhibit a 300-foot or greater mode C altitude deviation. For observed frequencies less than or equal to one, bar height is zero.

ROUTES. The routes most frequently traveled are plotted to the left of the graph and are coidentified by en route center (figure 24). The majority of aircraft were observed on routes J146, J4, J80, and J60. The number of aircraft on the remaining routes decreases gradually with route J72 containing the least amount (35 aircraft). On routes J4, J2, J6, J50, and J72, the observed frequency of 300-foot or greater errors was greater than expected. All these routes are over the Albuquerque en route center.

DIRECTION. The number of aircraft traveling east and west is nearly equal at 5,699 and 6,430, respectively (figure 25). The observed and expected frequencies of 300-foot or greater errors in both directions are also nearly equal. No aircraft were observed traveling north or south. This figure is representative of an attribute that does not exhibit any unusual characteristics and apparently does not relate to mode C altitude deviations.

SPEED. Figure 26 displays aircraft ground speed in 50-knot class intervals ranging from 100 to 700 knots. It indicates that the majority of aircraft observed traveled between 350 and 550 knots, and the aircraft count within these speeds is bimodal. That is, less aircraft were observed in the 450- and 500-knot class interval than in either adjacent intervals. This is apparently due to the prevailing winds, since 83 percent of the aircraft heading west were traveling between 350 and 450 knots, and 80 percent of the aircraft heading east were travelling between 450 and 550 knots (figures 27 and 28). These figures indicated that if the attribute of airspeed, rather than ground speed, was available during this data collection, it would have resulted in a similar pattern for both east and west traffic.

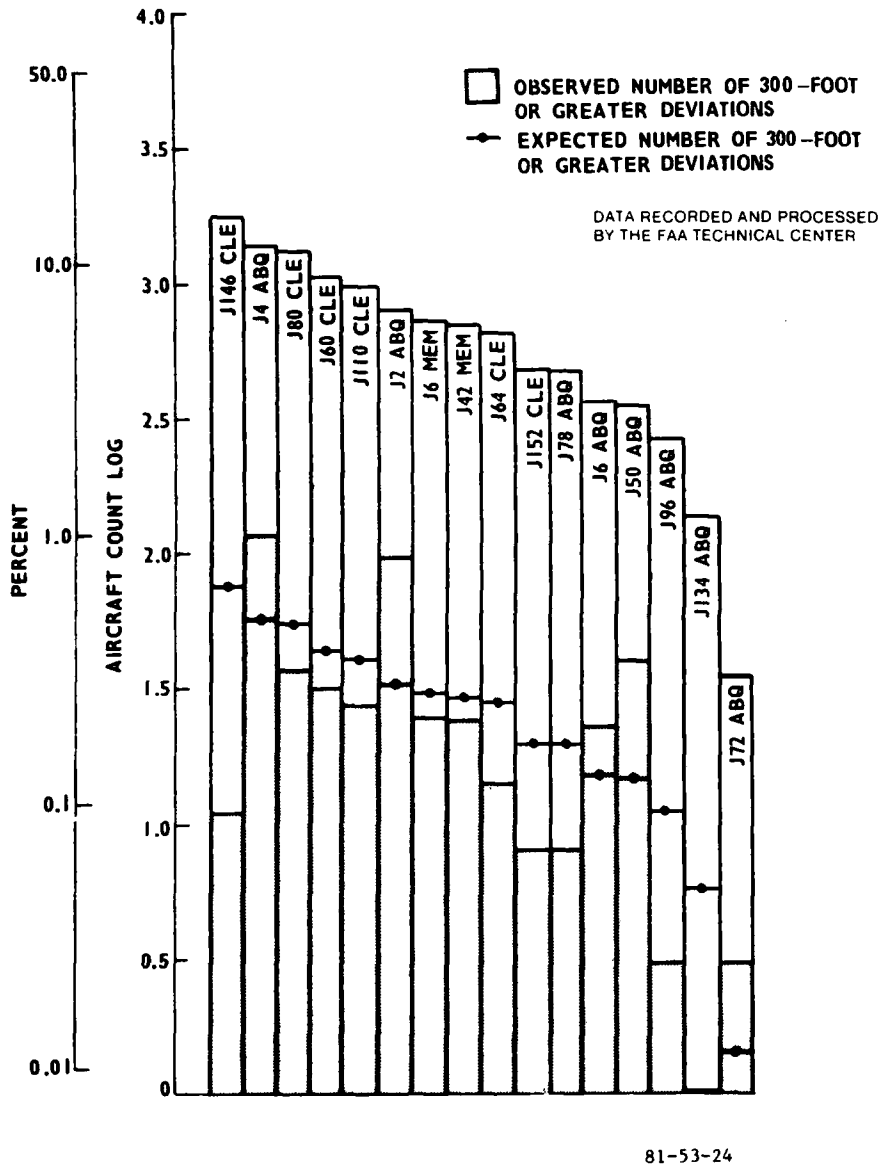

FIGURE 24. NUMBER OF AIRCRAFT PER ROUTE

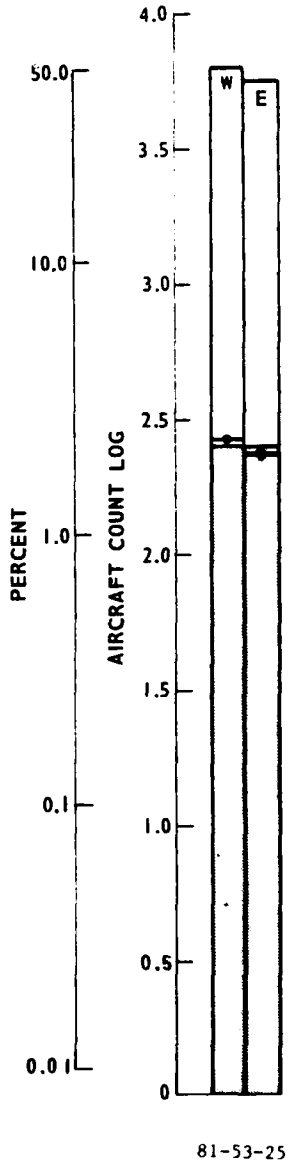

FIGURE 25. NUMBER OF AIRCRAFT PER DIRECTION

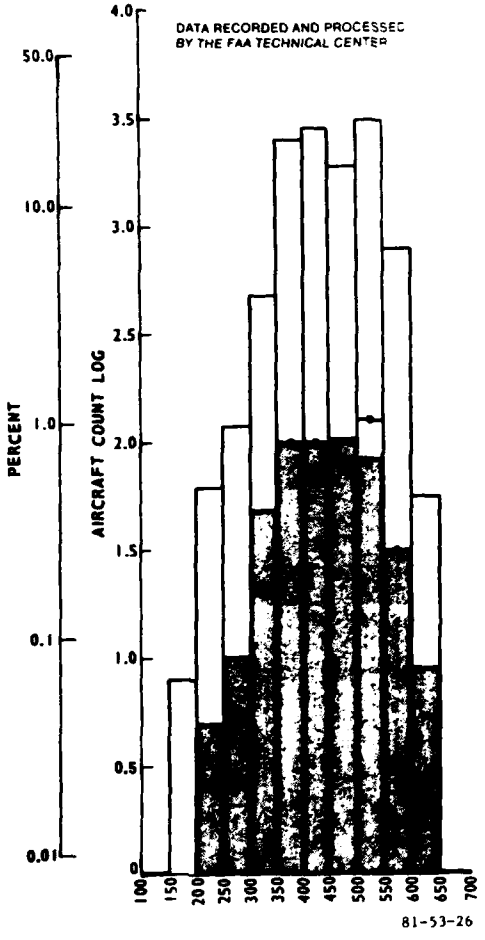

FIGURE 26. NUMBER OF AIRCRAFT AT 50-KNOT SPEED INTERVALS

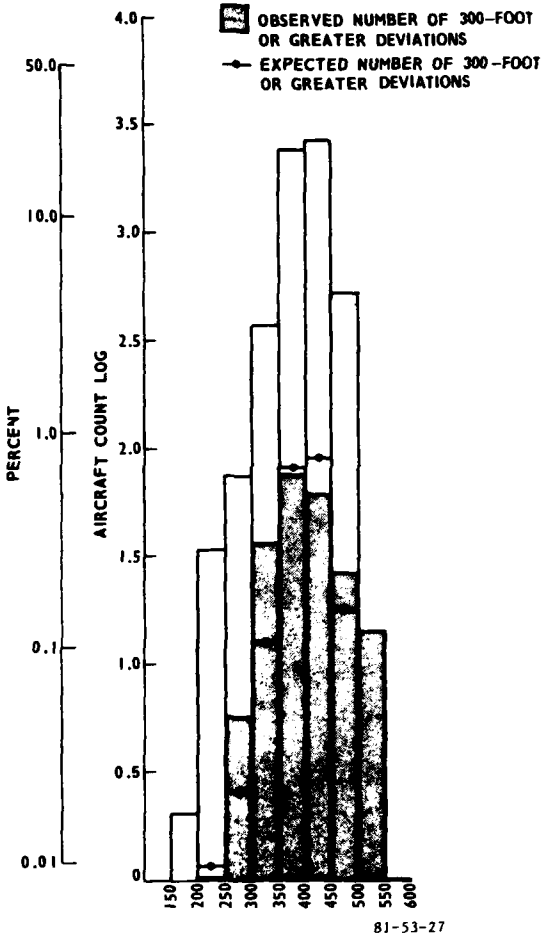

FIGURE 27. NUMBER OF AIRCRAFT AT 50-KNOT INTERVALS GOING WEST

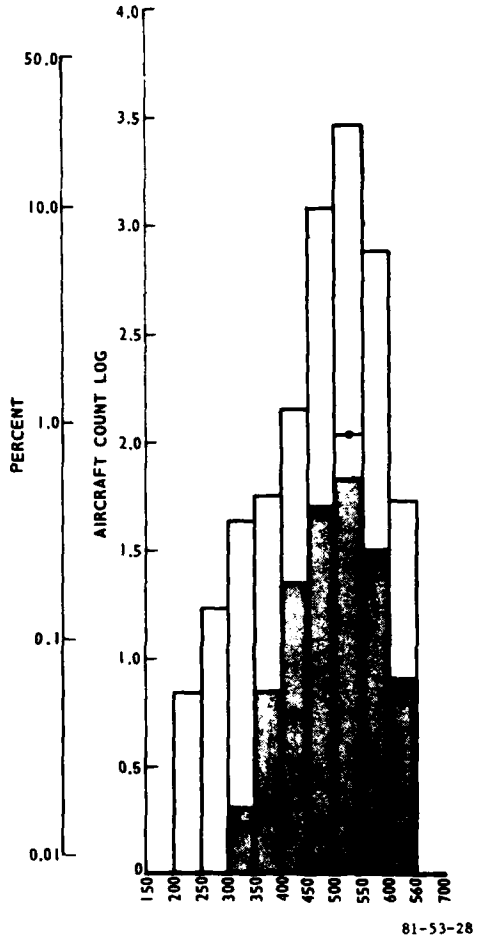

FIGURE 28. NUMBER OF AIRCRAFT AT 50-KNOT INTERVALS GOING EAST

Referring once again to figure 26, the number of 300-foot or greater errors is generally greater than expected for speeds less than 350 knots or greater than 600 knots. On aircraft headed west and east, the number of 300-foot or greater errors is larger than expected for speeds less than 350 knots or greater than 450 knots and less than 450 knots or greater than 600 knots, respectively. The distribution of speed is asymmetrical, with the number of aircraft at lower speeds decreasing less gradually than the number of aircraft at higher speeds.

AIRCRAFT USER. The number of commercial, general aviation, military, and unknown aircraft observed were 9,420, 1,683, 995, and 31, respectively (figure 29). Unknown aircraft are those indentified with foreign origin. Seventy-eight percent of the aircraft were commercial. The aircraft with 300-foot or greater errors were less than expected for commercial aircraft and greater than expected for general aviation, military, and unknown aircraft.

EN ROUTE CENTER. The number of aircraft observed at the en route centers of Cleveland, Memphis, and Albuquerque were 6,476, 3,851, and 1,802, respectively (figure 30). The majority of aircraft were observed over Cleveland. The observed number of aircraft with 300-foot or greater errors was less than expected for Cleveland, more than expected for Albuquerque, and nearly as expected for Memphis.

AIRCRAFT TYPE. Figure 31 displays the number of aircraft for a given type. There were 99 different aircraft types observed. Those observed at least 30 times are plotted in figure 28. Aircraft type B-727 is the most dominate and represents 47 percent of the observed aircraft. There were 43 aircraft types with more than the expected number of 300-foot or greater errors. Fifteen are plotted in figure 31.

AIRCRAFT WEIGHT. Aircrafts weights were divided into five categories, as defined in table 8. Small- and heavy-weight classes were obtained from the Federal Aviation Administration (FAA) Contractor's Handbook (reference 9). Weight A class interval was obtained from FAA Advisory Circular (reference 10), and weights B and C class intervals were chosen by the author. For each aircraft type, the minimum and maximum takeoff weights, as given in "Jane's All the World Aircraft" encyclopedia, were tabulated and the corresponding weight class designated (appendix F).

The object of subclassifying aircraft weights was to define a class interval for the large number of aircraft less than 300,000 pounds and still relatively heavy, and the large number of aircraft greater than 12,500 pounds and still relatively light (figure 32). As expected, weight category C contains almost 50 percent of the aircraft (B-727's are within this weight class interval), and weight category S contains the least number of aircraft (not many aircraft less than 12,500 pounds can maintain altitudes of 24,000 feet and above). Weight category A contains more aircraft than either B or S. The observed frequency of errors greater than 300 feet was more than expected for the two smallest weight class designations A and S.

FLIGHT LEVELS. The number of aircraft observed at and above flight level 240 are displayed in figure 33. It indicates that 80 percent were observed at or between flight levels 310 to 390. The uppermost flight level observed was 470.

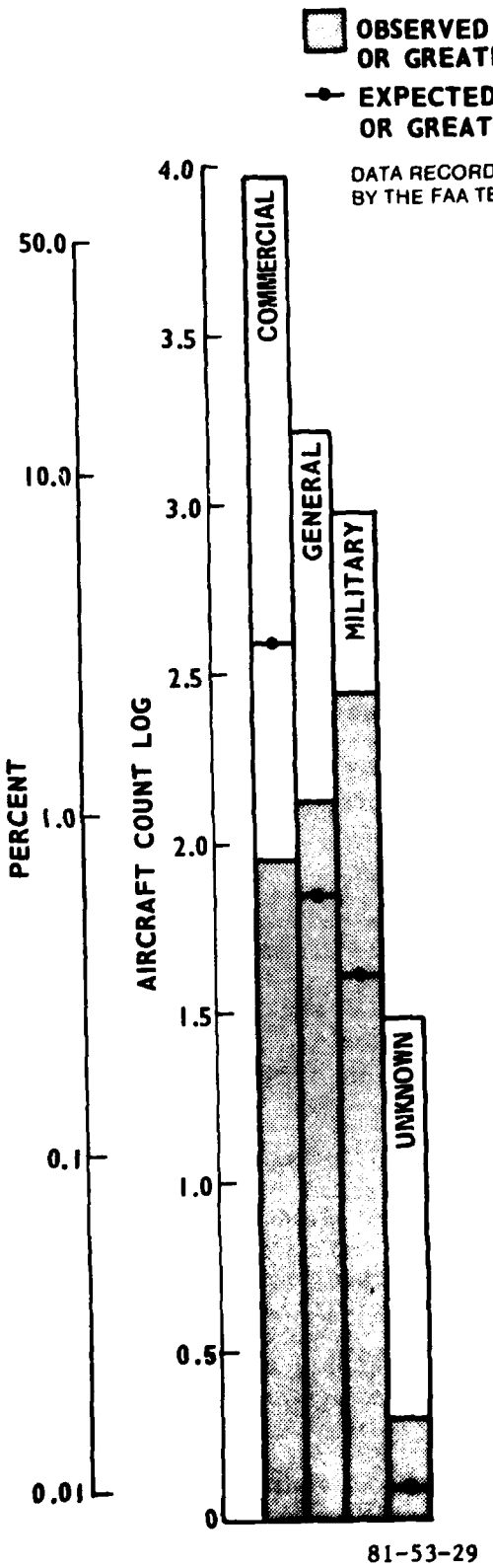

FIGURE 29. NUMBER OF AIRCRAFT PER USER

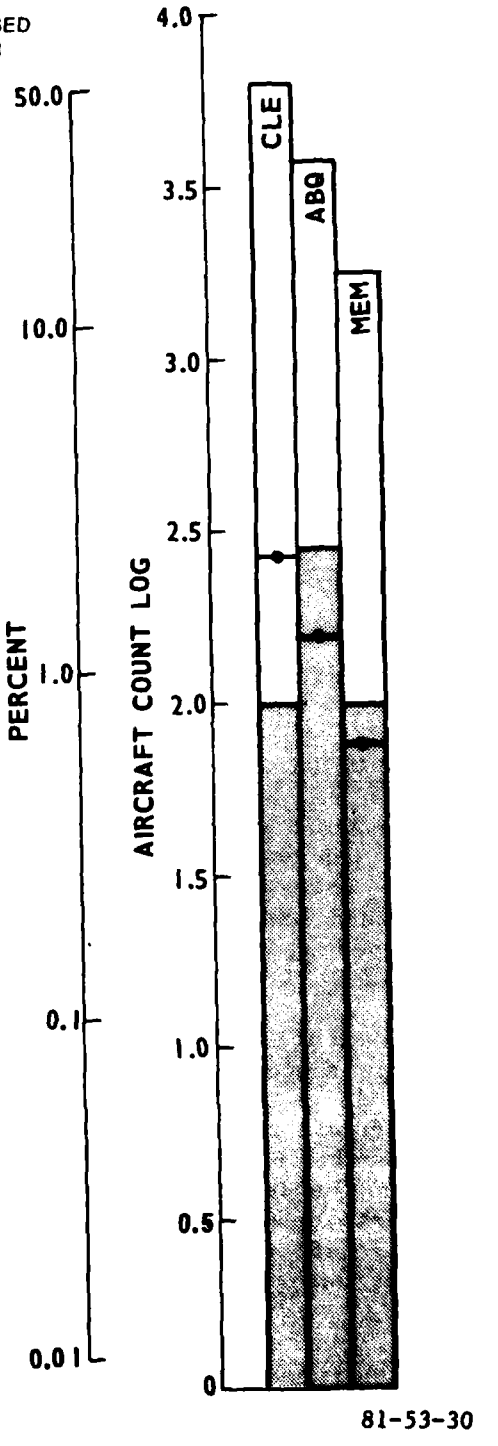

FIGURE 30. NUMBER OF AIRCRAFT PER EN ROUTE CENTER

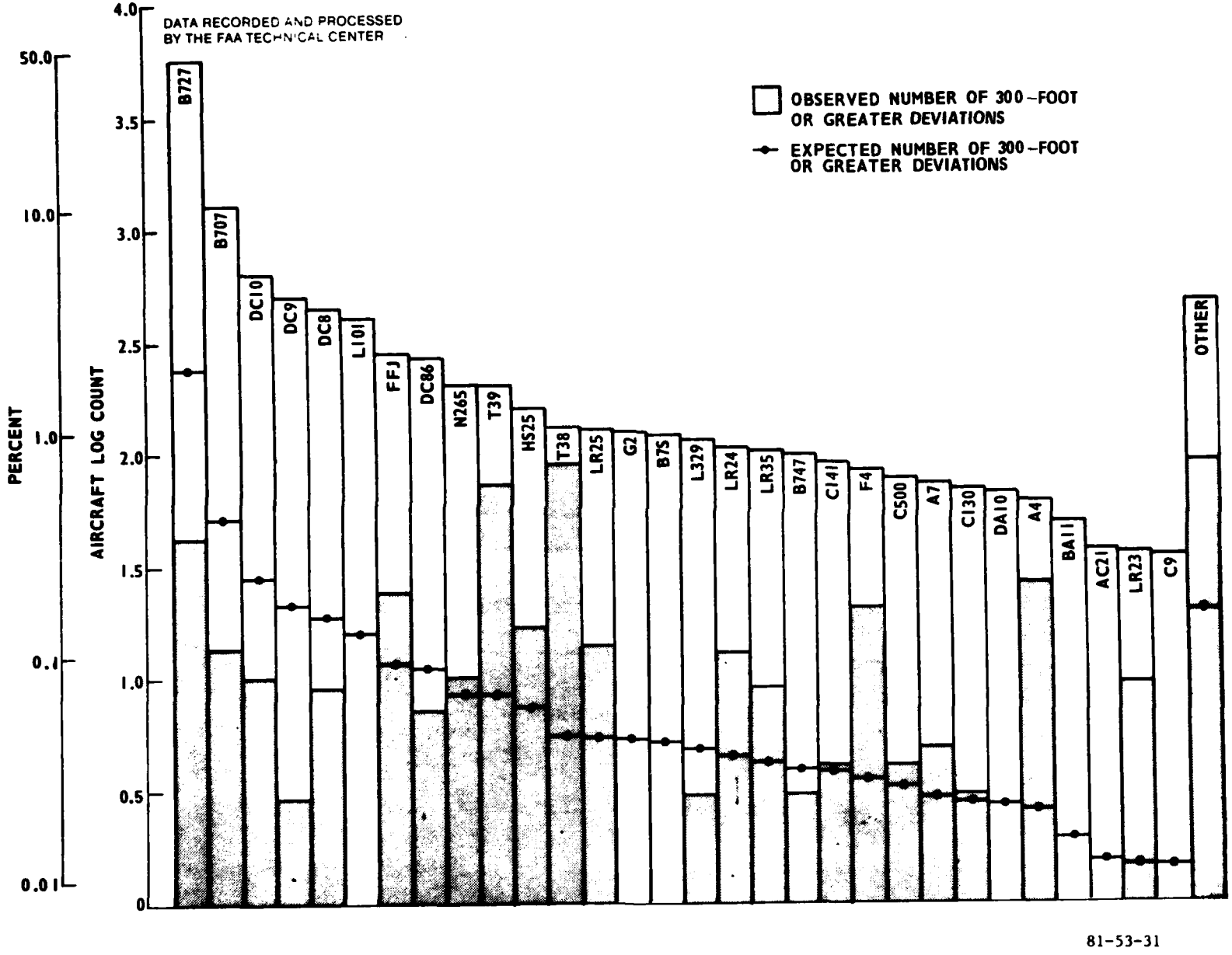

FIGURE 31. NUMBER OF AIRCRAFT PER TYPE

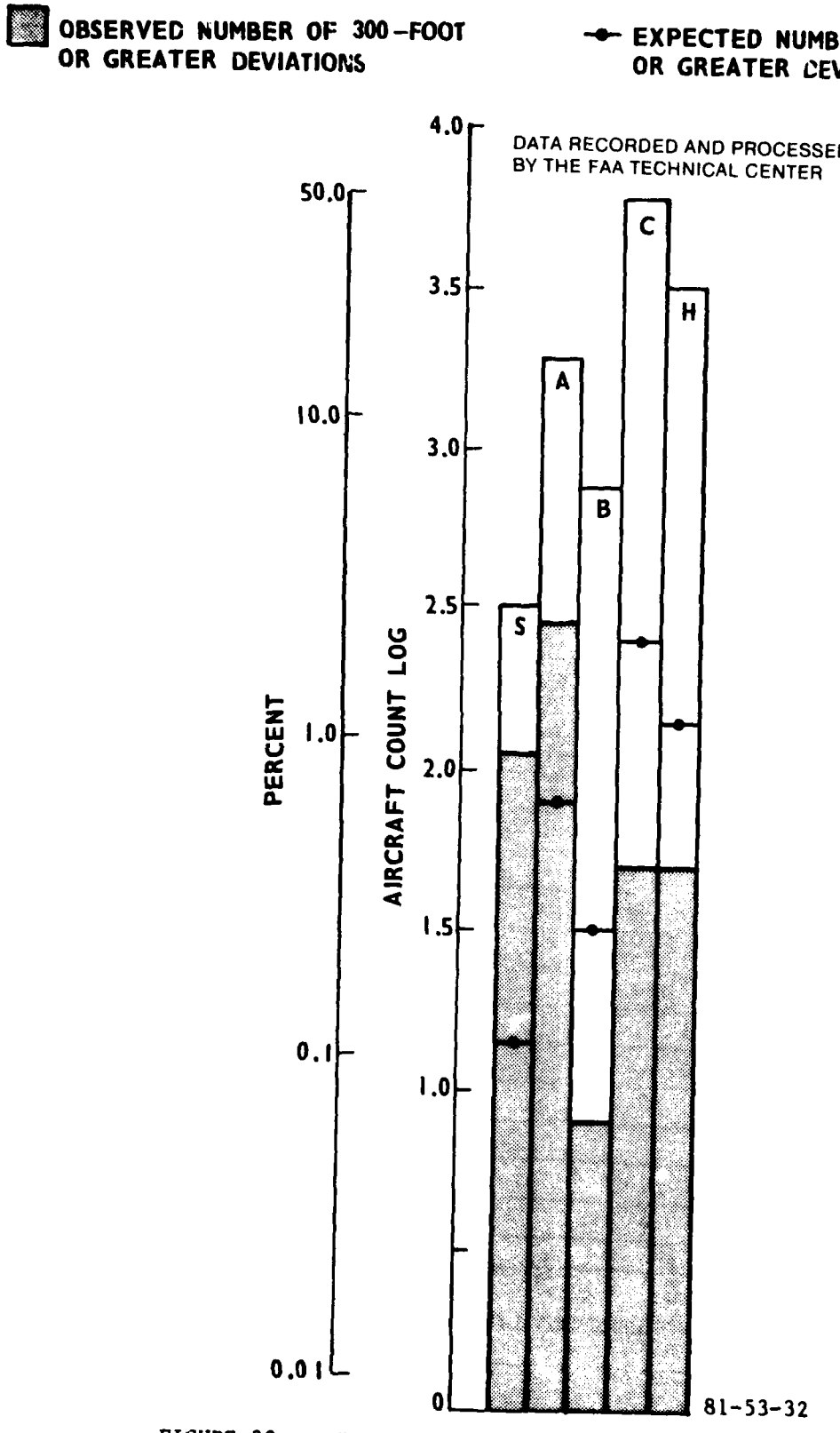

FIGURE 32. NUMBER OF AIRCRAFT PER WEIGHT CLASS

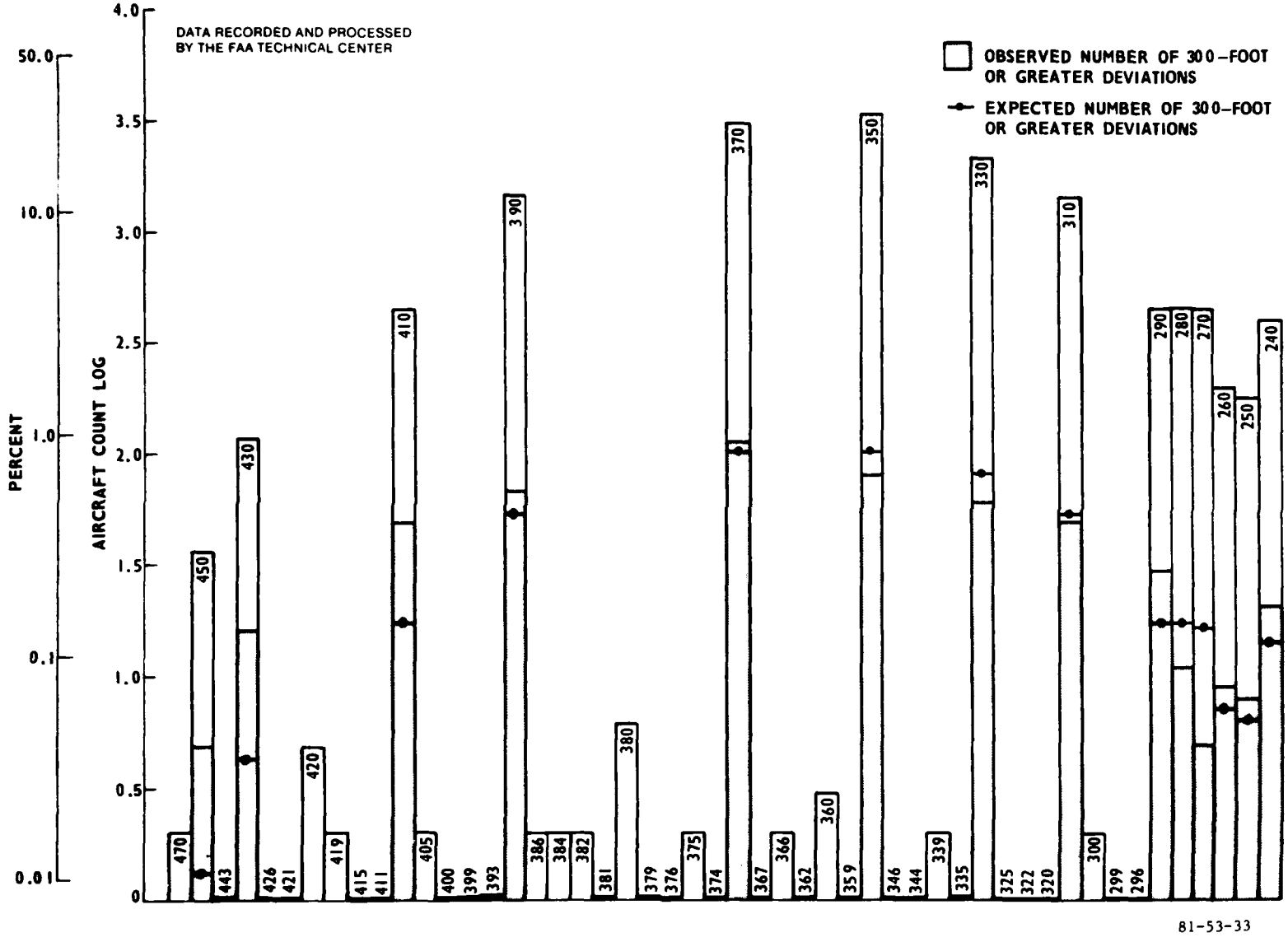

FIGURE 33. NUMBER OF AIRCRAFT PER FLIGHT LEVEL

TABLE 8. AIRCRAFT WEIGHT CLASS INTERVALS

Weight Designation	Weight Class Interval (Pounds)
S (Small)	Less than 12,500
A	12,500 to 60,000
B	60,000 to 120,000
C	120,000 to 300,000
H (Heavy)	Greater than 300,000

A feature that draws attention away from the odd-thousand-foot flight levels is the number of aircraft observed in level flight at other altitudes. Generally, those midway between odd-thousand-foot flight levels were aircraft assigned block altitudes, and those closer to odd-thousand-foot flight levels were aircraft step climbing. The most frequent occurrence of step climbing occurred at altitudes above flight level 370. The number of aircraft at lower flight levels (290 to 240) is fairly uniform and ranges from 200 to 400 aircraft. The number of aircraft at higher flight levels (410 to 470) decreases as flight level increases. The observed number of aircraft with 300-foot or greater errors occurs more frequently than expected for all flight levels above 350, with the difference getting larger for higher flight levels. It is also larger than expected for flight levels 290, 260, 250, and 240.

LEVEL-FLIGHT SEGMENTS. The duration of level flight for each aircraft observed was divided into 5-minute class intervals ranging from 0 to 80 minutes. Four aircraft were tracked for greater than 80 minutes and plotted within the last class interval. Ninety-four percent of the aircraft were observed in level flight for less than 40 minutes. Generally, the observed number of aircraft with 300-foot or greater deviations is much less than expected during short level-flight segments (less than 5 minutes), nearly equal to expected during the 5- to 35-minute level-flight segments, and greater than expected during 40-minute or greater level-flight segments.

ATTRIBUTE CLASSIFICATION.

During the examination of attribute data, it was apparent that some variables contained a larger number of 300-foot or greater errors than expected. This portion of the analysis will focus on these variables. Its purpose is to discover independent attributes, more fully understand the structure of data gathered during this study, and enhance follow-on data gathering efforts by ensuring that a sufficient quantity of data is obtained on those attributes considered most likely to contribute to mode C altitude deviations. This type of analysis requires that the observations associated with each attribute are obtained under equivalent conditions. Since the data gathered during this study were structured to examine lateral deviations on aircraft of opportunity and were not conditioned for the analysis described, they consisted of level-flight segments of variable time duration. Clearly, the likelihood of a given mode C altitude deviation increases with the amount of time an aircraft is observed. For example, it is more likely to observe a 300-foot mode C altitude deviation on an aircraft that is observed for

100 hours, than it is if the same aircraft was observed for 5 minutes. If the time duration between independent samples of mode C altitude were known, then it would be possible to divide the data into segments of proper length. Since the required time interval for independence of mode C altitude is not known, it is desirable to consider only those aircraft in level flight for a given time duration. However, if that limitation was introduced to the data gathered during this study, it would prohibitively reduce the number of aircraft analyzed.

Upon examining figure 34, it was noted that the difference between expected and observed frequencies of 300-foot or greater errors was almost the same from 5 to 35 minutes. Hence, this analysis will concentrate only on aircraft in level flight during that time interval. Under these loose conditions, it was possible to establish attributes that are very likely independent. However, a follow-on data collection, structured to gather information under equivalent conditions, is required to verify the results of this analysis.

With the above conditions established, contingency tables were constructed (appendix G). First, data were examined for those attributes that were divided into a small number of categories and exhibited apparently significant differences. One such attribute was en route centers (figure 30). A 2 by 3 contingency table was constructed, and a chi-square test performed at the 95 percent level with 2 degrees of freedom. The hypothesis of this test was that the proportion of errors greater than or equal to 300 feet was the same between en route centers. The test failed, indicating that the hypothesis was false. Upon further examination of the other attributes within each en route center, it was discovered that the frequency of 300-foot or greater errors was very different for each aircraft user (figures 35 to 37). Hence, a 2 by 3 contingency table was constructed for aircraft users. This hypothesis, that the proportion of errors greater than or equal to 300 feet was the same between aircraft users, was tested at the 95 percent level. Again, the test failed, indicating a false hypothesis. Now, is the difference of proportions computed in these two tests due to en route center, aircraft users, or yet another attribute? An attempt to answer the first part of this question was made by constructing two groups of three sets of 2 by 3 contingency tables. In the first group, one set was constructed for each en route center, and each set was divided into aircraft users. In the second group, one set was constructed for each aircraft user, and each set was divided into en route centers. Two hypothesis were tested, one for each group. The first hypothesis was that the proportion of 300-foot or greater errors within every en route center was the same, independent of the number of different aircraft users. So, although this proportion may vary from center to center, it does not vary within centers as a function of aircraft users. The second hypothesis was that the proportion of 300-foot or greater errors within every aircraft user was the same, independent of the center where the data were gathered. The first hypothesis failed at the 95 percent confidence level, not only when considered in toto, but also within each en route center. This indicates the hypothesis, that the proportion of 300-foot or greater errors within every en route center was the same independent of the number of different aircraft users, was false; and further, that the proportion of 300-foot or greater errors for each en route center was the same independent of the number of different aircraft users, was false.

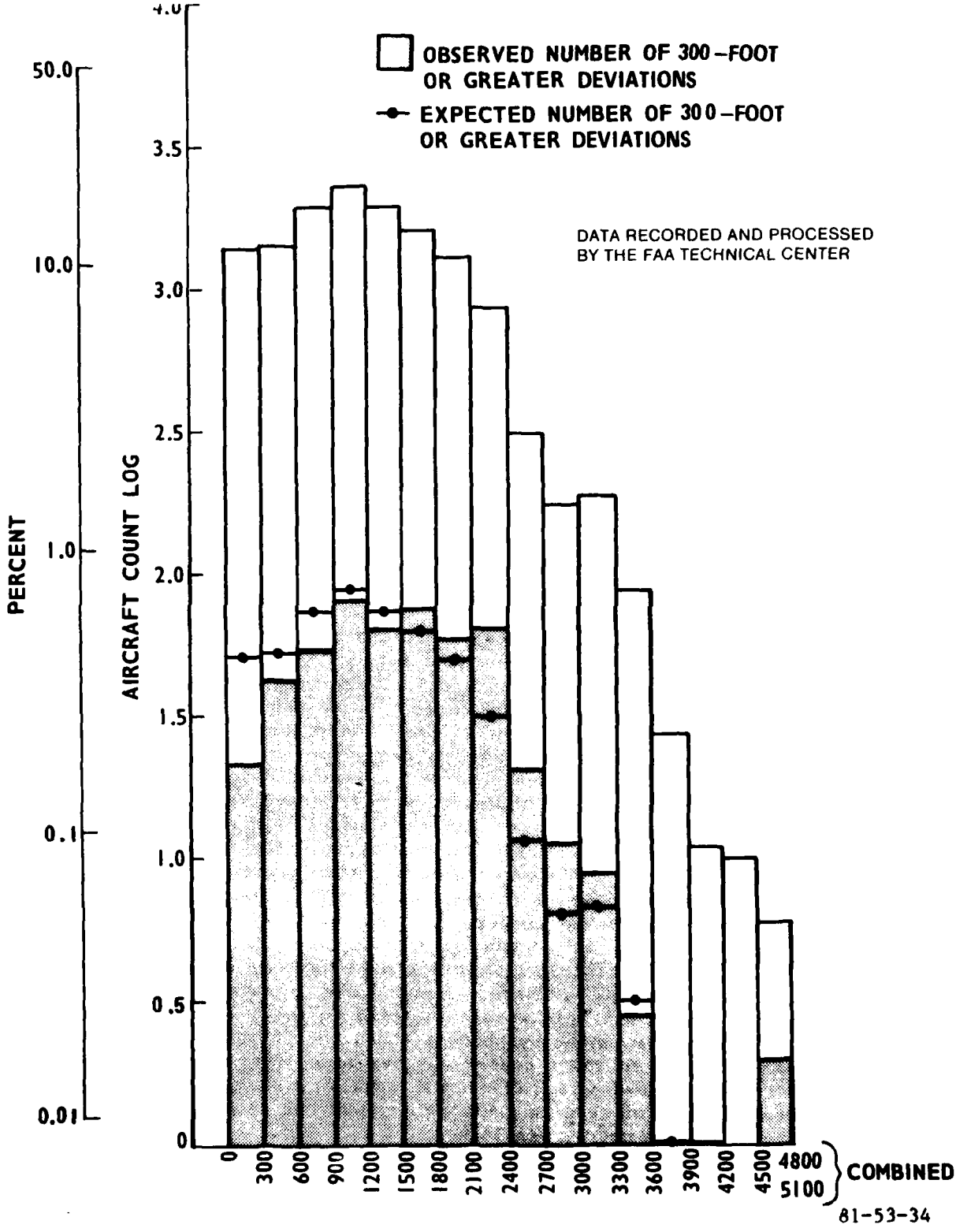

FIGURE 34. NUMBER OF AIRCRAFT AT 5-MINUTE INTERVALS

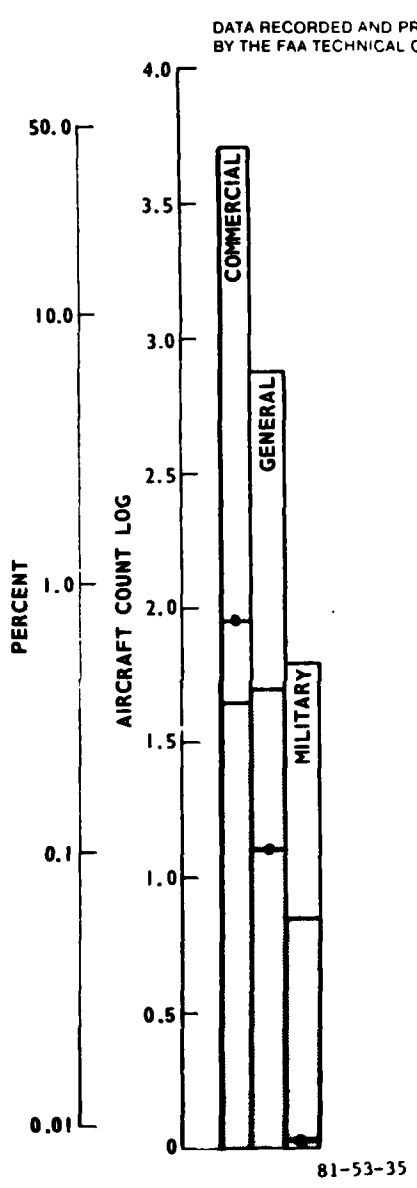

FIGURE 35. NUMBER OF AIRCRAFT USERS OVER CLEVELAND

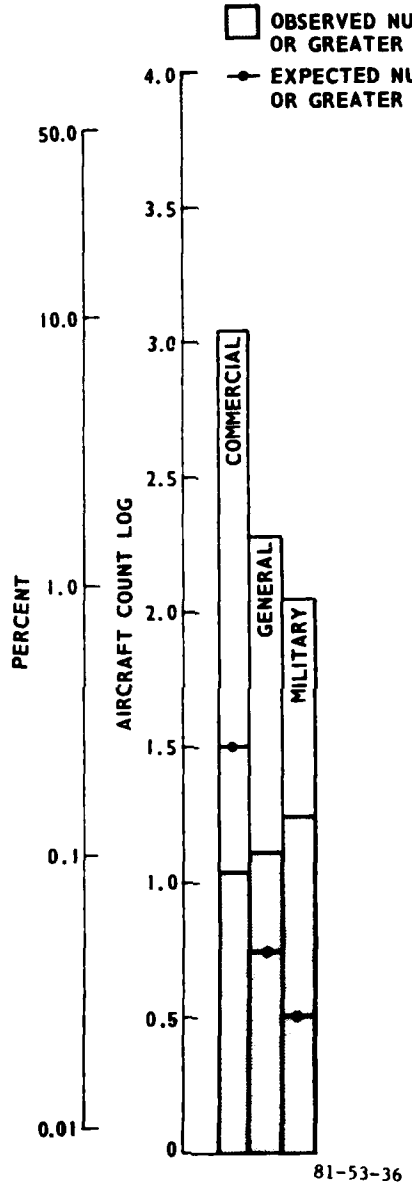

FIGURE 36. NUMBER OF AIRCRAFT USERS OVER MEMPHIS

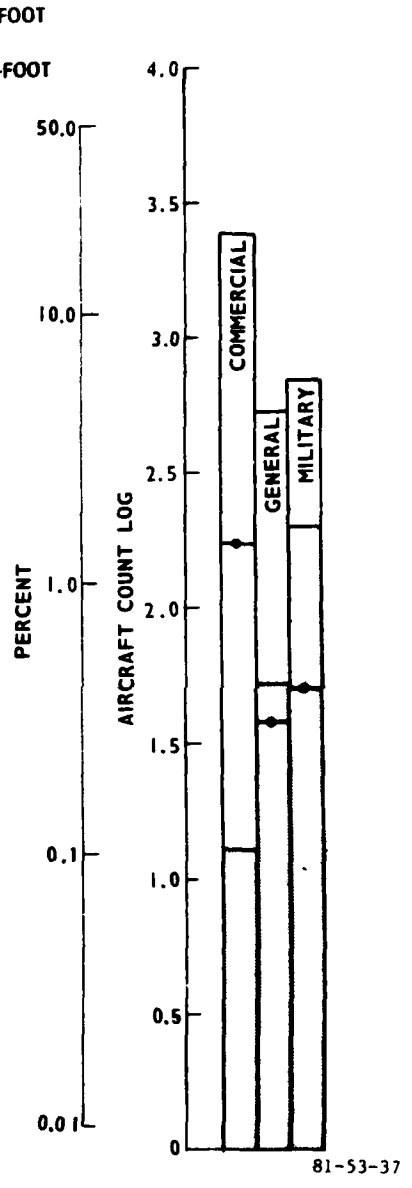

FIGURE 37. NUMBER OF AIRCRAFT USERS OVER ALBUQUERQUE

The second hypothesis also failed at the 95 percent confidence level when considered in toto, but passed when commercial or general aviation aircraft were considered separately. Hence, the hypothesis that the proportion of 300-foot or greater errors within every aircraft user was the same, independent of the center where the data were gathered, was rejected. However, the hypothesis that the proportion of commercial or general aviation aircraft 300-foot or greater errors was the same, independent of the center where the data were gathered, was accepted at the 95 percent confidence level.

The computed and critical chi-square values that were constructed for the second hypothesis are presented in table 9. The larger elements are observed in the second set under military aircraft and in the third set (third column) under general aviation Albuquerque aircraft, almost causing general aviation aircraft to fail the chi-square test. What is it about military aircraft or general aviation Albuquerque aircraft that might cause the observed frequency to be different from expected? Military aircraft weight classes indicate a possible further subdivision (figure 38). Albuquerque general aviation aircraft types indicate a possible further subdivision (figure 39). With further examination, it was discovered that NASA aircraft were classified as general aviation aircraft. They were removed from this classification, and the chi-square test on general aircraft was reconstructed. It resulted in a computed chi-square value of 0.48 (table 10), and the test passed. This indicated that the frequency of 300-foot or greater errors for general aviation aircraft, with NASA aircraft removed, was independent of the center where the data were gathered.

TABLE 9. AIRCRAFT USER — CENTER CONTINGENCY TABLES SUMMARY

Aircraft User	Cleveland	Memphis	Albuquerque	χ^2	χ^2 Critical Value At 95% Confidence	Degrees of Freedom
Commercial						
<300 ft.	0.0022	0.0047	0.0135			
				2.66	5.99	2
≥300 ft.	0.283	0.608	1.75			
Military						
<300 ft.	1.6	1.37	0.708			
				14.76	5.99	2
≥300 ft.	4.82	4.11	2.152			
General						
<300 ft.	0.14	0.02	0.284			
				5.70	5.99	2
≥300 ft.	1.63	0.243	3.384			
				23.12	12.6	6

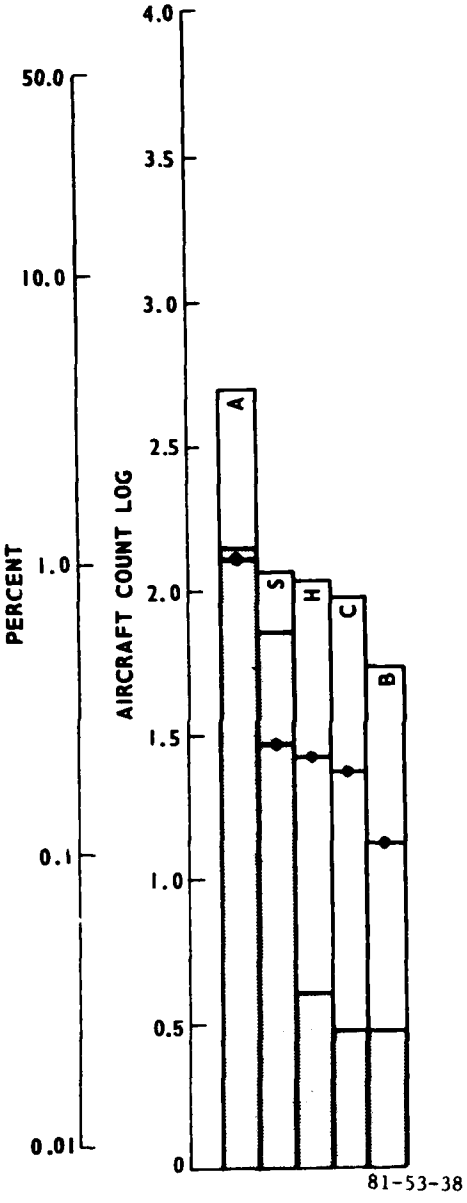

FIGURE 38. NUMBER OF MILITARY AIRCRAFT WEIGHT CLASSES

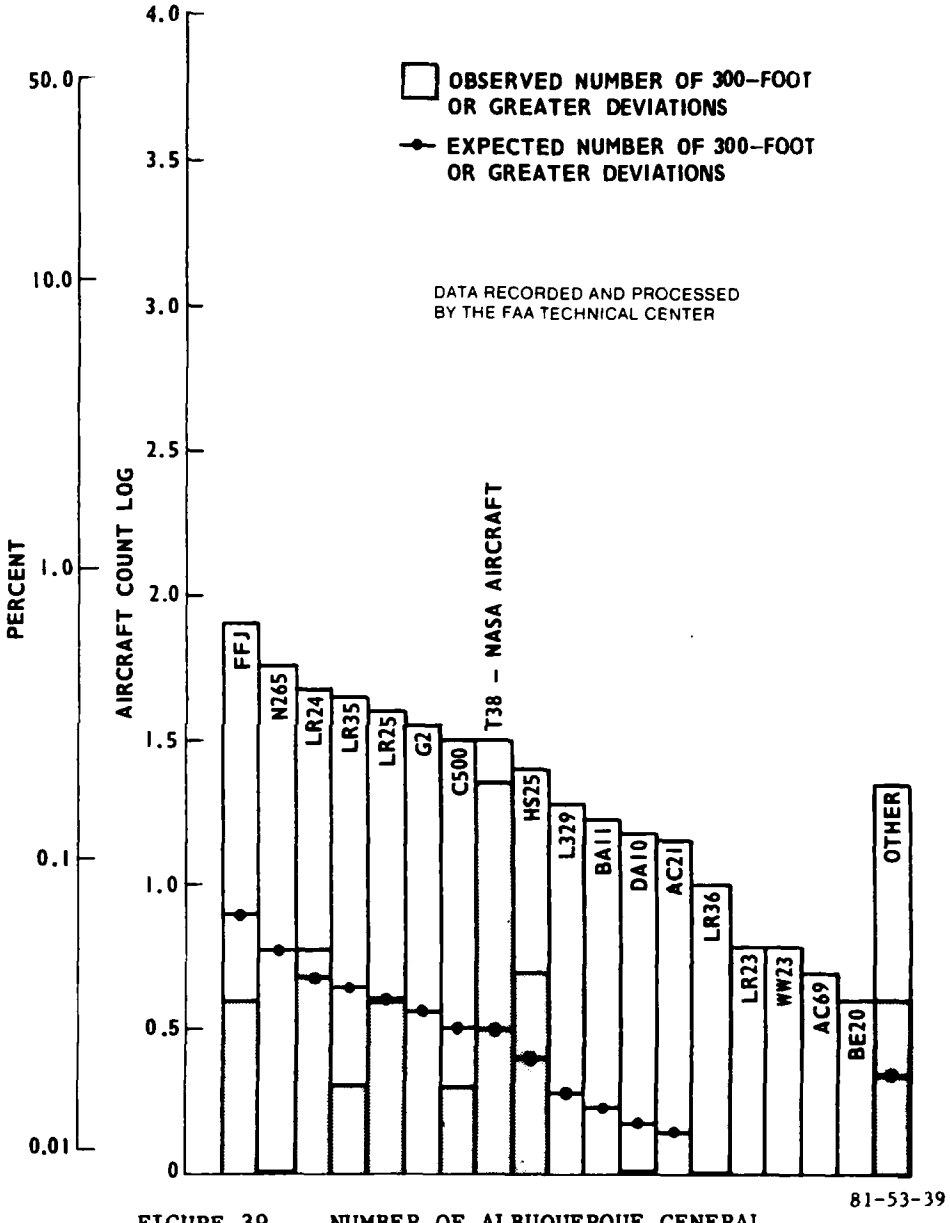

FIGURE 39. NUMBER OF ALBUQUERQUE GENERAL AIRCRAFT PER TYPE

Two sets of contingency tables were constructed for military aircraft. In these tables, the hypothesis tested was that the proportion of 300-foot or greater errors within two weight categories was the same, independent of whether the data were gathered over Albuquerque or the combined data of Cleveland and Memphis. The data within the latter two en route centers were combined to provide a sufficient quantity of information for each contingency table. Intermediate tests established that the proportion of 300-foot or greater errors was the same for military aircraft over the combined en route centers. Small and weight A classes were defined as W_1 (aircraft weighing less than 60,000 lbs), and large and heavy aircraft were defined as W_2 (aircraft weighing 60,000 lbs or greater). The chi-square tests failed with respect to W_1 and passed with respect to W_2. This implied the hypothesis that weight W_1 military aircraft exhibit the same proportion of 300-foot or greater errors over Albuquerque as over the combined data from Cleveland and Memphis was false, while the hypothesis that weight W_2 military aircraft exhibit the same proportion of errors under the same conditions was accepted. A test was conducted on weight W_1 general aviation aircraft. The hypothesis was that the proportion of 300-foot or greater errors was the same independent of the en route center where the data were gathered. The test passed. There were no weight W_1 commercial aircraft observed during this study. In summary, the data utilized in this analysis do not provide sufficient information to determine why weight W_1 military aircraft should exhibit different error characteristics over Albuquerque than over Cleveland or Memphis en route centers.

Another attribute that exhibited possible difference between observed and expected frequency of 300-foot deviations over its range of values was aircraft altitude. On figure 33, it was noted that the percentage of 300-foot or greater errors was larger than expected for altitudes above 350. Since previous analysis demonstrated that aircraft user was an important factor, the data were subdivided into altitude flight levels for each aircraft user (figures 40 to 42). Even within each user category, the frequency of errors 300-foot or greater seemed to increase at high altitudes. Three sets of 2 by 5 contingency tables were constructed. One for commercial aircraft, one for general aviation aircraft (NASA aircraft removed), and one for military weight W_1 aircraft over Albuquerque. There was insufficient data to construct tables for military weight W_2 aircraft, or military weight W_1 aircraft over Cleveland combined with Memphis. Each table was divided into five altitude intervals. They were [290,330), [330,370), [370,390] and greater than or equal to 410. For each user, the hypothesis that the porportion of aircraft with 300-foot or greater errors was the same, independent of altitudes, was tested. All three tests failed. Examining the table of chi-square values, a large number were observed for commercial and general aviation aircraft at altitudes 410 and above (appendix G). In both cases, the observed frequency of 300-foot or greater errors was larger than expected at these high altitudes. Military aircraft chi-square values exhibit a large number at altitudes below flight level 290 (appendix G). In this case, the observed frequency of 300-foot or greater errors was less than expected. Each table was reconstructed under weaker conditions. The commercial and general aircraft tables only considered aircraft below flight level 410, and the military aircraft table only considered aircraft at and above flight level 290. All three tests passed. This indicates the hypothesis that the proportion of 300-foot or greater errors is the same for commercial and general aircraft below flight level 410, and for military weight W_1 aircraft over Albuquerque at and above flight level 290 with expected percentages of 0.7, 4.76, and 38.86, respectively.

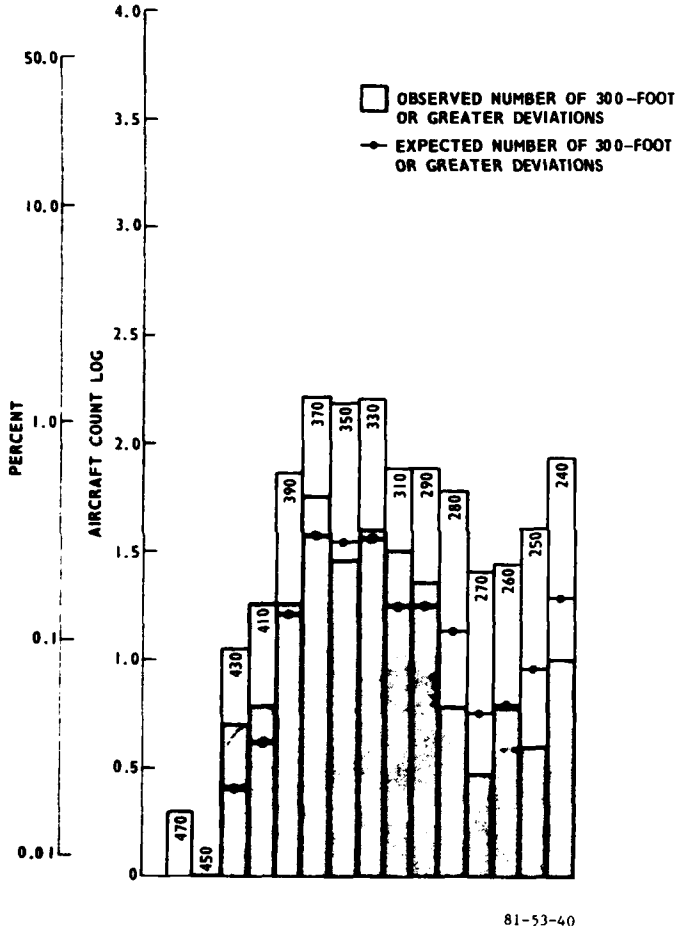

FIGURE 40. NUMBER OF MILITARY AIRCRAFT PER FLIGHT LEVEL

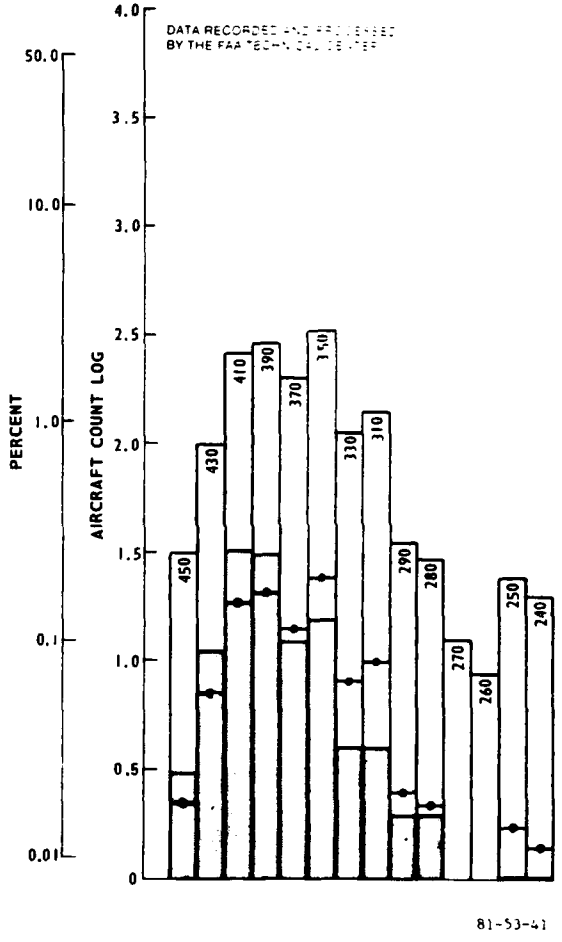

FIGURE 41. NUMBER OF GENERAL AVIATION AIRCRAFT PER FLIGHT LEVEL

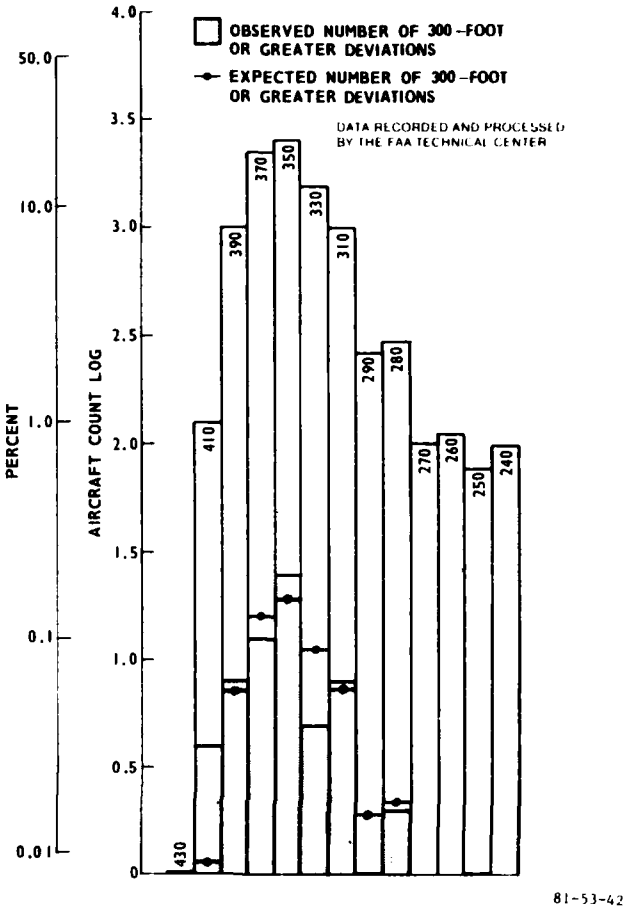

FIGURE 42. NUMBER OF COMMERCIAL AIRCRAFT PER FLIGHT LEVEL

Finally, it was previously noted that the frequency of 300-foot or greater errors was greater than expected for speeds less than 350 knots or greater than 600 knots. The data were again divided into commerical, general aviation (NASA aircraft removed), and military weight W_1 aircraft over Albuquerque. Further, they were subdivided into east and west traffic. Six sets of 2 by 4 contingency tables were constructed. Each table was divided into 4 speed intervals. They were less than or equal to 450, (450,500], (500,550] and greater than 550 for easterly traffic, and less than or equal to 350, (350,400], (400,450] and greater than 450 for westerly traffic. For each user and direction, the hypothesis that the proportion of aircraft with 300-foot or greater errors was the same, independent of speed was tested. For commercial aircraft, the chi-square test passed for aircraft traveling east and failed for aircraft traveling west.

When aircraft traveling less than 350 knots were removed from the westerly traffic, and a 2 by 3 contingency table defined, the test passed. For general aviation and military aircraft, the test passed for both east and west traffic. These tests indicate that the proportions of 300-foot or greater errors is independent of aircraft speed for general aviation, military weight W_1 aircraft over Albuquerque, and commercial aircraft traveling greater than 350 knots.

A summary of the results obtained during the analysis presented in this section is given in table 10. It demonstrates that the frequency of 300-foot or greater errors for commercial, general aviation (with NASA aircraft removed), and military weight W_2 aircraft are independent of where the data are gathered with expected precentages of 0.774, 6.23, and 3.8, respectively. Further, it shows a significant increase in the frequency of 300-foot or greater errors for military weight W_1 aircraft, as well as an unexplained distinction among this class of aircraft between data gathered over Albuquerque (35.3 percent with deviations greater than or equal to 300 feet), and data gathered over Cleveland and Memphis (23.7 percent with deviations greater than or equal to 300 feet).

The proportion of 300-foot or greater errors was found independent of altitude and speed for commercial aircraft at altitudes below 41,000 feet and speeds greater than 350 knots; for general aviation aircraft (NASA aircraft removed) at altitudes below 41,000 feet and all speeds observed; and for military aircraft weight W_1 over Albuquerque at altitudes at and above 29,000 feet and all speeds observed.

Due to the loose conditions assumed, and the data structure, a follow-on analysis is required by an independent data collection to validate the results obtained during this section of the analysis.

LARGE MODE C ALTITUDE ERROR CORRELATIONS.

LARGE MODE C ALTITUDE ERRORS VERSUS MODE C VELOCITY. A parameter frequently utilized in computing the probability of aircraft collisions is vertical velocity at a given distance above or below assigned altitude. It is recognized that vertical velocity is not totally composed of FTE's, rather it is a combination of static pressure error, altimeter instrument error, and FTE. However, since FTE is one component contributing to vertical velocity and knowledge of its characteristics provides information historically not available, a crude estimate of vertical FTE velocity at a given distance from altitude will be made utilizing mode C data.

The distances, above or below assigned altitude, of major interest when considering vertical separation are 500 feet or greater. To expedite this study, and reduce the number of aircraft analyzed, only those aircraft exhibiting mode C altitude deviations greater than or equal to 400 feet were examined.

Aircraft observed during this data collection were usually tracked asychronously by two or more surveillance radars. If the time difference between consecutive observations was very small, and this information was used to compute vertical velocity, mode C altitude (quantized into 100-foot increments) would erroneously produce large altitude changes. To alleviate this situation, a condition was placed on all velocity computations. If the time difference between consecutive observations was less than 12 seconds (scan rate of surveillance radars was generally from 10 to 12 seconds), then the data were compared with adjacent observations until the total time difference exceeded 12 seconds.

The altitude change during this expanded time interval was recorded and the velocity estimated. Care was taken not to combine data that consisted of opposite sign altitude changes unless the general trend was in one direction. This prevented the smoothing of modal data. Note, with an average time between observations of 12 seconds, the average velocity for a 100-foot change in altitude is 5 knots. This generally structured the data into 5-knot increments.

TABLE 10. ATTRIBUTE CLASSIFICATION SUMMARY

Test Description	x^2 Value	Degrees Of Freedom	Results	Estimated Percentage ≥ 300 Feet
Between en route centers	209	2	Failed	
Between aircraft users	1455	2	Failed	
Within en route centers by aircraft users	1685	6	Failed	
Cleveland Center by aircraft users	168	2	Failed	
Memphis Center by aircraft users	90	2	Failed	
Albuquerque Center by aircraft users	617	2	Failed	
Within aircraft users by en route centers	23.12	6	Failed	--
Commercial aircraft by en route center	2.66	2	Passed	0.774
Military aircraft by en route centers	14.76	2	Failed	
General aviation aircraft by en route center	5.71	2	Passed (Borderline)	7.7
General aviation aircraft by en route centers (NASA aircraft removed)	0.48	2	Passed	6.23
Weight W_1 general aviation aircraft by en route centers (NASA aircraft removed)	0.57	2	Passed	7.10
Military aircraft between Cleveland and Memphis en route centers	0.64	1	Passed	13.96
Weight W_1 military aircraft between Albuquerque and combined Cleveland with Memphis	5.06	1	Failed	
Weight W_2 military aircraft between Albuquerque and combined Cleveland with Memphis	2.05	1	Passed	3.8
Commercial aircraft by altitude	10.09	4	Failed (Borderline)	0.73
General aviation aircraft by altitude	13.2	4	Failed	
Military weight W_1 aircraft over Albuquerque by altitude	22.56	4	Failed	
Commercial aircraft by altitude (data above flight level 390 removed)	0.85	3	Passed	0.7

by en route centers				
Commercial aircraft by en route center	2.66	2	Passed	0.774
Military aircraft by en route centers	14.76	2	Failed	
General aviation aircraft by en route center	5.71	2	Passed (Borderline)	7.7
General aviation aircraft by en route centers (NASA aircraft removed)	0.48	2	Passed	6.23
Weight W_1 general aviation aircraft by en route centers (NASA aircraft removed)	0.57	2	Passed	7.10
Military aircraft between Cleveland and Memphis en route centers	0.64	1	Passed	13.96
Weight W_1 military aircraft between Albuquerque and combined Cleveland with Memphis	5.06	1	Failed	
Weight W_2 military aircraft between Albuquerque and combined Cleveland with Memphis	2.05	1	Passed	3.8
Commercial aircraft by altitude	10.09	4	Failed (Borderline)	0.73
General aviation aircraft by altitude	13.2	4	Failed	
Military weight W_1 aircraft over Albuquerque by altitude	22.56	4	Failed	
Commercial aircraft by altitude (data above flight level 390 removed)	0.85	3	Passed	0.7
General aviation aircraft by altitude (data above flight level 390 removed)	3.81	3	Passed	4.76
Military weight W_1 aircraft by altitude over Albuquerque (data below flight level 290 removed)	2.23	3	Passed	38.86
Commercial aircraft by speed (east)	3.48	3	Passed	0.69
Commercial aircraft by speed (west)	10.65	3	Failed	
General aviation aircraft by speed (east)	3.92	3	Passed	5.74
General aviation aircraft by speed (west)	2.04	3	Passed	6.49
Military weight W_1 aircraft by speed over Albuquerque (east)	0.25	3	Passsd	38.22
Military weight W_1 aircraft by speed over Albuquerque (west)	2.85	3	Passed	31.85
Commercial aircraft by speed (west with data below 350 knots removed)	3.87	2	Passed	0.79

2

Subsequent to velocity estimate computations, a matrix was constructed (table 11). Each row represented 5-knot velocity intervals ranging from 0 to 60 knots, each column represented 100-foot-altitude intervals ranging from 200 to 1,700 feet, and each element consisted of the time duration associated with the respective velocity and altitude interval. A time weighted average velocity at each altitude interval was then computed.

During this exercise, and as previously noted with regard to figure 33, it was discovered that situations occurred in which aircraft were in level flights at altitudes other than the odd-thousand-foot altitudes above flight level 290. In order to demonstrate the effect these values have on the computation of vertical velocity, they were separated by dividing the first row into two parts. The upper part consisted of the time duration with constant zero velocity at a given altitude (above dashed line). The lower part consisted of the time duration with nonzero velocity to 2.5 knots at a given altitude (below dashed line). This resulted in two computations of vertical velocity for each 100-foot-altitude interval. A regression line was computed for each set of velocity estimates, and the results are depicted in figure 43. The solid line was computed from time-weighted velocity estimates computed from constantly changing mode C altitude deviations and the broken line was computed from time-weighted velocity estimates computed from changing and nonchanging (zero velocity) mode C altitude deviations. This plot demonstrates two distinct estimates of vertical FTE velocity that diverge with increasing altitude deviation.

It becomes clear at this juncture in the analysis that, since vertical distances from assigned altitudes consist of both short- and long-term deviations, the estimate of vertical velocity requires precise definition. The construction of the FTE distribution, the enumeration of aircraft occupancies, the establishment of system procedures, and consequently, the computation of collision risk are closely hinged to this definition.

The other contributors to vertical velocity at large altitude deviations are pitot-static and altimeter instrument errors, and these are commonly thought to be long-term biases. The combination of short-term large vertical FTE velocity estimates and long-term altimeter system error velocity estimates must be thoroughly evaluated before being utilized in the computation of aircraft collision risk. This short study demonstrates that this entire area requires further careful analysis.

LARGE MODE C ALTITUDE DEVIATION VERSUS LATERAL DEVIATION. Corresponding to each mode C altitude deviation of 400 feet or greater, its time duration was recorded, and the average lateral deviation was computed. Four matrixes were then constructed. Each row represented average lateral deviation intervals in nautical miles, each column represented altitude deviation in 100-foot intervals, and each element consisted of the time duration in seconds associated with respective mode C altitude and lateral deviations. In matrix one, average lateral deviation ranged from -8.5 to 0 nautical miles, and altitude deviation ranged from -700 to -400 feet. Matrix two, average lateral deviation ranged from 0 to 13.5 nautical miles and altitude deviation ranged from -900 to -400 feet. Matrix three, average lateral deviation ranged from -8.5 to 0 nautical miles, and altitude deviation ranged from 400 to 1,100 feet. Matrix four, average lateral deviation ranged from 0 to 13.5 nautical miles over the same altitude range. A time-weighted lateral deviation for each altitude interval was computed. Each of the time-weighted

TABLE 11. MATRIX OF DURATION OF TIME (SECONDS) AT MODE C VELOCITY IN ALTITUDE DEVIATION INTERVALS

Vertical FTE Velocity (Knots)	Altitude Deviation (Feet)															
	(200 - 300]	(300 - 400]	(400 - 500]	(500 - 600]	(600 - 700]	(700 - 800]	(800 - 900]	(900 - 1000]	(1000 - 1100]	1200	1300	1400	1500	1600	1700	Greater Than 1700
0 to 2.5	202.3	882		597.5	212.8	321.4	81.0	374.7	369.5			141.3	152.0	232.7	252.8	1330.7
	95.3	407.7	208.2	392.8	5.7											
2.5 to 7.5	744.1	1744.4	571.5	51.8	37.5											
7.5 to 12.5	429.6	566.3	264.4	93.6	30.3	4.5	14.6									
12.5 to 17.5	99.6	121.6	11.7	64.2	12.1	14.5	14.5	9.7	9.7							
17.5 to 22.5	31.1	53.5	22.3	14.5												
22.5 to 27.5	20.5	22.8	6.7	4.3	1.9	1.9	2.5	2.1								
27.5 to 32.5		2	2	1.3	1.3	2.8	2.8									
32.5 to 37.5	5.1	4.1	2.5													
57.5 to 62.5	0.9	0.9	0.9	0.9	0.9	0.9	1.6									
V below dashed line	7.62	6.19	6.75	4.24	9.05	18.21	16.83	16.77	15.00			--	--	--	--	--
V all	6.67	4.75	6.75	2.16	2.68	1.29	5.17	0.51	0.38			0.0	0.0	0.0	0.0	0.0

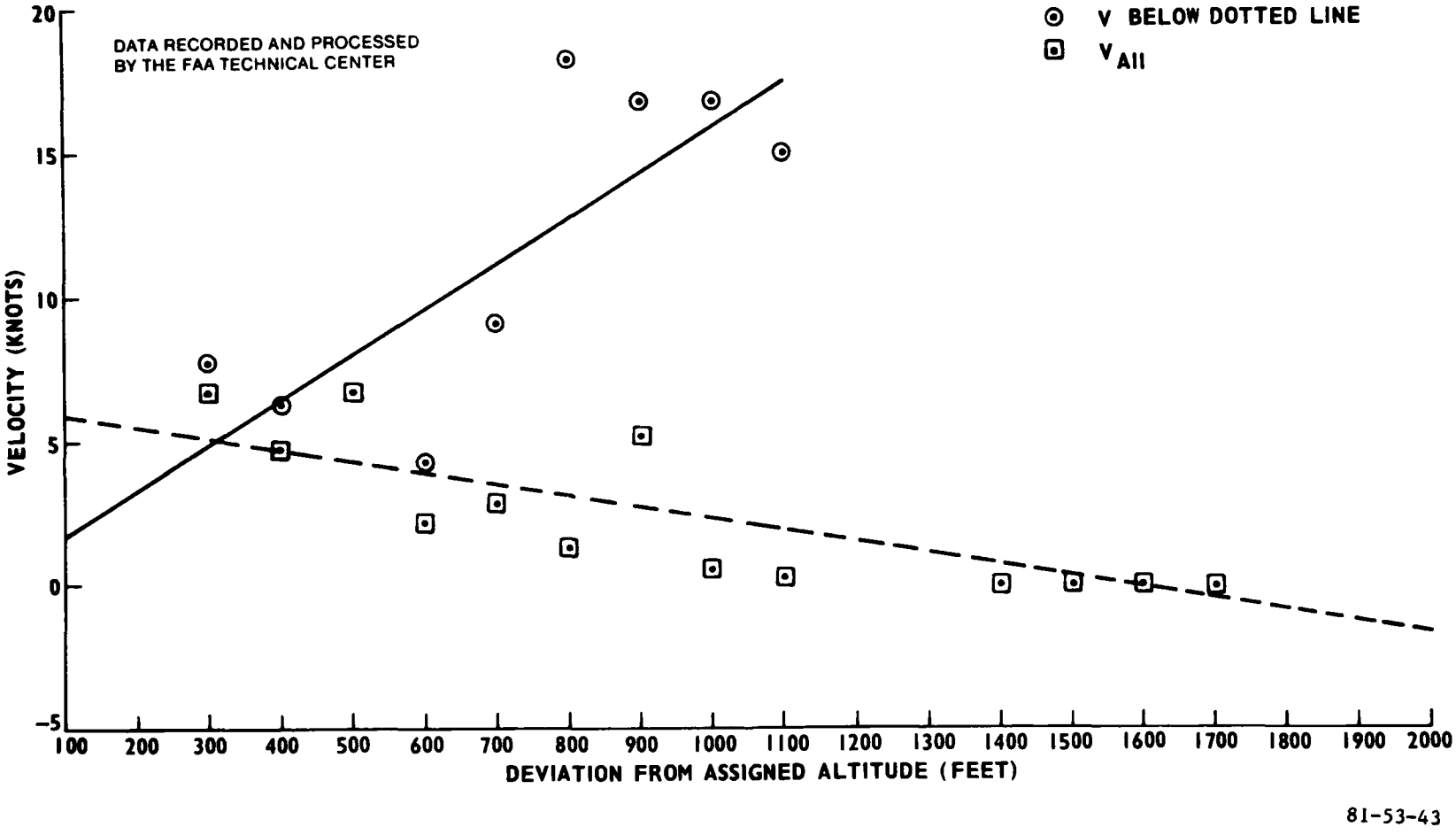

FIGURE 43. LINEAR REGRESSION OF MODE C VELOCITY ON LARGE MODE C ALTITUDE

values were plotted, and adjacent values were connected by a straight line (figure 44). The matrix of time durations was overlayed on this plot to demonstrate the scatter and magnitude of matrix elements. No obvious trend was detected within this data. It is concluded that, given a large mode C altitude deviation occurs, the associated lateral deviation is expected to be random.

SPECIAL CASES.

Each aircraft data set observed with a deviation from assigned altitude of 400 feet or greater (after processing anomalies were removed) was the subject of a detailed investigation. This included careful replay and transcription of voice communication magnetic tapes, reexamination of digital data flight strips and observer logs, construction of vertical plots, and consultation with an air traffic controller. It uncovered 126 aircraft with 400-foot errors, 60 aircraft with 500-foot or greater errors, 2,910 aircraft without altitude verification, 512 aircraft without augmenting flight strip data, 55 aircraft assigned block altitudes or step climbing, 8 aircraft with uncertain or dual beacon radar codes, 2 aircraft maneuvered due to turbulent conditions, 7 aircraft maneuvered due to conflicting traffic, 10 aircraft with altimeter system or mode C malfunctions, 6 aircraft too heavy to attain or maintain assigned altitude, 9 aircraft with a long-term 300-foot bias, and 6 aircraft identified as unusual cases.

Those aircraft with 400-foot or greater deviations were commonly characterized by turbulence or aircraft system error. Turbulence was confirmed in many cases and resulted in isolated downdrafts or updrafts and continuous or violent disturbances. Typical examples of each case are plotted in figures 45, 46, and 47, respectively. Each plot includes julian day and place of data collection, aircraft type, speed, flight level, weight class, route, and direction traveled. The y-axis is of constant scale ranging $\pm$ 5,000 feet from flight level. The x-axis is of variable scale to accommodate different track lengths and has units of minutes. If the level flight track length employed to compute the time histogram is smaller than total track length, it is indicated by vertical lines labeled S (start) and E (end). Only the data between start and end vertical lines were used in the analysis. Ascending or descending aircraft data are not shown once they go beyond 5,000 feet from assigned altitude. The dots represent recorded mode C altitude, and the connecting line was generated to demonstrate the relationship of contiguous points. In the first two cases (figure 45 and 46), controller intervention is unusual because either (1) the time duration of the disturbance is so short that it is over before he is able to respond or (2) he is aware of existing turbulent weather conditions. In the third case (figure 47), turbulence was so severe the pilot requested flight level 410, found conditions to be worse at approaching this lower level, and, once again, requested and was granted flight level 430. Aircraft system error was also confirmed in many cases and resulted in aircraft drifting from assigned altitude (figure 48 and 49), overshooting or undershooting flight level on approach or descent (figure 50), and cyclical oscillation about flight level (figure 51 and 52). In the first two cases, air traffic controller intervention is common, and the situation is usually corrected. In both of these examples, the pilots were informed of altitude inconsistencies. In the third case (figure 50), controller intervention is uncommon. It is considered as an adjustment time period before stablization and usually corrected within a reasonably short time after attaining or before leaving the desired flight level. When not corrected within a reasonable time (typically less than 5 minutes), the controller normally queries the pilot (figure 53). If possible, the situation is remedied. If not, a block altitude is assigned. The fourth and fifth cases (figures 51 and 52) represent smooth cyclical short- or long-term oscillations about flight level.

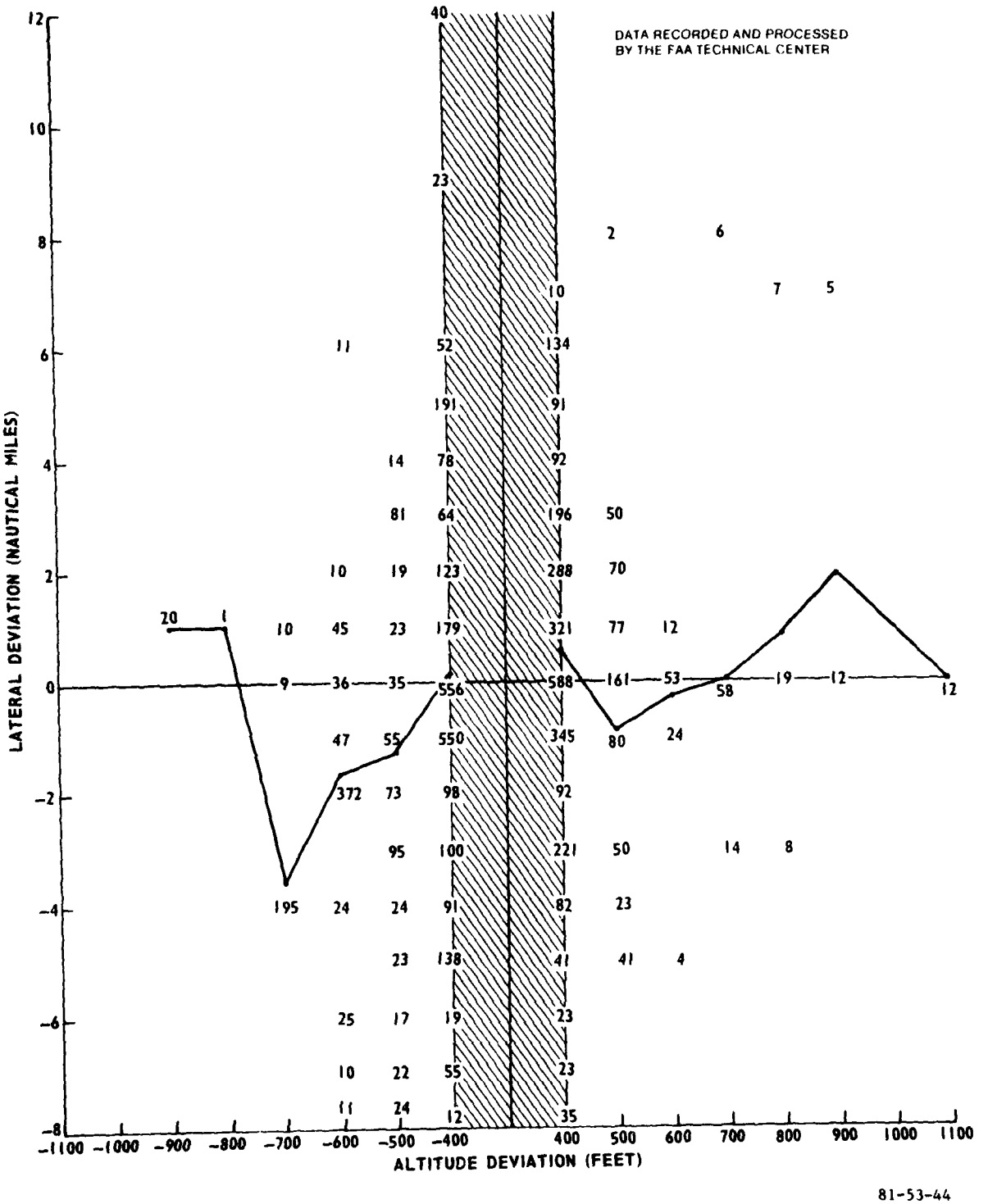

FIGURE 44. LARGE MODE C ALTITUDE VERSUS LATERAL DEVIATION TIME SCATTER PLOT

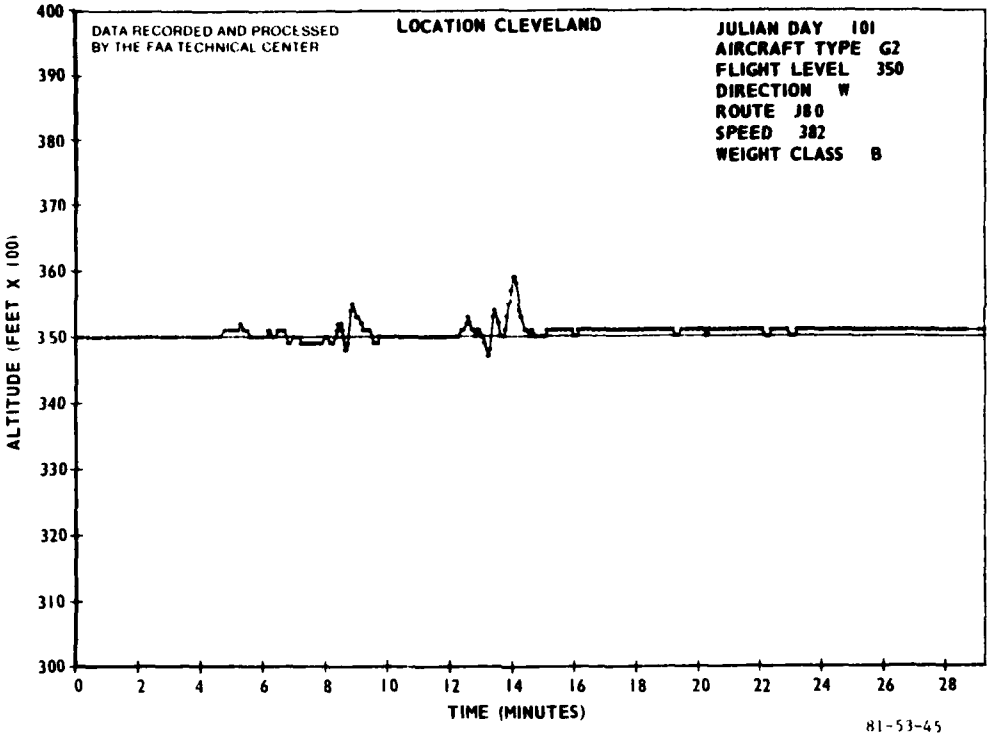

FIGURE 45. SPECIAL CASE 1

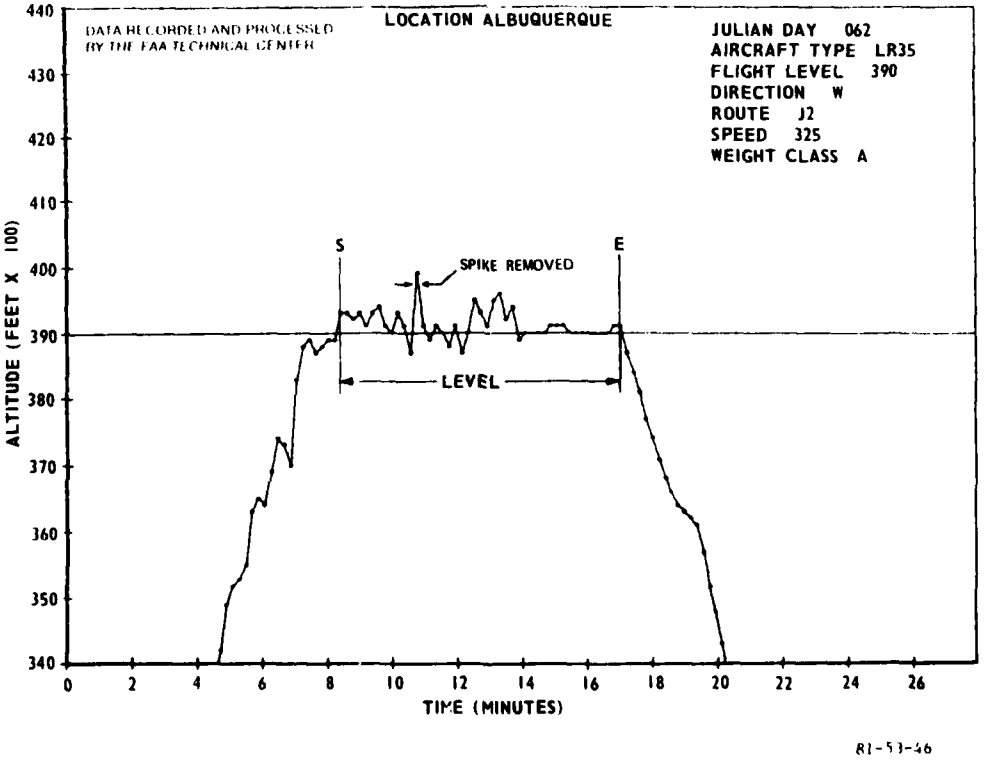

FIGURE 46. SPECIAL CASE 2

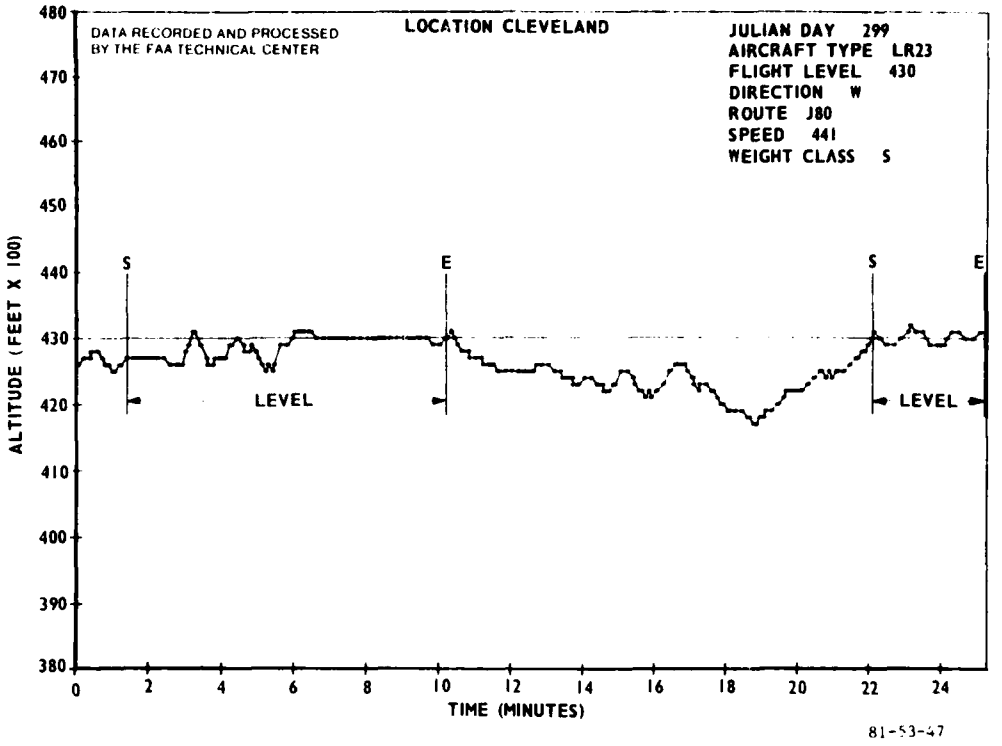

FIGURE 47. SPECIAL CASE 3

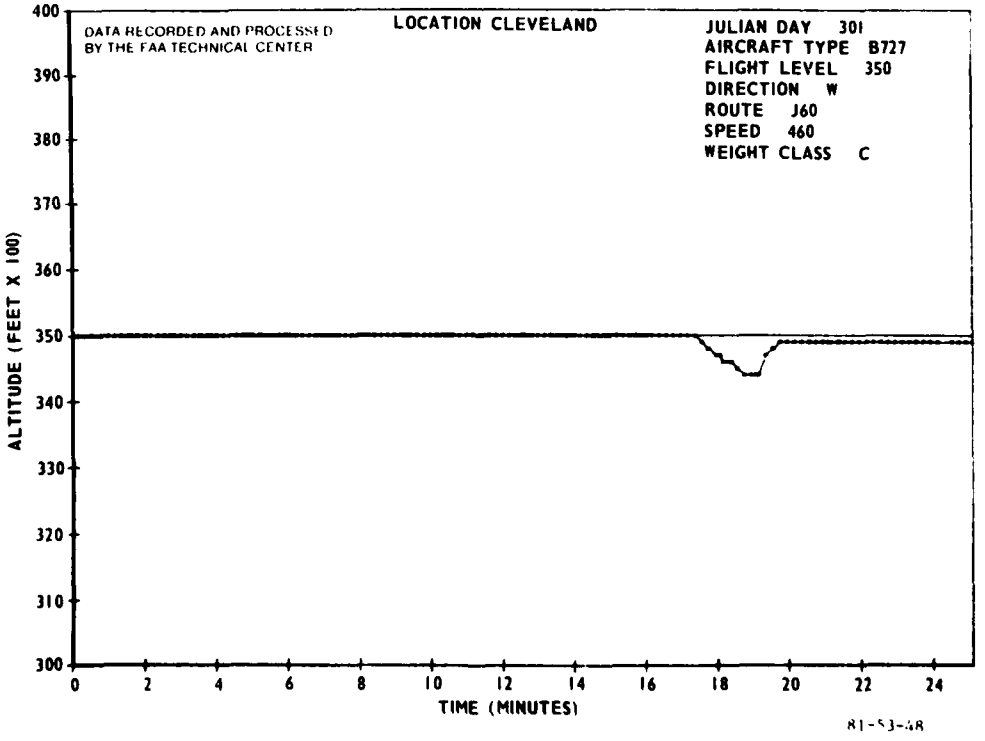

FIGURE 48. SPECIAL CASE 4

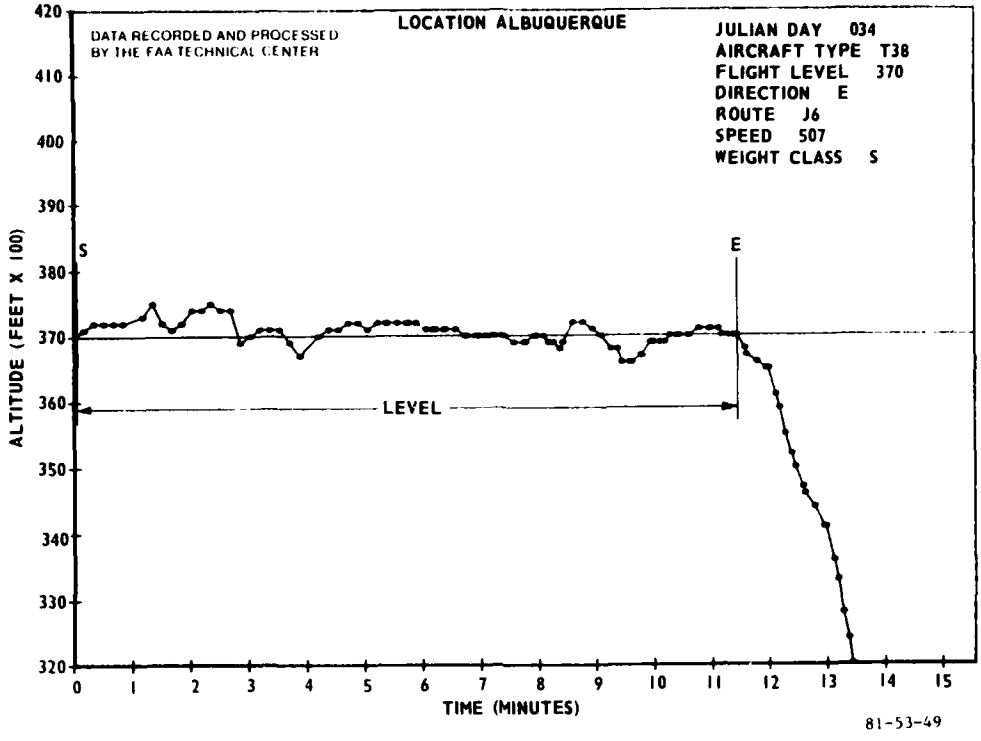

FIGURE 49. SPECIAL CASE 5

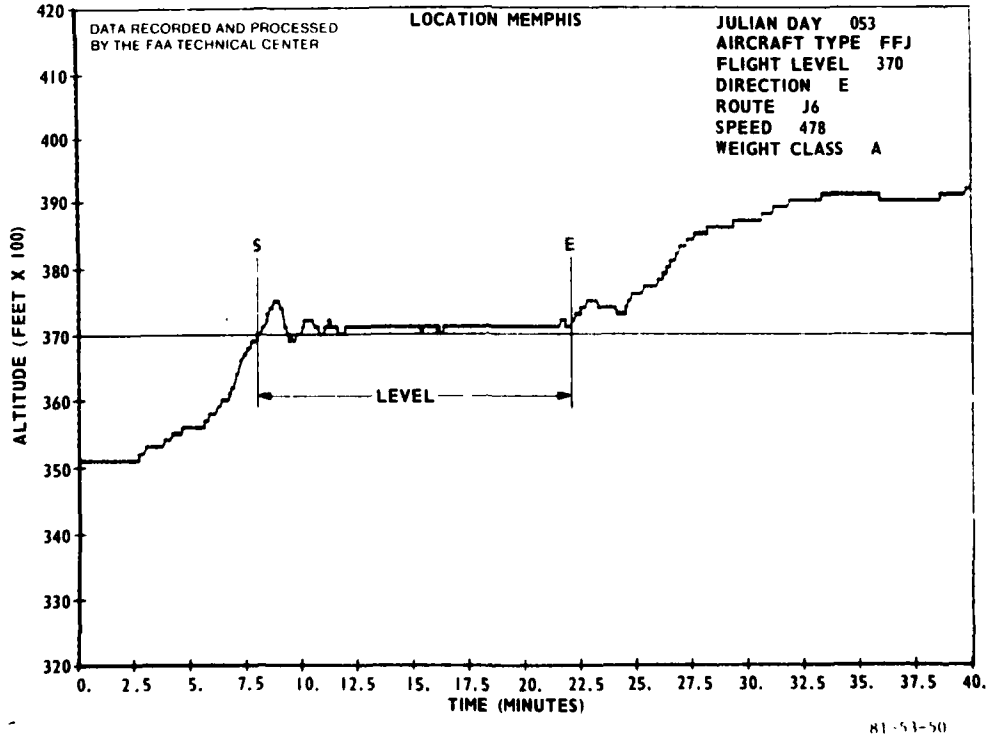

FIGURE 50. SPECIAL CASE 6

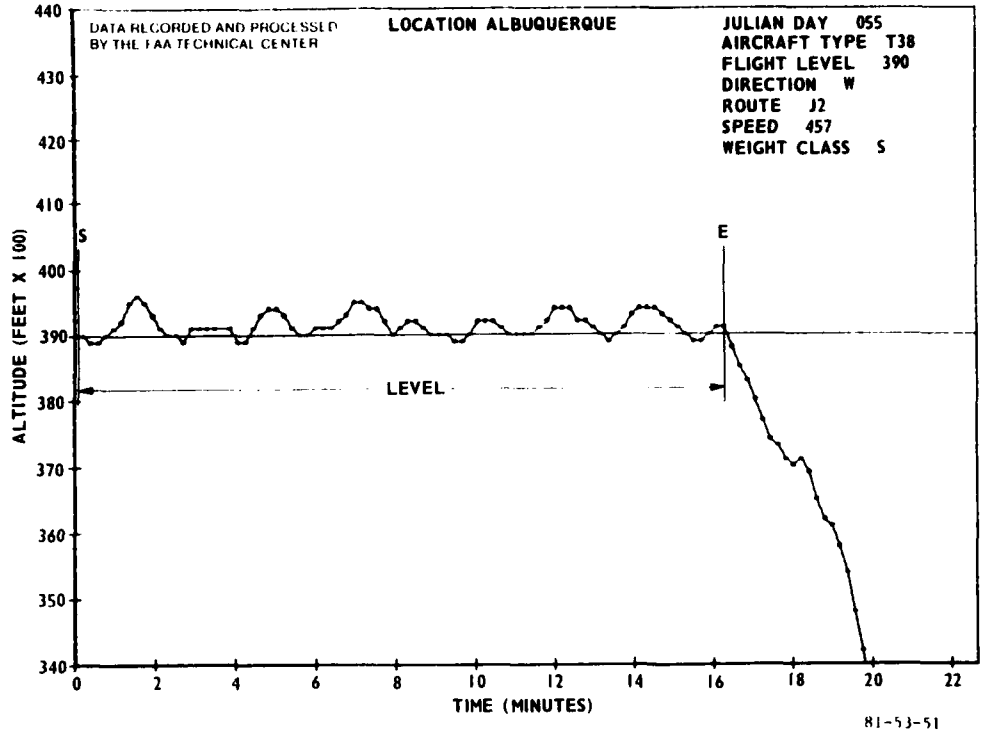

FIGURE 51. SPECIAL CASE 7

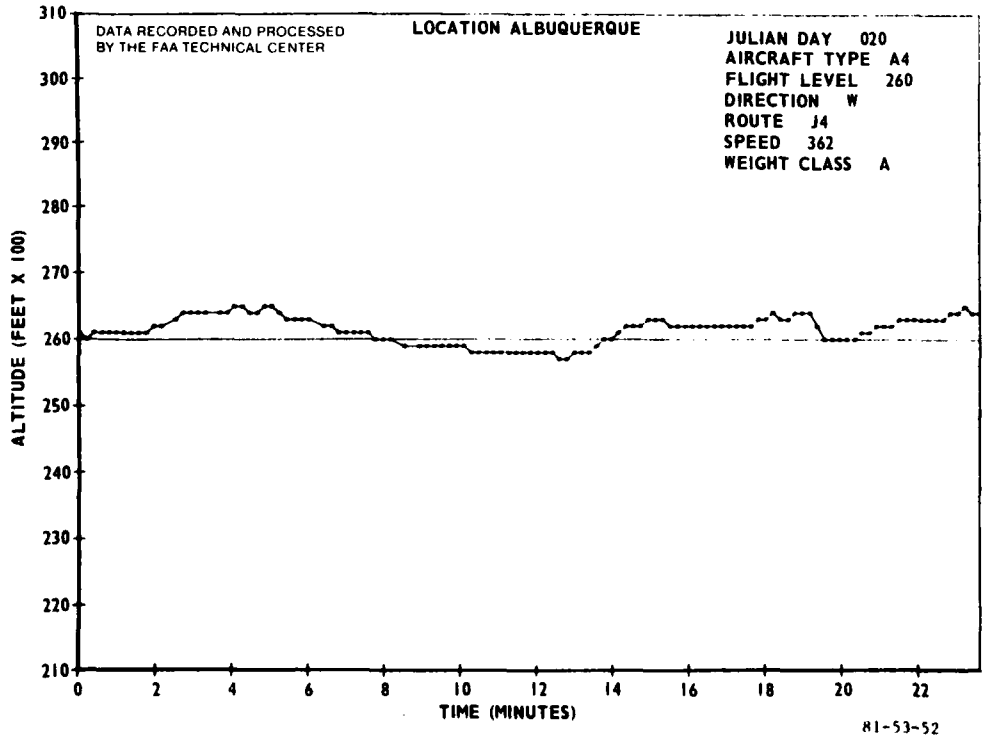

FIGURE 52. SPECIAL CASE 8

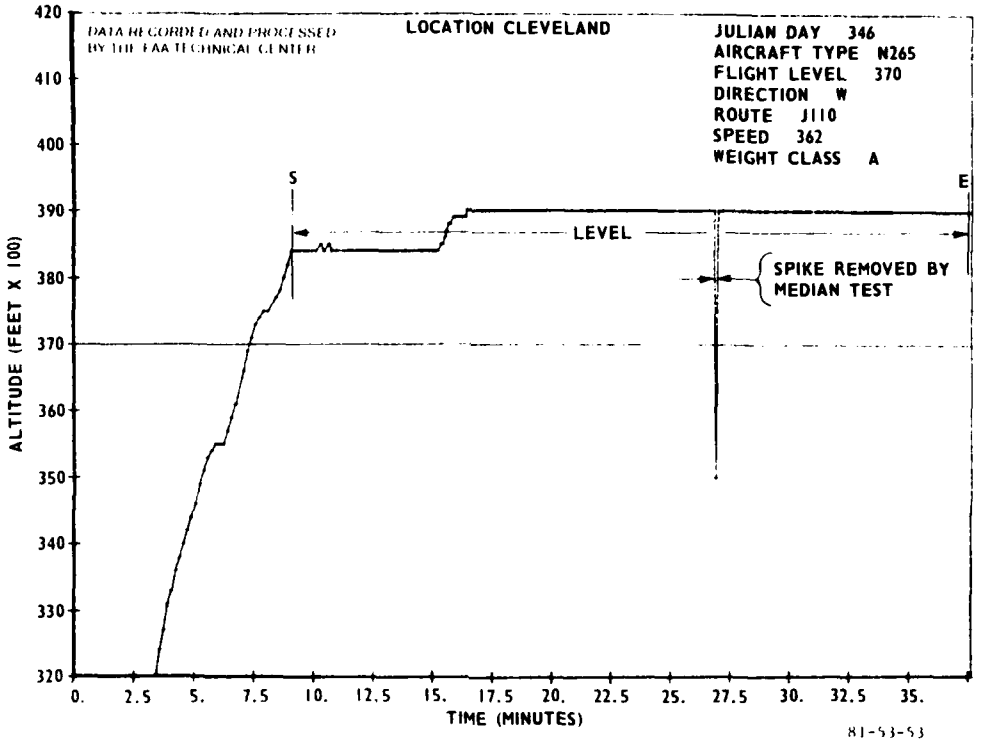

FIGURE 53. SPECIAL CASE 9

Several aircraft performed unexpected maneuvers because of conflicting traffic, weather conditions, or aircraft system constraints. Figures 54 to 56 are typical of maneuvers initiated by air traffic controllers to avoid conflicting traffic. In the first example (figure 54), the aircraft was directed from flight level 330 to a lower flight level, to avoid crossing traffic, and then back to flight level 330. In the second example (figure 55), the aircraft was in a normal descent from flight level 430 to 390, was instructed to climb and maintain flight level 410 until flight level 390 was clear, and 6 minutes later was instructed to proceed with descent to flight level 390. In the third example (figure 56), this aircraft was directed from flight level 240 to flight level 250; the crossing aircraft descended to a lower flight level; and this aircraft directed to return to flight level 240. Figure 57 is typical of a maneuver requested by pilots due to turbulent weather conditions. Not satisfied with the ride at flight level 330, he requested flight level 370; on ascent he decided to return to flight level 330; and he then requested and was granted flight level 290. Figures 58 and 59 are typical of maneuver employed when aircraft are too heavy to attain or maintain assigned altitude, respectively. In the first example (figure 58), the aircraft is in a slow climb to flight level 350, levels off at flight level 346 for about 4 minutes (step climbs), and then resumes climb to flight level 350. In the second example (figure 59), the aircraft is having trouble maintaining flight level 370 and requests a lower flight level. However, the controller was not able to approve a lower level due to traffic, and he was instructed to maintain altitude until lower flight levels were cleared.

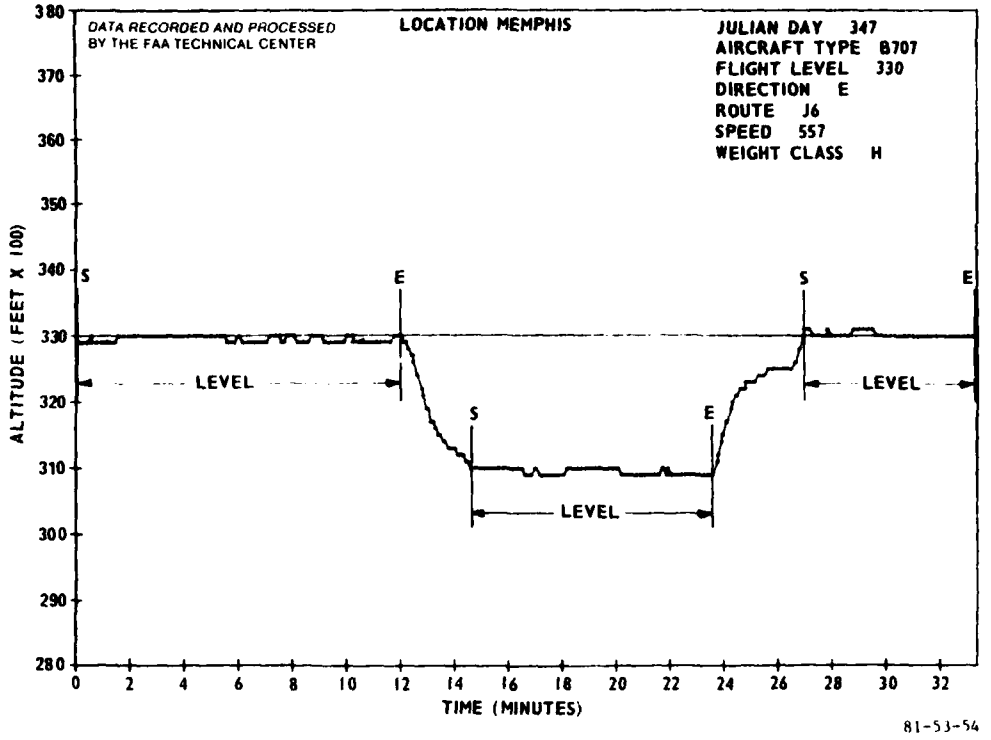

FIGURE 54. SPECIAL CASE 10

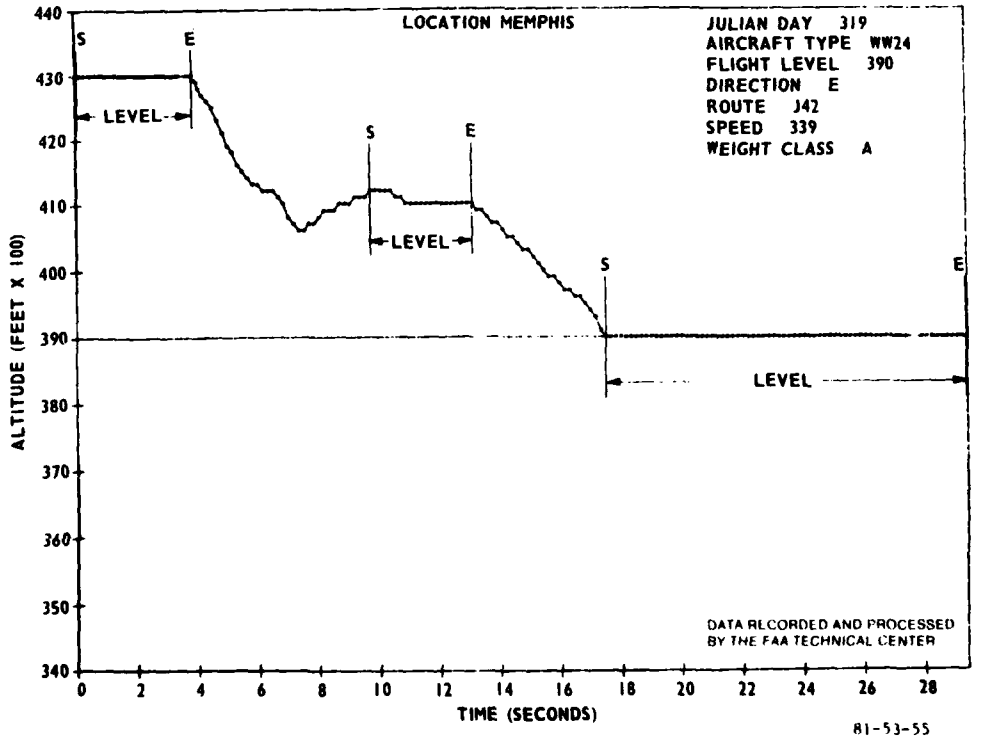

FIGURE 55. SPECIAL CASE 11

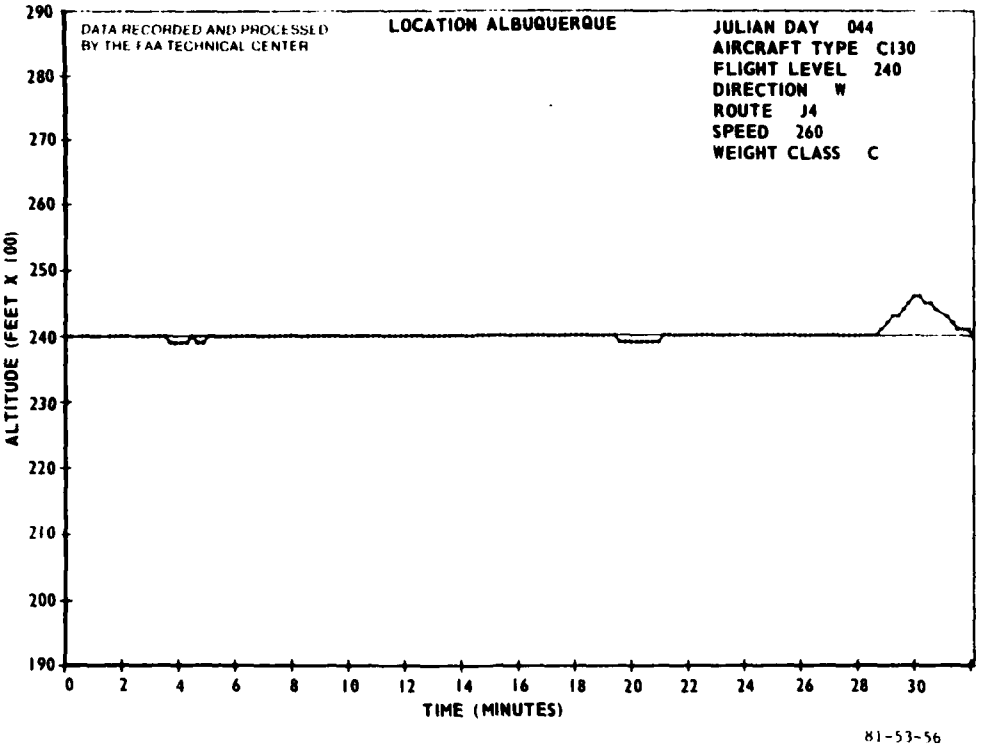

FIGURE 56. SPECIAL CASE 12

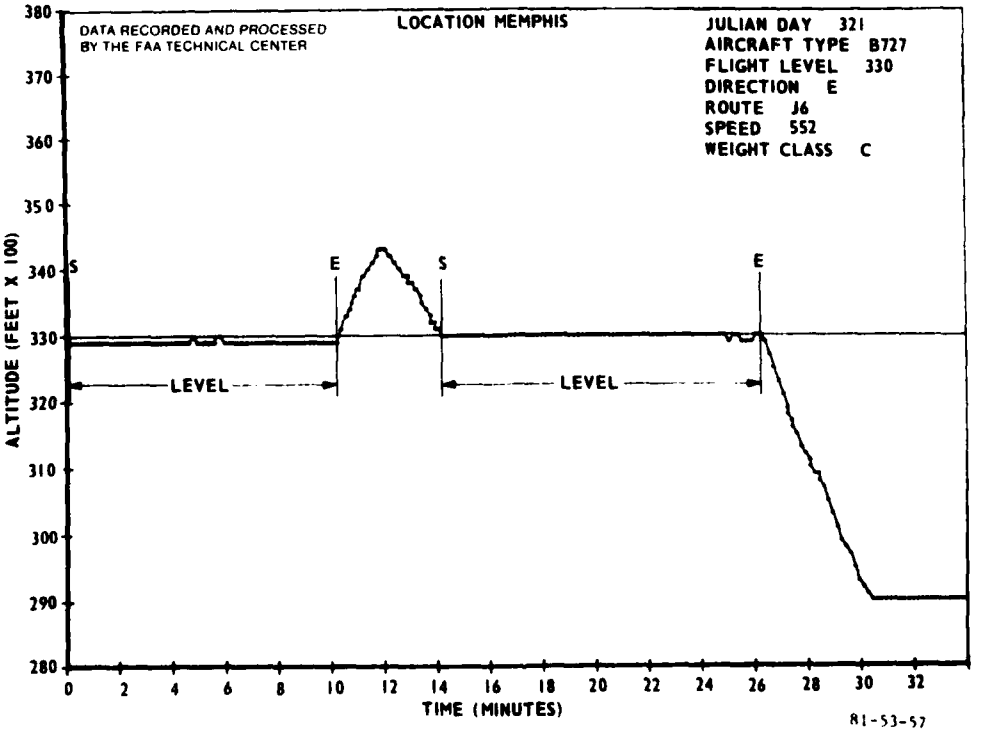

FIGURE 57. SPECIAL CASE 13

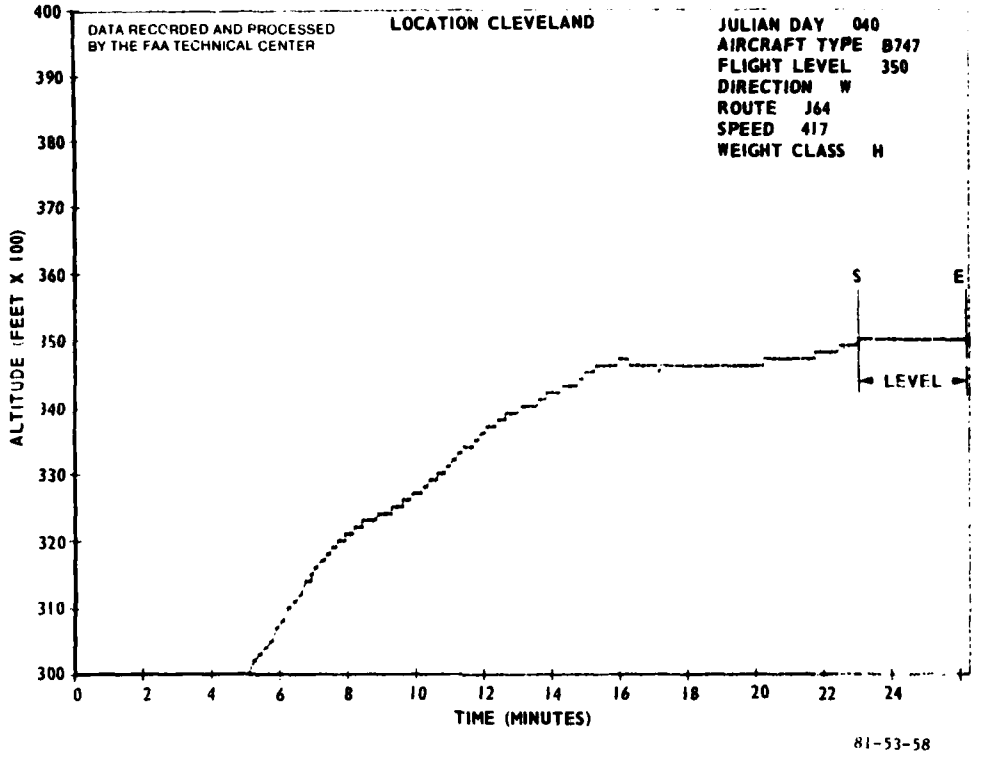

FIGURE 58. SPECIAL CASE 14

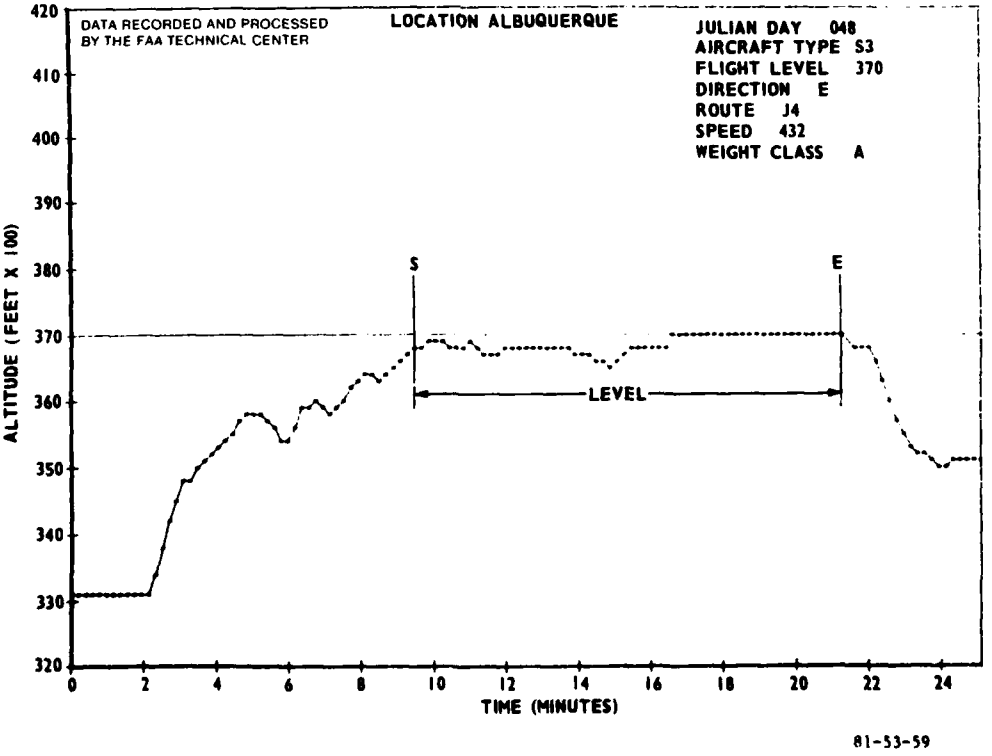

FIGURE 59. SPECIAL CASE 13

Malfunctions exhibited several unique situations. All situations characterized as malfunctions were deleted from the analysis. This is indicated on the figures by start and end vertical lines plotted at the same time-point. In some cases, the recorded data did not reflect any inconsistencies (figure 60). In this example, the pilot observed an inconsistency between his barometric altitude reading of 356 and his mode C altitude reading of 348 (an 800-foot difference!) He informed the controller of a probable air-data computer problem and requested a block altitude between 350 and 360. It was approved. Shortly after, the controller requested the pilot cut his altitude transmission to avoid confusion. This case demonstrates the reality of large vertical FTE's existing above flight level 290 that cannot be measured by the ATC system, even though both the pilot and controller are aware of the deviation and take precautionary actions. In other cases (figures 61 to 63), the recorded data reflect obvious inconsistencies that were later found to be the result of transponder, altimeter system, or autopilot malfunctions. The y scale on figure 61 is changed to 1,000 feet from flight level to more clearly demonstrate the 200-foot oscillations. At approximately 11 minutes into the track of figure 62, a malfunction exhibits an instantaneous change in transponded altitude of almost 4,000 feet. In this case the aircraft was in level flight at 370, and both the pilot and controller were aware of the malfunction. In figure 63, the pilot quickly informs the controller of an autopilot malfunction. The case shown in figure 64 is an extreme case of an aircraft system malfunction. In this example, the aircraft experienced an engine stall at about 36,000 feet during its ascent to flight level 370. It reported descending to flight level 240, and before the controller was able to assess the situation and issue an approval (less than 24 seconds), the aircraft already descended 1,400 feet. This was the only occurrence of its kind during this data collection. On descent, the engine was restarted and the aircraft resumed approved level flight at 290. This case demonstrates the possibility of an unapproved descent through several lower flight levels. The y scale in this case was changed to $\pm$ 10,000 feet to illustrate the entire vertical profile.

A final unique case is presented in figure 65. In this example, two aircraft with similar identities were within the same sector at flight levels 370 and 350. The controller instructed the aircraft at flight level 350 to ascend to flight level 390. Both aircraft started ascent to flight level 390. The controller intervened and corrected the misunderstanding. In this interval, the aircraft at flight level 370 was 1,100 feet above assigned flight level before returning.

Aircraft at other than odd-thousand-foot flight levels were confirmed as those given block altitudes or step-climbing. Once confirmed, these data were used in the analysis with assigned altitude set to confirmed altitude. One situation occurred where an aircraft was assigned an even-thousand-foot flight level of 300. Aircraft with misidentified beacon codes or those with the same beacon code as aircraft in other sectors were deleted from the analysis.

All but 133 aircraft altitudes were verified, and all augmented strip data were supplied except for 49 aircraft. These 182 aircraft were deleted from the analysis.

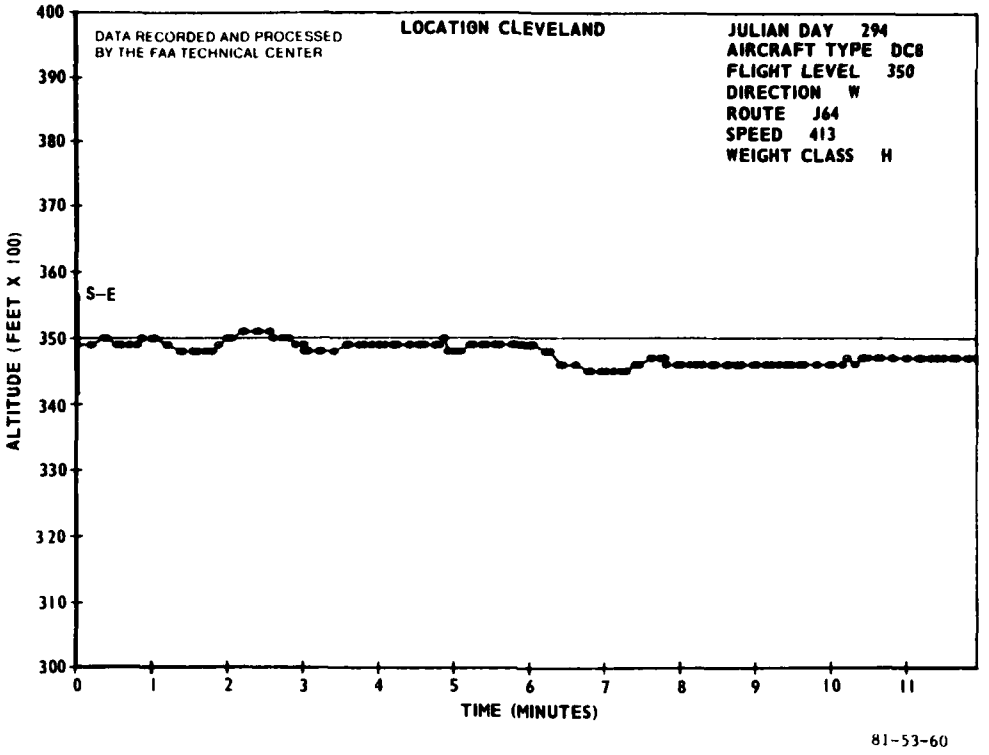

FIGURE 60. SPECIAL CASE 16

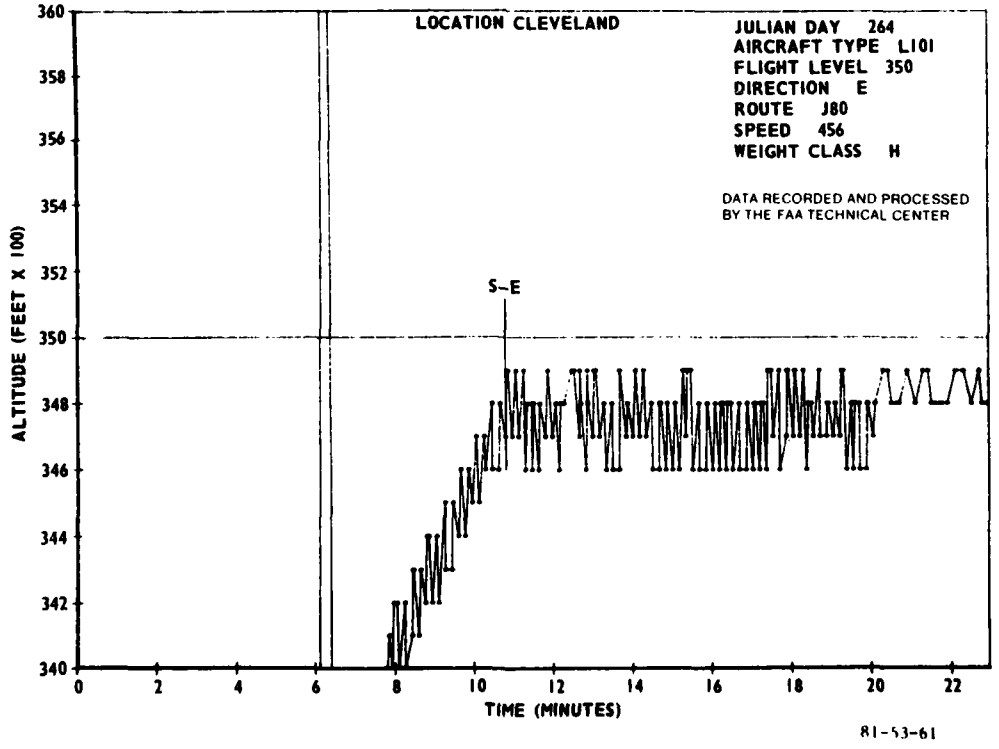

FIGURE 61. SPECIAL CASE 17

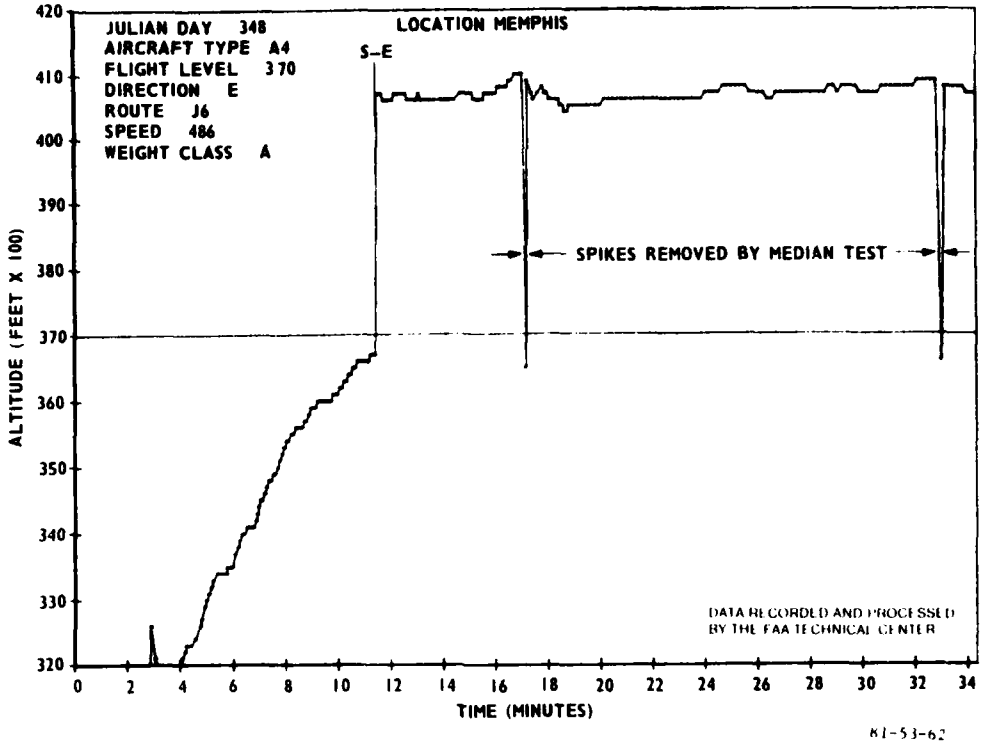

FIGURE 62. SPECIAL CASE 18

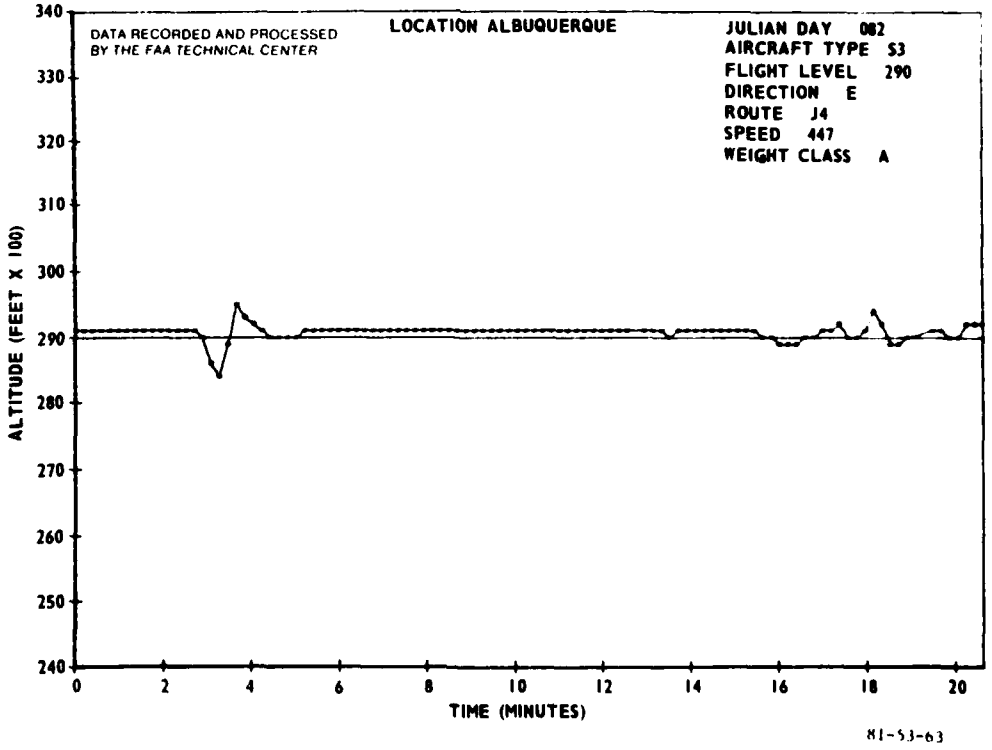

FIGURE 63. SPECIAL CASE 19

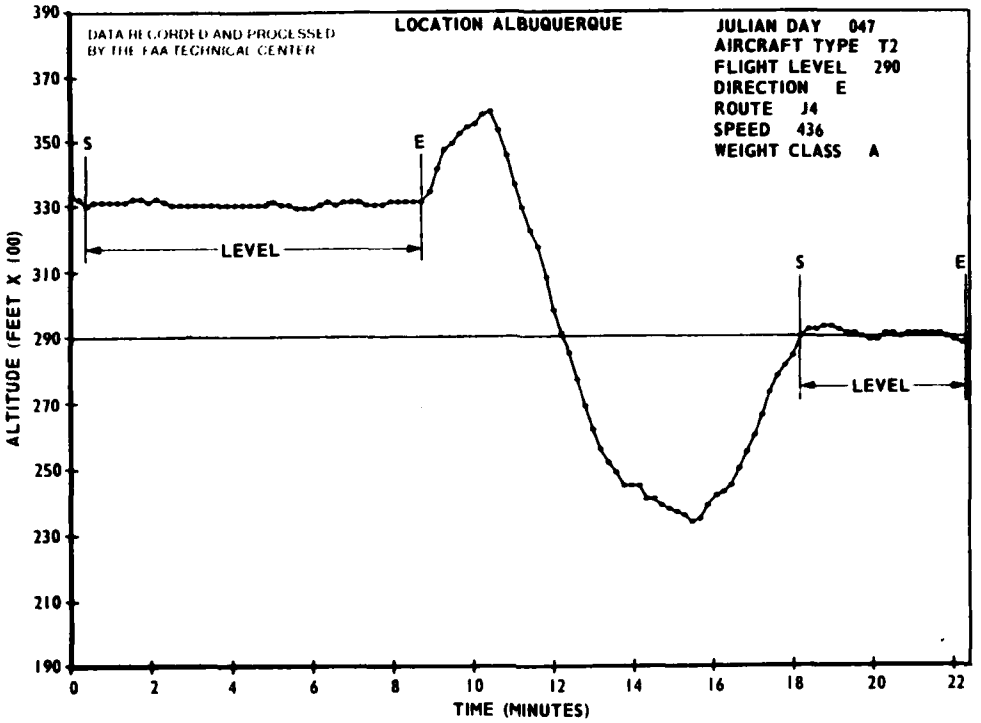

FIGURE 64. SPECIAL CASE 20

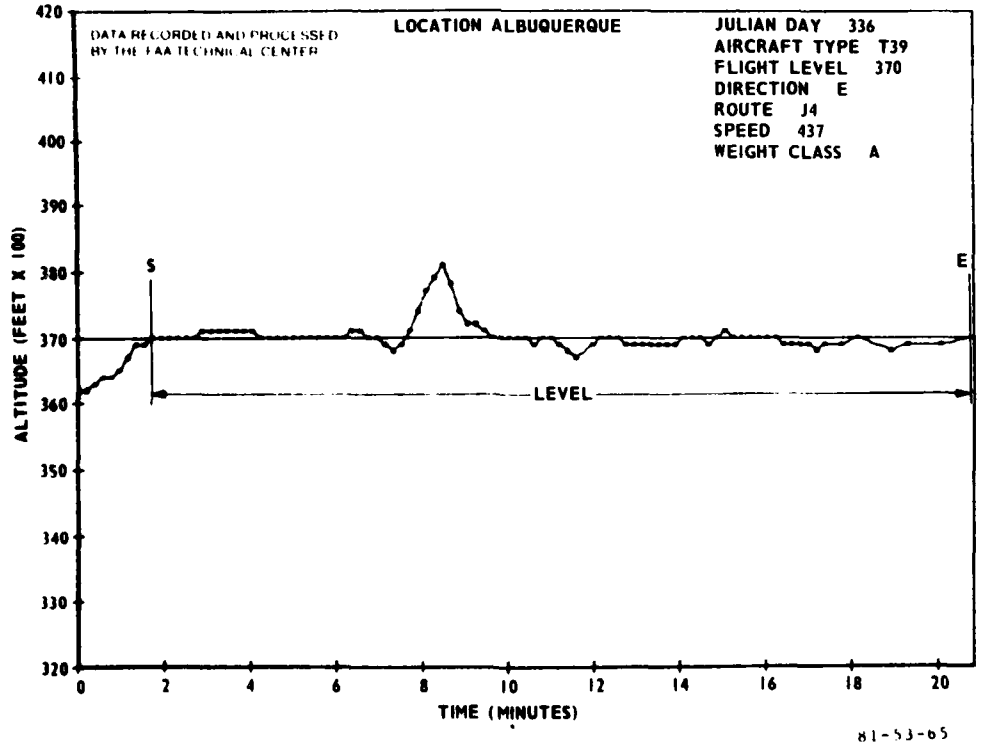

FIGURE 65. SPECIAL CASE 21

CONCLUSIONS

This report was written to demonstrate the utility of transponded mode C altitude in defining the nature of vertical flight technical error (FTE) and in discovering factors that would aid in properly structuring further data collection and analysis efforts designed to establish the feasibility of reducing vertical separation. It was apparent early on in this analysis that mode C afforded a distorted view of FTE. It included transmission and data processing errors, was quantized into 100-foot increments, and did not account for factors related to the aircraft's linkage system between the pressure input source, the encoder, the transponder, and the altimeter. An attempt was made to remove the majority of observable transmission and data processing errors with emphasis on mode C deviations from assigned altitude exceeding 300 feet. Quantization contributed to distorting statistical estimates mostly related to the frequency of small errors, and it prevented the smoothing of data, thus inhibiting the analysis of vertical velocity. However, it contributed little to the distortion of the frequency of large errors and was successfully handled by a distribution model building procedure. The factors related to the aircraft linkage system are believed to contribute mostly to the frequency of small errors related to defining the FTE core, and hopefully, did not adversely affect the frequency of large errors. By remaining aware of the distortions mentioned previously and taking precautionary measures in making inferences, mode C altitude provided a wealth of information related to FTE. Although the frequency of small errors (the distribution core) is surely distorted due to this approach, the frequency of large errors (the distribution tail) is felt to be a representative estimate of FTE. These assumptions can only be verified in a properly structured data collection effort — a necessary follow-on step to this report. Finally, a continual limitation to the construction of statistical procedures that plagued this, as well as previous efforts, was not being able to measure the time between independent observations.

HISTOGRAM DATA.

An aggregate time histogram was computed for the mode C altitude data collected during the lateral separation study over the en route centers of Cleveland, Memphis, and Albuquerque. It was a culmination of 14,168 aircraft level flight segments and represented 4,904 hours of data. The parametric estimates indicated a zero mean symmetric distribution heavier tailed than normal. Modified (the number of independent observations within each class interval were unknown) confidence intervals were computed about the height of each bar within the histogram. They illustrated a large uncertainty in values beyond 400 feet. This implies the lateral data collection was not large enough or structured properly to characterize the tail portion of vertical FTE.

MODEL DISTRIBUTION ESTIMATION.

A model distribution estimation procedure was established that enabled the computation of that portion of the vertical FTE distributior evidenced through mode C altitude. It indicated two suitable distribution types: a double-double exponential and the more general power-double exponential. The double-double exponential was more parsimonious and found to be adequate in representing the tail portion of the mode C altitude. The power-double exponential was required in order to evaluate the effect of quantization on parameter estimates.

The estimated mean, standard deviation, skewness, and kurtosis computed via the power-double exponential distribution were 0.0 feet, 57.1 feet, 0.0, and 7.4, respectively. It implied that quantization of vertical FTE, as represented in this effort, enlarged the standard deviation estimate by 4 feet (standard deviation estimate computed from quantized data was 61.2), and reduced the kurtosis estimate by 0.44 (kurtosis estimate computed from quantized data was 6.96). Since kurtosis is a measure of both core peakedness and tail heaviness, the fourth moment about the origin was instrumental in interpreting its distortion due to quantization.

ATTRIBUTE CLASSIFICATION.

Analysis of attribute data was conducted on all aircraft observed in level flight from 5 to 35 minutes. This range of time intervals was chosen in an attempt to provide homogeneous data sets. Again, if the time between independent samples were known, it would define the proper track length. Under these loose conditions, this portion of the analysis revealed that the proportion of 300-foot or greater errors for commercial, general aviation (with NASA aircraft removed), and large military (greater than 60,000 pounds) aircraft was 0.774, 6.23, and 3.8, respectively, independent of whether the data was gathered over Cleveland, Memphis, or Albuquerque En Route Centers. Light military aircraft (less than 60,000 pounds) exhibited a significantly larger percentage of 300-foot or greater errors than both commercial or general aviation aircraft. Further, the proportion of light military aircraft errors was not independent of data gathering locations with 35.3 percent over Albuquerque, and 23.7 percent over Cleveland and Memphis.

The proportion of 300-foot or greater errors was tested with respect to altitude and speed. It revealed independence for (1) commercial aircraft below flight level 410 and at speeds greater than 350 knots, with a higher incidence of errors at flight level 410 and at speeds less than 350 knots; (2) general aviation aircraft (NASA aircraft removed) below flight level 410 and at all speeds observed with a higher incidence of errors for flight levels at or greater than 410; and (3) military aircraft less than 60,000 pounds over Alburquerque, at and above flight level 290, and at all speeds observed with a lower incidence of errors below flight level 290. The loose condition that all aircraft in level flights from 5 to 35 minutes be employed during this analysis prevented conclusive results.

LARGE MODE C ALTITUDE ERROR CORRELATIONS.

A preliminary investigation was conducted to aid in revealing whether there existed some degree of correlation between (1) large mode C altitude deviations (400 feet or greater) and mode C velocity estimates and (2) large mode C altitude deviations and lateral deviations. During the first investigation, two divergent relationships emerged: one for FTE deviations occurring while in level flight at odd 1,000-foot increments and one for any occurrence of level flight other than at odd 1,000-foot increments. It became clear that this distinction would ripple into the computation of expected number of aircraft collisions. Further, the topic of statistically combining long-term deviations, as are expected in other aircraft height-keeping components (such as pitot-static and altimeter instrument) with short-term FTE deviations was addressed. This initial study did not provide a solution to this problem, rather it indicated an area that required further analysis. The second investigation did reveal any obvious relationship between large mode C altitude deviations and lateral deviations.

SPECIAL CASES.

A look at typical cases revealed many situations that cause an aircraft to be at altitudes other than those assigned. They range from mild turbulence to complete aircraft engine failure.

RECOMMENDATIONS

The data employed for this study were not structured for the vertical domain. It is recommended that an additional effort be conducted to confirm the results discovered during this analysis and that this effort include a preliminary study that (1) ensures the data collection is efficiently structured, (2) obtains auxiliary information not available through mode C data to establish the time between independent samples and determine the altimeter linkage system error distribution, and (3) ensures comparable data sets. Of the three en route centers employed for data gathering during this effort, Albuquerque provided the best mix of aircraft users. It is over mountainous terrain, is centrally located over CONUS, and exhibits aircraft in level flight for long-time durations. It is recommended that this location be utilized in further efforts.

Two other known major vertical error components (static pressure and altimeter instrument error) were not measured during this study. Estimating vertical velocity, statistical combining and gathering data with both short-term and long-term deviations, and processing aircraft in level flight at other than odd-thousand-foot increments requires further analysis. Vertical safety at higher altitude can only be evaluated if all contributing factors are considered.

It is recommended that a further data collection be structured to obtain the distribution of total vertical error. The effect of improvements to aircraft systems as related to the estimate of the potential risk of aircraft collisions and ultimately to vertical separation safety can only be evaluated when this distribution is known.

REFERENCES

1. Report on Vertical Separation Study NAT Region, IATA Document Gen. 1951, March 1964.

2. Kolniek, J., and Bentley, B., Random Deviations from Stabilized Cruise Altitude of Commercial Transports at Altitudes up to 40,000 Feet with Autopilot in Altitude Hold, NASA-TN-D-1950, July 1963.

3. Reich, P. G., Separation Standards in the North Atlantic Region, 1965-71, in the Light of Recent Measurements of Flying Errors, RAE-TR-64043, 1964.

4. Reich, P. G., and Anderson, R. G., Specifying the Calibration of Static Pressure Systems for the Safe Use of 1,000 Feet Vertical Separation Standard in North Atlantic Jet Traffic, RAE-TR-66156, 1966.

5. Edwards, Lloyd, DOD-AIMS Pitot-Static Systems Calibrations and AIMS Systems Test Summary Report, Edwards AFB, California, Technical Report No. 72-51, October 1973.

6. Lambdin, R., Maintenance of Pitot-Static System Calibration, Wright-Patterson AFB, Ohio, July 1976.

7. Bone, A. G., and Scard, M., Altimeter Systems for Automatic Altitude Reporting with Particular Reference to System and Instrument Accuracy, RAE-TR-70064, April 1970.

8. Sheppard, W. F., On the Calculation of the Most Probable Values of Frequency Constants for Data Arranged According to Equidistant Division of Scale, Vol. XXIX, 1898.

9. FAA Contractions Handbook, 7340.1F 1979, p. L-1.

10. FAA, Advisory Circular, 150/5325-5B, July 30, 1975, p. 3.

BLANK PAGE

APPENDIX A

CRITERIA FOR LEVEL FLIGHT TIME INTERVALS

This appendix defines the criteria for selecting starting and ending times of altitude data for the vertical FTE study. It was constructed to include as much data as possible for a preliminary analysis. Subsequent examination of those special cases that were not correctly bracketed by these general criteria were corrected manually.

Case 1: Aircraft maintains level flight, but with variation.

Criterion: Constant level flight is defined as the time interval that an aircraft flys about an assumed flight level with no obvious intention of ascending (descending).

Case 2: An aircraft ascends (descends) at a constant rate, and then maintains a constant flight level.

Criterion: Level flight starts at the time where ascention (descention) ends.

Case 3: An aircraft maintains constant level flight and then ascends (descends) at a constant rate.

Criterion: Level flight ends at the time ascention (descention) starts.

Case 4: An aircraft maintains a constant flight level, ascends (descends) at a very slow rate, or waivers about the assumed flight level, and then ascends (descends) at a higher constant rate.

Criterion: Level flight ends at the time there is no doubt that the aircraft's intention was to start ascent (descent).

Case 5: An aircraft ascends (descends) at a constant rate, then ascends (descends) at a very slow rate, or waivers about the assumed flight level, and then maintains a constant flight level.

Criterion: Level flight starts at the time there is no doubt that the aircraft's intention was to discontinue ascending (descending).

Case 6: An aircraft maintains a constant flight level and another aircraft is apparently transmitting on the same beacon code.

Criterion: Choose the portion of the data set that has only one aircraft transmitting.

APPENDIX B

COMPUTATION OF FLIGHT TECHNICAL ERROR MOMENTS FROM MODE C ALTITUDE HISTOGRAMS

This appendix will utilize the equivalence between the nth mean power

$$\overline{g^n(t)} = \lim_{T \to \infty} \frac{1}{2T} \int_{-T}^{T} g^n(t)dt \qquad (1)$$

of the time function g(t) and the nth moment

$$\gamma^{(n)} = \int_{-\infty}^{\infty} x^{(n)} f(x)dx \qquad (2)$$

of the frequency function f(x) to estimate moments about the origin from data samples of variable time duration. The proof of the equality between equations 1 and 2 is given in reference 1 and will not be repeated in this appendix. Only its generalization to samples of variable time duration and approximations that utilize 100-foot increments will be presented.

Consider an aircraft vertical track of time duration T with flight technical error (FTE) amplitude g(t) as depicted in figure B-1. Divide this interval into N elements of variable length Δt_i. Let $g(t_i)$ be the amplitude of g(t) during the time interval $\Delta t_i = (t_i, t_{i+1})$

Then

$$\overline{g^n(t)} = \lim_{\substack{T \to \infty \\ \Delta t_{max} \to 0}} \sum_{i=1}^{N} \frac{g^n(t_i) \cdot \Delta t_i}{T}$$

where Δt_{max} is the largest Δt_i. $i = 1, 2, ---N.$

For Δt_i small (in the case of mode C altitude less than or equal to 12 seconds), and g(t) a constant c_i over the interval Δt_i; the function $\overline{g^n(t)}$ can be approximated by

$$\widehat{g^n(t)} = \sum_{i=1}^{N} \frac{c_i^n \cdot \Delta t_i}{T}$$

Let the value c represent the average value of g(t) rounded to the nearest 100 feet. Due to this rounding procedure, it is very likely that a particular value of c will be repeated during r different intervals (figure B-1). Assume that c_i ranges over the values $k \cdot 100$ for $j = -10, -9, ---, 0, 1, ---, 10$. Then $\widehat{g^n(t)}$ can be rewritten as

$$\widehat{g^n(t)} = \sum_{j=-10}^{10} \frac{(j \cdot 100)^n \Delta t_j}{T}$$

where Δt_j is the total amount of time c is equal to $j \cdot 100$.

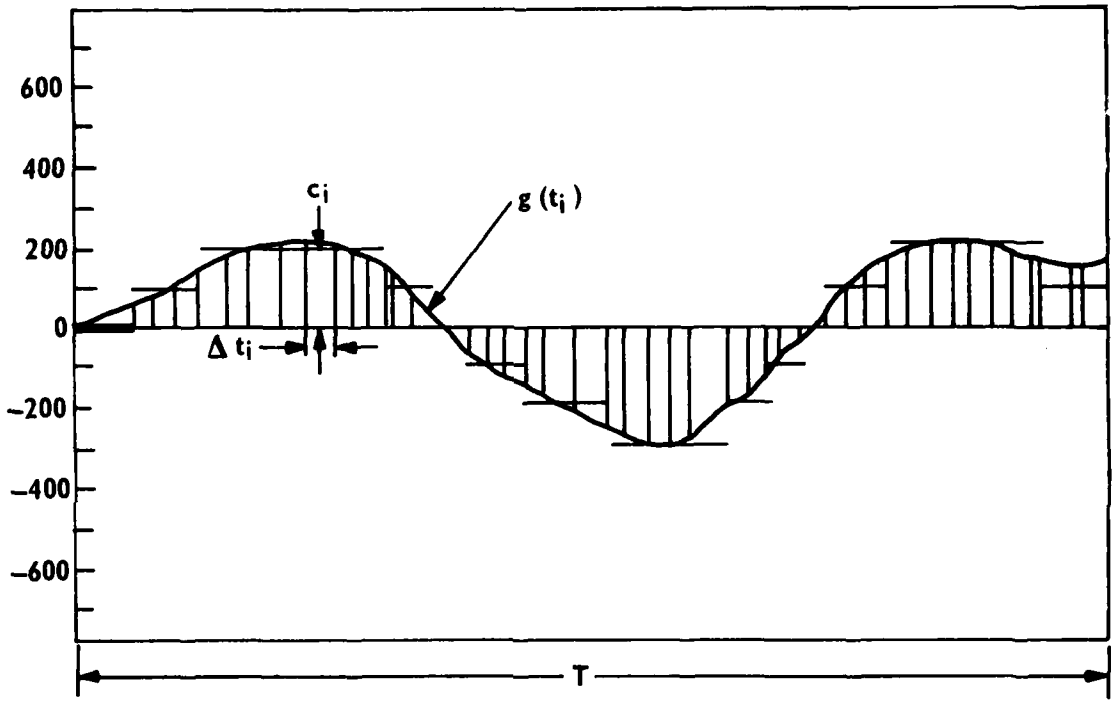

FIGURE B-1. FLIGHT TECHNICAL ERROR AMPLITUDE

REFERENCES

Statistical Theory of Communications, John Wiley and Sons, Y. W. Lee 1960, pp. 200-206.

APPENDIX C

QUANTILE CONFIDENCE LIMITS

From each observed frequency $\hat{h}$ within a class interval, the upper and lower confidence limits for any given probability θ can be obtained (reference 1). An upper limit $\overline{\theta}$ was chosen so that the probability of frequencies smaller than or equal to $\hat{h}$ was 2.5 percent. A lower limit $\underline{\theta}$ was chosen so that the probability of frequencies larger than or equal to $\hat{h}$ was 2.5 percent. Mathematically, these respective probabilities can be represented by the following two equations.

$$P_r(h \geq \hat{h}; \theta = \underline{\theta}) = \sum_{x=\hat{x}}^{n} \binom{n}{x} \underline{\theta}^{x}(1-\underline{\theta})^{n-x} = .025$$

and

$$P_r(h \leq \hat{h}; \theta = \overline{\theta}) = \sum_{x=o}^{\hat{x}} \binom{n}{x} \overline{\theta}^{x}(1-\overline{\theta})^{n-x} = .025$$

where n is the number of samples and $\hat{x} = \hat{h}\, n$.

For $\hat{h} \geq .1$ and n large, a transformation is implemented to obtain a variable independent of θ (reference 2). The confidence limits are approximated by

$$\begin{matrix} 2 \arcsin\left(\sqrt{\overline{\theta}}\right) \\ 2 \arcsin\left(\sqrt{\underline{\theta}}\right) \end{matrix} = 2 \arcsin \left[\sqrt{\frac{\hat{h} \cdot n \pm \frac{1}{2}}{n}}\right] \pm \frac{1.96}{\sqrt{n}}$$

For $\hat{h} \leq .1$ and n large, the probabilities approach a Poisson distribution, and the cumulative Poisson can be expressed by a chi-square variable (reference 3). The confidence limits are approximated by

$$n\,\overline{\theta} = \tfrac{1}{2}\chi^2_{.975} \qquad \text{for } f = 2(\hat{x}+1)$$

and

$$n\,\underline{\theta} = \tfrac{1}{2}\chi^2_{.025} \qquad \text{for } f = (2\hat{x})$$

where $x = \chi^2_\gamma$ represents the 100γ percent probability that a chi-square distributed variable with f degrees of freedom is less than or equal to x.

REFERENCES

1. Statistical Theory with Engineering Applications, John Wiley and Sons, A. Hald, 1952, pp. 697, 700.

2. Ibid., p. 685

3. Ibid., p. 722

APPENDIX D

DISTRIBUTION MODELS

A. Normal Probability Density Function (Reference 1)

$$f(x) = \frac{1}{\sqrt{2\pi}\,\sigma}\, e^{\frac{-x^2}{2\sigma^2}} \qquad -\infty < x < \infty \qquad 0 < \sigma^2 < \infty$$

Mean = zero

Skewness = zero

Variance = σ^2

*Kurtosis = 3

B. Double Exponential Probability Density Function (Reference 2)

$$f(x) = \frac{1}{2\beta}\, e^{\frac{-|x|}{\beta}} \qquad -\infty < x < \infty \qquad 0 < \beta < \infty$$

Mean = zero

Skewness = zero

Variance = $2\beta^2$

Kurtosis = 6

C. Double-Double Exponential Probability Density Function (Reference 3)

$$f(x) = \alpha\left[\frac{1}{2\beta_1}\, e^{\frac{-|x|}{\beta_1}}\right] + (1-\alpha)\left[\frac{1}{2\beta_2}\, e^{\frac{-|x|}{\beta_2}}\right] \qquad -\infty < x < \infty \qquad 0 < \beta_1 < \beta_2 < \infty \qquad 0 \leq \alpha \leq 1$$

Mean = zero

Skewness = zero

$$\text{Variance} = 2\left[\alpha\,\beta_1{}^2 + (1-\alpha)\,\beta_2{}^2\right]$$

$$\text{Kurtosis} = 6\left\{\frac{\left[\alpha + (1-\alpha)\,\rho^4\right]}{\left[\alpha + (1-\alpha)\,\rho^2\right]^2}\right\}$$

where $\rho = \dfrac{\beta_2}{\beta_1}$

D. Power Exponential Probability Density Function (Reference 4)

$$f(x) = k\,\phi^{-1}\,e^{-\frac{1}{2}\left|\frac{x}{\phi}\right|^{\left(\frac{2}{1+\beta}\right)}} \qquad -\infty < x < \infty$$

$$-1 < \beta \leq 1$$

$$0 < \phi < \infty$$

where $k^{-1} = \Gamma\left(1 + \dfrac{1+\beta}{2}\right) 2^{\left(1 + \frac{1+\beta}{2}\right)}$

Mean = zero

Skewness = zero

$$\text{Variance} = 2^{(1+\beta)}\left[\frac{\Gamma\left(\frac{3}{2}(1+\beta)\right)}{\Gamma\left(\frac{1}{2}(1+\beta)\right)}\right]\phi^2$$

$$\text{Kurtosis} = \frac{\Gamma\left(\frac{5}{2}(1+\beta)\right)\cdot\Gamma\left(\frac{1}{2}(1+\beta)\right)}{\left[\Gamma\left(\frac{3}{2}(1+\beta)\right)\right]^2}$$

E. Generalized t Probability Density Function (Reference 5)

$$f(x) = \frac{c\,\eta(\phi,c)}{2\Gamma\left(\frac{1}{c}\right)}\left[\nu^{\frac{1}{c}}\frac{\Gamma\left(\nu+\frac{1}{c}\right)}{\Gamma(\nu)}\right]\left[1+\frac{(\eta(\phi,c)\,|x|)^c}{\nu}\right]^{-\left(\nu+\frac{1}{c}\right)}$$

$$-\infty < x < \infty$$

$$0 < c < \infty$$

$$c\,\nu > 2$$

$$0 < \phi < \infty$$

where $\eta(\phi,c) = \phi^{-1}\left[\frac{\Gamma\left(\frac{3}{c}\right)}{\Gamma\left(\frac{1}{c}\right)}\right]^{\frac{1}{2}}$

ν = degrees of freedom

Mean = zero

Skewness = zero

$$\text{Variance} = \left[\nu^{\frac{2}{c}}\frac{\Gamma\left(\nu-\frac{2}{c}\right)}{\Gamma(\nu)}\right]\phi^2$$

Kurtosis - not computed.

F. Power - Double Exponential Probability Density Function

$$f(x) = \alpha\left[k\,\phi^{-1}\,e^{-\frac{1}{2}\left|\frac{x}{\phi}\right|^{\left(\frac{2}{1+\beta_1}\right)}}\right] + (1-\alpha)\left[\frac{1}{2\beta_2}\,e^{-\frac{|x|}{\beta_2}}\right]$$

$$-\infty < x < \infty$$

$$-1 < \beta_1 \leq 1$$

$$0 < \phi < \infty$$

$$0 < \beta_2 < \infty$$

$$0 \leq \alpha \leq 1$$

where $k^{-1} = \Gamma\left[1+\left(\frac{1+\beta_1}{2}\right)\right]2^{\left(1+\left(\frac{1+\beta_1}{2}\right)\right)}$

Mean = zero

Skewness = zero

$$\text{Variance} = \alpha\left[2^{(1+\beta_1)}\,\frac{\Gamma\left(\frac{3}{2}(1+\beta_1)\right)}{\Gamma\left(\frac{1}{2}(1+\beta_1)\right)}\,\phi^2\right] + 2(1-\alpha)\,\beta_2{}^2$$

$$\text{Kurtosis} = \frac{\alpha\left\{2^{2\cdot(1+\beta_1)}\left[\frac{\Gamma\left(\frac{5}{2}(1+\beta_1)\right)}{\Gamma\left(\frac{1}{2}(1+\beta_1)\right)}\right]\right\} + 24(1-\alpha)\,\rho^4}{\left[\alpha\left\{2^{(1+\beta_1)}\left[\frac{\Gamma\left(\frac{3}{2}(1+\beta_1)\right)}{\Gamma\left(\frac{1}{2}(1+\beta_1)\right)}\right]\right\} + 2(1-\alpha)\,\rho^2\right]^2}$$

where $\rho = \frac{\beta_2}{\phi}$

*Kurtosis = $\frac{\text{4th moment about the orign}}{(\text{2nd moment about the orign})^2}$

REFERENCES

1. Abromowitz, M., and Stegun, I. A., Handbook of Mathematical Functions, Dover Publications Inc., New York, 1972, p. 930.

2. Ibid, p. 930.

3. Busch, A., and Colamosca, B., Navigational System Requirements Via Collision-Risk Model, p. 4.

4. Box, G., and Tiao, G., Bayesian Inference In Statistical Analysis, Addison-Wesley Publishing Company, 1973, pp. 156-158.

5. Hunter, Prof. S., Notes On A Generalized Cauchy Distribution, Princeton University.

APPENDIX E

MODIFIED MAXIMUM LIKELIHOOD TECHNIQUE

Assume that $f(x,\theta)$ is a known density function with an unknown parameter θ. One method of estimating θ was given by R. A. Fisher and is called the method of maximum likelihood. It consists of constructing the joint probability density function

$$L = f(x_1, x_2, ---x_n, \theta) = f(x_1, \theta)\ f(x_2, \theta) --- f(x_n, \theta)$$

of n random samples $x_1, x_2, ---x_n$ taken from the population of $f(x,\theta)$. The maximum likelihood estimate is that value $\hat{\theta}$ which maximizes L for the given random sample (Reference 1).

Let the n random samples be grouped into k class intervals with n_i observations in class interval i. Then L, the maximum likelihood function, can be approximated

$$L = p(y_1)^{n1}\ p(y_2)^{n2} --- p(y_k)^{nk} = \prod_{i=1}^{k} p(y_i)^{n_i}$$

where $p(y_i)$ is the probability of an observation falling into the ith class interval centered at y_i (reference 2).

If only the proportion of random samples $l_i = \frac{n_i}{n}$ within each class interval i were known, instead of the number of random samples n_i, the maximum likelihood function L could be replaced by a modified maximum likelihood function $\hat{L}$.

Consider that $\hat{L} = p(y_1)^{l1}\ p(y_2)^{l2} --- p(y_k)^{lk} = \prod_{i=1}^{k} p(y_i)^{li}$

then $$\ln \hat{L} = \ln \left[p(y_1)^{l1}\ p(y_2)^{l2} --- p(y_k)^{lk} \right]$$

$$= \sum_{i=1}^{k} \ln \left[p(y_i)^{li} \right]$$

$$= \sum_{i=1}^{k} l_i . \ln \left[p(y_i) \right]$$

$$= \sum_{i=1}^{k} \left(\frac{n_i}{n}\right) \ln \left[p(y_i)\right]$$

$$= \frac{1}{n} \sum_{i=1}^{k} \ln \left[p(y_i)^{n_i}\right]$$

$$= \frac{1}{n} \left\{ \ln \left[p(y_1)^{n1} \quad p(y_2)^{n2} \quad \text{---} \quad p(y_k)^{nk} \right] \right\}$$

$$= \frac{1}{n} \ln L$$

Since lnL and $\ln\hat{L}$ only differ by the constant n, then the value $\hat{\theta}$ that maximizes L will also be the maximum value for $\hat{L}$.

REFERENCES

1. Advanced Theory of Statistics, Vol. 2, 3rd Edition, Kendall, M., and Stuart, A., 1973, Hafner Pub. Co. p.37.

2. Ibid, p. 49.

APPENDIX F

AIRCRAFT WEIGHT CATEGORIES

This appendix was constructed by cross-referencing each aircraft type observed in the data collection with "Jane's All the World's Aircraft" encyclopedia, and estimating the average takeoff weight for each aircraft. These weights were then grouped into one of five classes as defined in table 8 in the main section of this report. Each aircraft type and weight class are listed below.

Aircraft Type	Weight Class	Aircraft Type	Weight Class	Aircraft Type	Weight Class
A3	B	C500	S	L329	A
A4	A	C501	A	L382	B
A5	B	C5A	H	LR23	S
A6	A	CT39	A	LR24	A
A7	A	DA10	A	LR25	A
A10	A	DC8	C	LR35	A
AC6	S	DC9	B	LR36	A
AC21	A	DC10	H	MU2	S
AC69	S	DC85	C	N265	A
AC6T	S	DC86	C	P3	C
AV8	S	DC9A	B	P51	S
B52	H	E2	A	PAYE	S
B57	A	F4	A	RF8	S
B707	H	F5	A	S3	A
B720	C	F8	A	SW2	S
B727	C	F14	B	T2	A
B737	B	F15	A	T33	S
B747	H	F16	A	T37	A
BA11	B	F28	B	T38	S
BE10	S	F100	A	T39	A
BE20	S	F101	A	T43	B
BE58	S	F102	A	T43A	B
BE60	S	F104	A	TA4	A
BE90	S	F106	A	TA4J	A
B7S	C	F111	B	TC4	A
C5	H	FA10	A	VC9	B
C9	B	FFJ	A	WW23	A
C12	S	G2	B	WW24	A
C130	C	G159	A	YA7	A
C135	H	HF32	A		
C137	H	HS25	A		
C140	A	KC35	H		
C141	C	KC97	C		
C340	S	L101	H		
C421	S	L188	B		

BLANK PAGE

AD-A114 655 FEDERAL AVIATION ADMINISTRATION TECHNICAL CENTER ATL--ETC F/G 1/2
REDUCTION AND ANALYSIS OF MODE C ALTITUDE DATA COLLECTED AT HI--ETC(U)
MAR 82 R RIGOLIZZO

UNCLASSIFIED DOT/FAA/CT-81/53 DOT/FAA/EM-82/9 NL

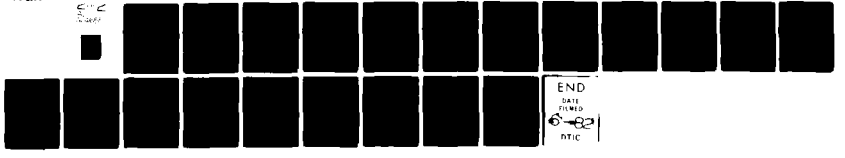

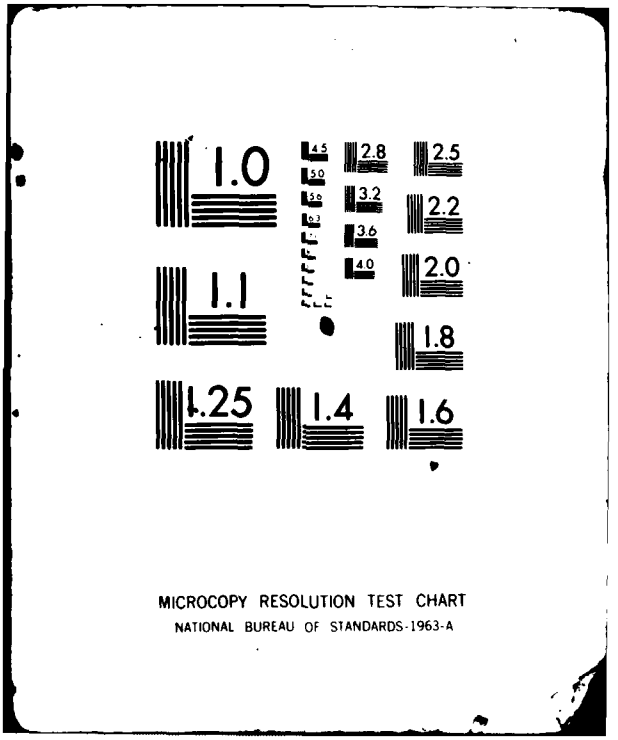
1.0
1.1
1.25
1.4
1.6
1.8
2.0
2.2
2.5
2.8
3.2
3.6
4.0
4.5
5.0
5.6
6.3
MICROCOPY RESOLUTION TEST CHART
NATIONAL BUREAU OF STANDARDS-1963-A

APPENDIX G

CONTINGENCY TABLES

Table G-1 to G-18

BLANK PAGE

LIST OF TABLES

TABLE 1. AIRCRAFT EN ROUTE CENTER CONTINGENCY TABLE

Observed Frequency

Number Of Aircraft	Cleveland	Memphis	Alburquerque	Total
<300	6109	1391	3409	10909
≥300	102	42	266	410
Total	6211	1433	3675	11319
%≥300	1.6	2.9	7.2	3.62

Expected Frequency

<300	5986	1381	3541
≥300	225	52	133

$(Obs-Exp)^2/Exp$

<300	2.5	.07	4.92
≥300	67.2	1.89	133

Note: Computed X^2 (2) = 209

$X^2_{.95}$ (2) = 5.99

TABLE 2. AIRCRAFT USER CONTINGENCY TABLE

Observed Frequency

Number Of Aircraft	Commercial	Military	General	Total
<300	8851	677	1381	10909
≥300	69	225	116	410
Total	8920	902	1497	11319
%≥300	.773	24.94	7.74	3.62

Expected Frequency

<300	8597	869	1443
≥300	323	33	54

$(Obs-Exp)^2/Exp$

<300	7.5	42.5	2.6
≥300	199.8	1130.8	70.5

Note: Computed χ^2 (2) = 1454

$\chi^2_{.95}$ (2) = 5.99

TABLE 3. RECONSTRUCTED GENERAL AVIATION AIRCRAFT CONTINGENCY TABLE (NASA AIRCRAFT REMOVED)

Observed Frequency

Number Of General Aircraft	Cleveland	Memphis	Albuquerque	Total
<300	724	179	467	1370
≥300	50	13	28	91
Total	774	192	495	1461
%≥300	6.46	6.77	5.66	6.23

Expected Frequency

<300	726	180	464
≥300	48	12	31

$(Obs-Exp)^2/Exp$

<300	005	.005	.019
≥300	.08	.08	.29

Note: Computed X^2 (2) = .48

$X^2_{.95}$ (2) = 5.99

TABLE 4. WEIGHT W_1 MILITARY AIRCRAFT CONTINGENCY TABLE

Number Of Military Aircraft Weight W_1	Albuquerque	Cleveland And Memphis	Total
	Observed Frequency		
<300	350	77	427
≥300	191	24	215
Total	541	101	642
%≥300	35.3	23.7	33.4
	Expected Frequency		
<300	360	.67	
≥300	181	34	
	$(Obs-Exp)^2/Exp$		
<300	.28	1.49	
≥300	.552	2.94	

Note: Computed χ^2 (1) = 5.26

χ^2 (1) = 3.84
.95

TABLE 5. WEIGHT W_2 MILITARY AIRCRAFT CONTINGENCY TABLE

Number Of Military Aircraft Weight W_2	Albuquerque	Cleveland And Memphis	Total
Observed Frequency			
<300	173	77	250
≥300	9	1	10
Total	182	78	260
%≥300	4.9	1.3	3.8
Expected Frequency			
<300	175	75	
≥300	7	3	
$(Obs-Exp)^2/Exp$			
<300	.02	.05	
≥300	.57	1.33	

Note: Computed χ^2 (1) = 1.97

$\chi^2_{.95}$ (1) = 3.84

TABLE 6. COMMERCIAL AIRCRAFT ALTITUDE CONTINGENCY TABLE

Observed Frequency

Number Of Commercial Aircraft	≤280	[290,330)	[330,370)	[370,390]	≥410	Total
<300	675	1292	4201	3206	124	9498
≥300	3	9	30	24	4	70
Total	678	1301	4231	3230	128	9568
%≥300	.442	.691	.709	.743	3.12	.732

Expected Frequency

<300	673	129.1	4200.0	3206	127	
≥300	5	10	31	24	1	

$(Obs-Exp)^2/Exp$

<300	.006	0	0	0	.07	
≥300	.8	.03	.03	0	10	

Note: Computed χ^2 (4) = 10.94

$\chi^2_{.95}$ (4) = 9.49

TABLE 7. GENERAL AVIATION AIRCRAFT ALTITUDE CONTINGENCY TABLE
(NASA Aircraft Removed)

Observed Frequency

Number Of General Aircraft	≤280	[290,330)	[330,370)	[370,390]	≥410	Total
<300	97	168	434	462	348	1509
≥300	4	6	18	30	35	93
Total	101	174	452	492	383	1602
%≥300	3.96	3.45	3.98	6.10	9.14	5.81

Expected Frequency

<300	95	164	426	463	361
≥300	6	10	26	29	22

$(Obs-Exp)^2/Exp$

<300	.042	.097	.15	.002	.468
≥300	.67	1.6	2.46	.02	7.68

Note: Computed χ^2 (4) = 13.2

$\chi^2_{.95}$ (4) = 9.49

TABLE 8. MILITARY WEIGHT W_1 AIRCRAFT OVER ALBUQUERQUE ALTITUDE CONTINGENCY TABLE

Observed Frequency

Number Of Military Aircraft	≤280	[290,330)	[330,370)	[370,390]	≥410	Total
<300	111	78	110	74	18	391
≥300	24	44	64	59	11	202
Total	135	122	174	133	29	593
%≥300	17.8	36.1	36.8	44.4	37.9	34.06

Expected Frequency

<300	89	80	115	88	19
≥300	46	41	59	45	10

$(Obs-Exp)^2/Exp$

<300	5.44	.05	.22	1.19	.05
≥300	10.52	.22	.42	4.35	.1

Note: Computed X^2 (4) = 22.56

X^2 (4) = 9.49
.95

TABLE 9. RECONSTRUCTED COMMERCIAL AIRCRAFT ALTITUDE CONTINGENCY TABLE
(Data Above 390 Removed)

Observed Frequency

Number Of Commercial Aircraft	<280	[290,330)	[330,370)	[370,390]	Total
<300	675	1292	4201	3206	9374
≥300	3	9	30	24	66
Total	678	1301	4231	3230	9440
%≥300	.442	.691	.709	.743	.7

Expected Frequency

<300	673	1292	4201	3207
≥300	5	9	30	23

$(Obs-Exp)^2/Exp$

<300	.0059	0	0	0
≥300	.8	0	0	.043

Note: Computed χ^2 (3) = .85

χ^2 (3) = 7.81
.95

TABLE 10. RECONSTRUCTED GENERAL AVIATION AIRCRAFT ALTITUDE CONTINGENCY TABLE (NASA Aircraft Removed, Data Above 390 Removed)

Number Of General Aircraft	≤280	[290,330)	[330,370)	[370,390]	Total
			Observed Frequency		
<300	97	168	434	462	1161
≥300	4	6	18	30	58
Total	101	174	452	492	1219
%≥300	3.96	3.45	3.98	6.10	4.76
			Expected Frequency		
<300	96	160	430	469	
≥300	5	8	21	23	
			$(Obs-Exp)^2/Exp$		
<300	.01	.4	.04	.1	
≥300	.2	.5	.43	2.13	

Note: Computed χ^2 (3) = 3.81

χ^2 (3) = 7.81
.95

TABLE 11. RECONSTRUCTED MILITARY WEIGHT W_1 AIRCRAFT OVER ALBUQUERQUE ALTITUDE CONTINGENCY TABLE (Data Below 290 Removed)

Number Of Military Aircraft	[290,330)	[330,370)	[370,390]	≥410	Total
Observed Frequency					
<300	78	110	74	18	280
≥300	44	64	59	11	178
Total	122	174	133	29	458
%≥300	36.1	36.8	44.4	37.9	38.86
Expected Frequency					
<300	75	106	81	18	
≥300	47	68	52	11	
$(Obs-Exp)^2/Exp$					
<300	.12	.15	.60	0	
≥300	.19	.23	.94	0	

Note: Computed χ^2 (3) = 2.23

$\chi^2_{.95}$ (3) = 7.81

TABLE 12. COMMERCIAL AIRCRAFT SPEED CONTINGENCY TABLE (EASTERLY TRAFFIC)

Observed Frequency

Number Of Commercial Aircraft (East)	≤450	(450,500]	(500,550]	>550	Total
<300	32	871	2557	691	4151
≥300	1	6	19	3	29
Total	33	877	2576	694	4180
%≥300	3.03	.68	.74	.43	.69

Expected Frequency

<300	33	871	2558	689
≥300	.23	6	18	5

$(Obs-Exp)^2/Exp$

<300	.03	0	0	.006
≥300	2.6	0	.05	.8

Note: Computed χ^2 (3) = 3.49

χ^2 (3) = 7.81
.95

TABLE 13. COMMERCIAL AIRCRAFT SPEED CONTINGENCY TABLE (WESTERLY TRAFFIC)

Observed Frequency

Number Of Commercial Aircraft (West)	≤350	(350,400]	(400,450]	>450	Total
<300	88	1747	2394	470	4699
≥300	3	16	14	7	40
Total	91	1763	2408	477	4739
%≥300	3.23	.91	.51	1.47	.844

Expected Frequency

<300	90.23	1748	2388	473
≥300	.77	15	20	4

$(Obs-Exp)^2/Exp$

<300	.055	0	.015	.02
≥300	6.45	.06	1.8	2.25

Note: Computed χ^2 (3) = 10.65

$\chi^2_{.95}$ (3) = 7.81

TABLE 14. RECONSTRUCTED COMMERCIAL AIRCRAFT SPEED CONTINGENCY TABLE (WESTERLY TRAFFIC, DATA <350 KNOTS REMOVED)

Number Of Commercial Aircraft (West)	(350,400]	(400,450]	>450	Total
		Observed Frequency		
<300	1747	2394	470	4611
≥300	16	14	7	37
Total	1763	2408	477	4648
%≥300	.91	.51	1.47	.79
		Expected Frequency		
<300	1749	2389	473	
≥300	14	19	4	
		$(Obs-Exp)^2/Exp$		
<300	.002	.01	.019	
≥300	.28	1.31	2.25	

Note: Computed χ^2 (2) = 3.87

$\chi^2_{.95}$ (2) = 5.99

TABLE 15. GENERAL AVIATION AIRCRAFT SPEED CONTINGENCY TABLE (EASTERLY TRAFFIC, NASA AIRCRAFT REMOVED)

Number Of General Aircraft (East)	≤450	(450,500]	(500,550)	≥550	Total
Observed Frequency					
<300	112	182	156	26	476
≥300	8	9	8	4	29
Total	120	191	164	30	505
%≥300	6.6	4.71	4.87	13.3	5.74
Expected Frequency					
<300	113	180	155	28.3	
≥300	7	11	9	1.7	
$(Obs-Exp)^2/Exp$					
<300	0	.02	0	.18	
≥300	.14	.36	.11	3.11	

Note: Computed χ^2 (3) = 3.92

$\chi^2_{.95}$ (3) = 7.81

TABLE 16. GENERAL AVIATION AIRCRAFT SPEED CONTINGENCY TABLE (WESTERLY TRAFFIC, NASA AIRCRAFT REMOVED)

Observed Frequency

Number Of General Aircraft (West)	≤300	(300,350]	(350,400]	>400	Total
<300	48	187	466	192	893
≥300	2	17	29	14	62
Total	50	204	495	206	955
%≥300	4.0	8.33	5.85	6.79	6.49

Expected Frequency

<300	47	191	463	193
≥300	3	13	32	13

$(Obs-Exp)^2/Exp$

<300	.02	.08	.02	.005
≥300	.33	1.23	.28	.08

Note: Computed χ^2 (3) = 2.04

$\chi^2_{.95}$ (3) = 7.81

TABLE 17. MILITARY WEIGHT W_1 AIRCRAFT SPEED CONTINGENCY TABLE (ALBUQUERQUE EASTERLY TRAFFIC)

Number Of Military Aircraft (East)	≤450	(450,500]	(500,550]	>550	Total
		Observed Frequency			
<300	38	53	55	35	181
≥300	21	33	35	23	112
Total	59	86	90	58	293
%≥300	35.6	38.4	38.8	39.65	38.22
		Expected Frequency			
<300	36	53	55	36	
≥300	22	33	34	22	
		$(Obs-Exp)^2/Exp$			
<300	11	0	0	.03	
≥300	.04	0	.03	.04	

Note: Computed χ^2 (3) = .25

$\chi^2_{.95}$ (3) = 7.81

TABLE 18. MILITARY WEIGHT W_1 AIRCRAFT SPEED CONTINGENCY TABLE (ALBUQUERQUE WESTERLY TRAFFIC)

Observed Frequency

Number Of Military Aircraft (West)	≤350	(350,400]	(400,450]	≥450	Total
<300	35	54	55	25	169
≥300	16	19	27	17	79
Total	51	73	82	42	248
%≥300	31.4	26.0	32.9	40.4	31.85

Expected Frequency

<300	35	50	56	29
≥300	16	23	26	13

$(Obs-Exp)^2/Exp$

<300	0	.32	.02	.55
≥300	0	.69	.04	1.23

Note: Computed χ^2 (3) = 2.85

$\chi^2_{.95}$ (3) = 7.81

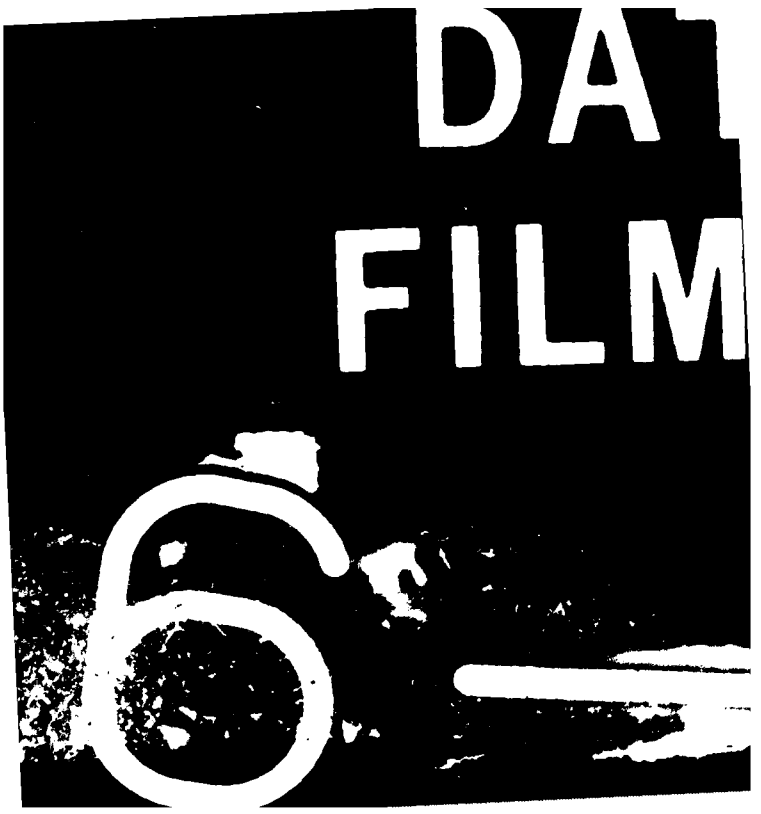
DA
FILM
6